BIOLOGICAL EFFECTS AND CANCER RISK OF COMPUTED TOMOGRAPHY

UNDERSTANDING THE BIOLOGICAL EFFECTS AND CANCER RISK OF MEDICAL DIAGNOSTIC COMPUTED TOMOGRAPHY

By

NGHI PHAN, BHSc (Hon)

A Thesis

Submitted to the School of Graduate Studies

in Partial Fulfilment of the Requirements

for the Degree

Doctor of Philosophy

McMaster University

DOCTORATE OF PHILOSOPHY (2011) McMaster University
(Radiation Biology) Hamilton, Ontario

TITLE: Understanding the biological effects and cancer risk of medical diagnostic computed tomography

AUTHOR: Nghi Phan, BHsc (McMaster University)

SUPERVISOR: Dr. Douglas R. Boreham, PhD

NUMBER OF PAGES: ix, 173

Abstract

The need to understand and accurately assess the health risks of low dose ionizing radiation is more important now than ever before. The global applications of ionizing radiation in medicine, mining, manufacturing, and the nuclear industry have increased exponentially in recent years. Parallel to this increase are the health concerns regarding occupational and medical exposures to radiation. The research presented here investigates the biological and health effects of ionizing radiation, specifically from medical diagnostic exposures.

Medical diagnostic procedures such as x-rays and computed tomography (CT) scans account for a notable portion of the public's exposure to ionizing radiation. The health risk to humans associated with these low dose exposures is unknown. Often times they are correlated with risk estimates derived from much higher radiation doses. There is no doubt that very high dose ionizing radiation can be harmful; however, the same notion does not exist regarding exposures to low dose ionizing radiation such as that from medical diagnostic CT exposures.

The objective of this research is to address the effects and risks associated with diagnostic CT scans. This research focuses on the biological outcome of cancer which remains a primary concern in health care and the development of radiation risk policies. The investigation utilized various mouse models that have differing sensitivities to radiation and susceptibilities to developing radiation-induced cancer.

Results from this research found that low-dose diagnostic CT scans do not increase risk and can, in fact, induce protective effects. The hypothesis that harmful effects increase linearly with radiation dose is not supported by this research. With low doses of CT scans, protective biological effects such as reduced chromosomal aberrations, decreased radiation-induced oxidative DNA damage, and enhanced clearance of damaged cells have been observed. In cancer-prone mice, CT scans can increase longevity and reduce cancer risk by delaying the latency of specific cancers.

This research advances the understanding of the biological effects and health risk associated with low-dose medical diagnostic procedures. This research is timely and important to allow medical practitioners, policy makers, and regulators to make informed decisions about using ionizing radiation in the clinic. Such knowledge is valuable as better, more complex, and perhaps more damaging modalities are being used to image and manage disease.

Acknowledgements

The acknowledgement section is my favourite part to read in any thesis. For me, it is an opportunity to share the secrets of my accomplishments and candidly provide key highlights of my post-graduate experience.

The biggest secret to my accomplishments is that I have a team of GIANTS; no, not a football or baseball reference, but GIANTS as in Goodhearted Individuals And Never Tiring Supporters. The Latin phrase "*nanos gigantium humeris insidentes"* perfectly captures my feelings. My accomplishments and successes are not mine alone; I am merely a "dwarf standing on the shoulders of giants". There are many people that I am greatly indebted to for the work in this thesis. My greatest fear of writing this section is the tragic omission of a name; please accept my apologies in advance.

Dr. Doug Boreham, we first met when I was a first year undergraduate student looking for a summer job at McMaster Shad Valley in 2004. You were a great speaker with an inspiring persona. I was sold on everything that you uttered. I often joke with my friends that had you gone into business, Jim Balsillie would just be an average Joe in comparison. You are a mentor with great vision for his students. Your guidance has been as valuable personally as they are academically. The opportunities that you have provided for me are countless. Thus far, I can only thank you by offering souvenirs that we *will* one day enjoy together.

Lisa, Nicole, and Mary Ellen, I can definitely say that none of the work in this thesis would be what it is without you. Your dedication to laboratory excellence and technical expertise does not go unnoticed and is very much valued. Kristina, my lab partner in crime, thanks for putting up with my shannanigans. Together, we witnessed and thankfully overcame the many difficulties associated with conducting a 3000+ mice study. I think I would still be around for another decade completing the PhD if I had to head the study myself. Thank you for your support and the many fond memories of working late hours at night / early mornings. The next time I "cart", "sort", "irradiate", or "health check" mice, I will be thinking of you.

Dr. Jennifer Lemon, you were my undergraduate honours thesis supervisor and my first mentor in real scientific research. The research in this thesis is built upon the framework of the impressive DOE grant that you worked on. Without your vital contribution to the application of this grant, I would probably be an expert on the effects of CT scans in fish and not mice. Thank you.

Thank you to my committee members and mentors: Drs. G. Parise, F. McNeil, D. Chettle, and T. Farrell, your counsel and guidance throughout my post-graduate studies have been highly

appreciated. From advice on experiments and statistics to scholarship recommendations, you have provided great insight into the intricacies of academia.

Zoe, my better half, thank you for being so supportive of my endeavours and understanding of the nuances associated with those endeavours. Our lives have been separated, physically, for most of the last four years, but the care and encouragement that you gave made the distance and time apart bearable. Thank you for being the catalyst for the various adventures we had over the years, and the much needed distraction from the research scene. I look forward to sharing our lives together in the same city.

Thank you to my mother, although you probably don't understand much of what is written in this thesis, the work here is not possible without the many sacrifices you have made for me. I could write a novel on how you have shaped my life; and if this was baseball, all my accomplishments would have an asterisk beside them to note that they were achieved with your unconditional love. I dedicate this thesis to you, and hope that you understand how big of a role you played in its completion. Mom, thank you!

To all the GIANTS whom I have not personally named, your advice and help over the years have been important. I hope to be a supporting figure in your lives, as you have been in mine. Thank you all.

Table of Contents

List of Figures

List of Tables

Chapter 1

Introduction

Radiation biology is the study of the effects of ionizing radiation on living things. The discovery of x-rays by Wilhelm Conrad Roentgen in 1895 led to its inception as a relatively new field of research *(1)*. The first reported medical use of x-rays was to locate a metal fragment in the spine of a drunken sailor who had been temporary paralyzed by the injury *(2)*. By 1897, physicians were using x-rays to treat abnormal growths such as hairy moles, ulcers, and warts *(2)*. However, adverse effects from radiation exposure were noted early on amongst radiation scientists and radiotherapy patients. Dermatitis of the hands, irritation of the eyes, and hair loss were common signs *(3)*, and their observation prompted systematic research on the biological and health effects of ionizing radiation.

The idea that ionizing radiation exhibits stimulatory effects at low doses and detrimental effects at high doses, called radiation hormesis, gained prominence by the first decade of the 20th century. Low doses of radiation were found to have positive results in treating a spectrum of ailments and diseases *(4-7)*. Conversely, high doses of radiation caused cancer, inhibition of bone growth, sterilization, and degeneration of blood and bone marrow compartments *(1, 2, 3, 8)*. Although some thought that low doses were inherently genotoxic and carcinogenic, the majority at the time believed that ionizing radiation was beneficial up to a certain threshold *(4, 9)*.

The positive effects of ionizing radiation were not only observed in humans, but also in mammalian cells, plants, and animals. By the 1920's, there was substantial evidence that ionizing radiation had stimulatory effects on growth *(9)*. Studies published in prominent journals showed

that low-dose radiation enhanced cell division in chick embryo and other cell types *(4, 9, 10)*. Research on the effects of radiation in plants led to a patent in 1923, which described the procedure to use radiation to stimulate plant growth *(4, 11)*. By the 1940's, there were reports that low-dose radiation exposure could enhance longevity in insects and small animals *(4, 12-14)*.

Despite these positive biological effects of ionizing radiation, there were mounting concerns that even low doses of radiation exposure could have harmful effects. A series of ill-timed historical events strengthened this belief *(15)*: 1) the discovery by Herman J. Muller in 1927 that x-rays could cause mutations in fruit flies heightened concerns that radiation was genotoxic; 2) the death of Eben M. Byers in 1932, a wealthy entrepreneur who had chronically consumed radium water for the supposed health benefits, brought the use of radioactive health products to a halt; 3) the outright rejection of a threshold for radiation effects by Nobel laureate Herman J. Muller in 1946 substantiated fears about radiation at low doses; and 4) the 1972 introduction of the unvalidated linear, no threshold (LNT) model for radiation risk estimates supported the growing radiation-phobia. Although there were other key events that led to the demise of radiation hormesis *(4, 10, 15)*, these events shaped the way popular culture and the media negatively portray exposure to ionizing radiation. One area where this is most prominent is in the field of medical diagnostic radiology.

Diagnostic medicine has used ionizing radiation since the discovery of x-rays. Advances in computer technology have allowed for more powerful diagnostic modalities such as computed tomography (CT) to render 3-dimensional projections of patient anatomy. Introduced in 1972, the use of CT scans has increased rapidly, and it is estimated that there were over 390 million CT procedures performed worldwide in 2010 *(16, 17)*. In Canada, CT scans account for only 12% of

all diagnostic radiological procedures, but is estimated to be responsible for more than 70% of the total radiation dose delivered to patient populations *(18, 19)*. A study by *Lee et al*. found that patients, physicians, and radiologists are unable to provide accurate estimates of CT doses *(18)*, let alone risk. The estimated average dose range for a single CT examination is between 10-30 mGy, but can be as high as 80 mGy depending on the procedure and size of the individual *(20-23)*. To put this into perspective, the global average background radiation dose is 2.4 mGy annually *(24)*. In some places such as Guarapari Beach, Brazil and Ramsar, Iran, the annual dose can be over 150 mGy *(25-29)*. The regulatory limit for nuclear workers is 50 mGy per year; however, most workers receive less than 20 mGy over their entire lifetime on the job *(30, 31)*. A return flight from New York to London is approximately 0.1 mGy *(32)*, and a simple bone x-ray radiograph is five times less at 0.02 mGy *(33)*. Although these dose estimates vary moderately from study to study, the risk estimates associated with them do not only vary in magnitude but also in direction *(33-36)*.

Using the LNT assumption, there are published studies claiming increased risk associated with low-dose radiation exposure, specifically from CT scans *(36-43)*. In a recent publication, Brenner and Hall estimate that a 1.5-2% increase in cancer risk can be attributed to CT scans *(42)*. Based on the most recent BEIR (Biological Effects of Ionizing Radiation) VII report, the overall solid cancer fatality risk for both males and females from a 10 mGy CT scan is 0.00041 *(33)*. Although this risk figure is small, some researchers have inappropriately multiplied it by the number of CT scans performed annually to estimate the number of fatal cancers induced by CT procedures each year *(40)*. This method of risk assessment is invalid and misleading. These LNT-based risk studies have been repeatedly challenged *(29, 44-48)*. Scott *et al*. argue that the evidence is lacking for the assertion that current usage of CT scans will increase cancer incidence *(46)*. They purport that available cell biology *(49-55)*, animal cancer models *(56-67)*, and human

epidemiological data *(29, 68-71)* show that occasional exposure to low-dose diagnostic x-rays could reduce the risk of cancers *(46)*.

Low-dose radiation exposure has been shown to induce protective mechanisms against genomic and cellular damage *(48, 72, 73)*. Radiation doses less than 100 mGy can enhance the detoxification of reactive oxygen species by up-regulating antioxidants such as glutathione and superoxide dismutase *(74)*. Priming doses from 1-500 mGy have been reported to effectively protect against chromosomal aberrations and/or micronuclei formation following high-dose challenges in human lymphocytes and tissue culture cells *(26, 47, 75-78)*. Apoptosis induced by low-dose radiation is theorized to be an anti-oncogenic mechanism by which pre-cancerous cells are eliminated *(50, 51)*. Similarly, low-dose radiation can reduce the incidence of cancer metastases by increasing the number of cytotoxic lymphocytes *(52-55)*. Cell cycle delay is another way by which low dose radiation has been shown to prevent genomic damage from being passed on to daughter cells *(73, 79, 80)*. These various radiation-induced protective mechanisms involve changes in gene expression *(60, 81-84)*. Low doses can up-regulate the expression of thousands of stress response and DNA repair-related genes *(84, 85)*. Taken together, these radiation-induced effects are indicative of reduced risk following low dose exposure, not increased risk, as would be predicted under the LNT model.

The work in this thesis investigated the biological outcomes and carcinogenic effects of low-dose radiation exposure. The main objective was to directly address the risk associated with diagnostic CT scans and attempt to relate the mechanism of that risk with chromosomal aberrations, genomic instability, DNA oxidative stress damage, and apoptosis.

There were three specific aims to this research:

1) To determine the biological effects of single and repeated CT scans;

2) To determine if a single CT scan can alter cancer risk;

3) To determine if repeated CT scans administered after high dose exposure can alter cancer risk.

A mouse model was used to extrapolate radiation risk to humans. Although there are obvious limitations to using a non-human model, similarities between mice and humans at the cellular level make the findings of this research valuable to the understanding of the biological responses and cancer risk of diagnostic radiation exposure at low doses.

References

1. Upton AC. Radiation hormesis: Data and interpretations. Crit Rev Toxicol. 2001 Jul;31(4-5):681-95.
2. Hall EJ, Amato J. Radiobiology for the radiologist, 6th edition. 6th ed. New York: Lippincott Williams & Wilkins; 2006.
3. Upton AC. The first hundred years of radiation research: What have they taught us? Environ Res. 1992 Oct;59(1):36-48.
4. Calabrese EJ, Baldwin LA. Tales of two similar hypotheses: The rise and fall of chemical and radiation hormesis. Hum Exp Toxicol. 2000 Jan;19(1):85-97.
5. Desjardins AU. Roentgen treatment for hodgkin's disease and lymphosarcoma of the chest. Dis Chest. 1945 Nov-Dec;11:565-89.
6. Desjardins AU. Salient factors in the treatment of hodgkin's disease and lymphosarcoma with roentgen rays. Am J Roentgenol Radium Ther. 1945 Dec;54:707-22.
7. Desjardins AU. The action of roentgen rays or radium on inflammatory processes. Radiology. 1937(29):436-445.
8. Stone RS. The concept of a maximum permissible exposure. Radiology. 1952 May;58(5):639-61.
9. Calabrese EJ, Baldwin LA. Radiation hormesis: The demise of a legitimate hypothesis. Hum Exp Toxicol. 2000 Jan;19(1):76-84.
10. Calabrese EJ. Muller's nobel lecture on dose-response for ionizing radiation: Ideology or science? Arch Toxicol. 2011 Jun 30.
11. Adams RR. Radioactive spray material. The Official Gazzete of the U.S. Patent Office 1923. 1923(312):320.
12. Davey WP. The effect of X-rays on the length of life of *tribolium consusm*. Journal of Experimental Zoology. 1917(22):573-592.
13. Lorenz E, Heston WE. Biological studies in the tolerance range. Radiology. 1947 Sep;49(3):274-85.
14. Lorenz E, Jacobson LO, Heston W, Shimkin M, Eschenbrenner AB, Deringer MK, et al. Effects of long-continued total-body gamma irradiation of mice, guinea pigs, and rabbits. III. effects of life span, weight, blood picture, and carcinogenesis and the role of the intensity of radiation. Zirkle RE (ed) Biological Effects of External X and Gamma Radiation. 1954:24–248.
15. Calabrese EJ, Baldwin LA. Tales of two similar hypotheses: The rise and fall of chemical and radiation hormesis. Hum Exp Toxicol. 2000 Jan;19(1):85-97.
16. Frush DP. Review of radiation issues for computed tomography. Semin Ultrasound CT MR. 2004 Feb;25(1):17-24.
17. Berrington de Gonzalez A, Mahesh M, Kim KP, Bhargavan M, Lewis R, Mettler F, et al. Projected cancer risks from computed tomographic scans performed in the united states in 2007. Arch Intern Med. 2009 Dec 14;169(22):2071-7.
18. Lee CI, Haims AH, Monico EP, Brink JA, Forman HP. Diagnostic CT scans: Assessment of patient, physician, and radiologist awareness of radiation dose and possible risks. Radiology. 2004 May;231(2):393-8.
19. Canadian Institute for Health Information. Medical imaging in canada, 2007. Ottawa, ON: CIHI, 2008; 2008.
20. Mettler FA,Jr, Wiest PW, Locken JA, Kelsey CA. CT scanning: Patterns of use and dose. J Radiol Prot. 2000 Dec;20(4):353-9.
21. Frush DP, Applegate K. Computed tomography and radiation: Understanding the issues. J Am Coll Radiol. 2004 Feb;1(2):113-9.

22. Fujii K, Aoyama T, Yamauchi-Kawaura C, Koyama S, Yamauchi M, Ko S, et al. Radiation dose evaluation in 64-slice CT examinations with adult and paediatric anthropomorphic phantoms. Br J Radiol. 2009 Dec;82(984):1010-8.
23. Shrimpton PC, Hillier MC, Lewis MA, Dunn M. National survey of doses from CT in the UK: 2003. Br J Radiol. 2006 Dec;79(948):968-80.
24. UNSCEAR. Sources and effects of ionizing radiation: United nations scientific committee on the effects of atomic radiation: UNSCEAR 2000 report to the general assembly. New York: United Nations; 2000.
25. Hendry JH, Simon SL, Wojcik A, Sohrabi M, Burkart W, Cardis E, et al. Human exposure to high natural background radiation: What can it teach us about radiation risks? J Radiol Prot. 2009 Jun;29(2A):A29-42.
26. Mohammadi S, Taghavi-Dehaghani M, Gharaati MR, Masoomi R, Ghiassi-Nejad M. Adaptive response of blood lymphocytes of inhabitants residing in high background radiation areas of ramsar- micronuclei, apoptosis and comet assays. J Radiat Res (Tokyo). 2006 Nov;47(3-4):279-85.
27. Attar M, Molaie Kondolousy Y, Khansari N. Effect of high dose natural ionizing radiation on the immune system of the exposed residents of ramsar town, iran. Iran J Allergy Asthma Immunol. 2007 Jun;6(2):73-8.
28. Shetty PK, Narayana Y. Variation of radiation level and radionuclide enrichment in high background area. J Environ Radioact. 2010 Dec;101(12):1043-7.
29. Sanders CL. Radiation hormesis and the linear-no-threshold assumption. New York: Springer-Verlag Berlin Heidelberg; 2010.
30. Cardis E, Vrijheid M, Blettner M, Gilbert E, Hakama M, Hill C, et al. The 15-country collaborative study of cancer risk among radiation workers in the nuclear industry: Estimates of radiation-related cancer risks. Radiat Res. 2007 Apr;167(4):396-416.
31. Cardis E, Gilbert E, Carpenter L, Howe G, Kato I, Armstrong B, et al. Effects of low doses and low dose rates of external ionizing radiation: Cancer mortality among nuclear industry workers in three countries. Radiat Res. 1995;142(2):117-32.
32. Brenner DJ, Doll R, Goodhead DT, Hall EJ, Land CE, Little JB, et al. Cancer risks attributable to low doses of ionizing radiation: Assessing what we really know. Proc Natl Acad Sci U S A. 2003 Nov 25;100(24):13761-6.
33. BEIR VII.
Health risks from exposure to low levels of ionizing radiation — BEIR VII. Washington, DC: National Academies Press; 2005.
34. Tubiana M, Aurengo A, Averbeck D, Masse R. The debate on the use of linear no threshold for assessing the effects of low doses. J Radiol Prot. 2006 Sep;26(3):317-24.
35. Tubiana M, Aurengo A, Averbeck D, Masse R. Recent reports on the effect of low doses of ionizing radiation and its dose-effect relationship. Radiat Environ Biophys. 2006 Mar;44(4):245-51.
36. Preston RJ. Update on linear non-threshold dose-response model and implications for diagnostic radiology procedures. Health Phys. 2008 Nov;95(5):541-6.
37. Little MP, Wakeford R, Tawn EJ, Bouffler SD, Berrington de Gonzalez A. Risks associated with low doses and low dose rates of ionizing radiation: Why linearity may be (almost) the best we can do. Radiology. 2009 Apr;251(1):6-12.
38. Smith-Bindman R, Lipson J, Marcus R, Kim KP, Mahesh M, Gould R, et al. Radiation dose associated with common computed tomography examinations and the associated lifetime attributable risk of cancer. Arch Intern Med. 2009 Dec 14;169(22):2078-86.
39. Martin DR, Semelka RC. Health effects of ionising radiation from diagnostic CT. Lancet. 2006 May 27;367(9524):1712-4.

40. Boone JM. Multidetector CT: Opportunities, challenges, and concerns associated with scanners with 64 or more detector rows. Radiology. 2006 Nov;241(2):334-7.
41. Tien HC, Tremblay LN, Rizoli SB, Gelberg J, Spencer F, Caldwell C, et al. Radiation exposure from diagnostic imaging in severely injured trauma patients. J Trauma. 2007 Jan;62(1):151-6.
42. Brenner DJ, Hall EJ. Computed tomography--an increasing source of radiation exposure. N Engl J Med. 2007 Nov 29;357(22):2277-84.
43. Brenner DJ, Elliston CD. Estimated radiation risks potentially associated with full-body CT screening. Radiology. 2004 Sep;232(3):735-8.
44. Blecher CM. Alarm about computed tomography scans is unjustified. Med J Aust. 2010 Jun 21;192(12):723-4.
45. Scott BR. Low-dose radiation risk extrapolation fallacy associated with the linear-no-threshold model. Hum Exp Toxicol. 2008 Feb;27(2):163-8.
46. Scott BR, Sanders CL, Mitchel REJ, Boreham DR. CT scans may reduce rather than increase risk of cancer. Journal of American Physicians and Surgeons. 2008;13(1).
47. Rithidech KN, Scott BR. Evidence for radiation hormesis after in vitro exposure of human lymphocytes to low doses of ionizing radiation. Dose Response. 2008;6(3):252-71.
48. Scott B. Low-dose-radiation activated natural protection and LNT. Health Phys. 2011 Mar;100(3):337-9.
49. Redpath JL, Elmore E. Radiation-induced neoplastic transformation in vitro, hormesis and risk assessment. Dose Response. 2006 Dec 6;5(2):123-30.
50. Portess DI, Bauer G, Hill MA, O'Neill P. Low-dose irradiation of nontransformed cells stimulates the selective removal of precancerous cells via intercellular induction of apoptosis. Cancer Res. 2007 Feb 1;67(3):1246-53.
51. Bauer G. Low dose radiation and intercellular induction of apoptosis: Potential implications for the control of oncogenesis. Int J Radiat Biol. 2007 Nov-Dec;83(11-12):873-88.
52. Nowosielska EM, Cheda A, Wrembel-Wargocka J, Janiak MK. Anti-neoplastic and immunostimulatory effects of low-dose X-ray fractions in mice. Int J Radiat Biol. 2011 Feb;87(2):202-12.
53. Cheda A, Nowosielska EM, Wrembel-Wargocka J, Janiak MK. Production of cytokines by peritoneal macrophages and splenocytes after exposures of mice to low doses of X-rays. Radiat Environ Biophys. 2008 Apr;47(2):275-83.
54. Nowosielska EM, Wrembel-Wargocka J, Cheda A, Lisiak E, Janiak MK. Enhanced cytotoxic activity of macrophages and suppressed tumor metastases in mice irradiated with low doses of X- rays. J Radiat Res (Tokyo). 2006 Nov;47(3-4):229-36.
55. Cheda A, Wrembel-Wargocka J, Lisiak E, Nowosielska EM, Marciniak M, Janiak MK. Single low doses of X rays inhibit the development of experimental tumor metastases and trigger the activities of NK cells in mice. Radiat Res. 2004 Mar;161(3):335-40.
56. Mitchel REJ, Jackson JS, Morrison DP, Carlisle SM. Low doses of radiation increase the latency of spontaneous lymphomas and spinal osteosarcomas in cancer-prone, radiation-sensitive Trp53 heterozygous mice. Radiat Res. 2003;159(3):320-7.
57. Mitchel RE, Jackson JS, Carlisle SM. Upper dose thresholds for radiation-induced adaptive response against cancer in high-dose-exposed, cancer-prone, radiation-sensitive Trp53 heterozygous mice. Radiat Res. 2004 Jul;162(1):20-30.
58. Mitchel REJ, Jackson JS, McCann RA, Boreham DR. The adaptive response modifies latency for radiation-induced myeloid leukemia in CBA/H mice. Radiat Res. 1999;152(3):273-9.
59. Plews M, Simon SL, Boreham DR, Parchaliuk D, Wyatt H, Mantha R, et al. A radiation-induced adaptive response prolongs the survival of prion-infected mice. Free Radic Biol Med. 2010 Nov 15;49(9):1417-21.

60. Shin SC, Lee KM, Kang YM, Kim K, Lim SA, Yang KH, et al. Differential expression of immune-associated cancer regulatory genes in low- versus high-dose-rate irradiated AKR/J mice. Genomics. 2011 Jan 23.
61. Shin SC, Kang YM, Kim HS. Life span and thymic lymphoma incidence in high- and low-dose-rate irradiated AKR/J mice and commonly expressed genes. Radiat Res. 2010 Sep;174(3):341-6.
62. Ina Y, Sakai K. Activation of immunological network by chronic low-dose-rate irradiation in wild-type mouse strains: Analysis of immune cell populations and surface molecules. Int J Radiat Biol. 2005 Oct;81(10):721-9.
63. Ina Y, Tanooka H, Yamada T, Sakai K. Suppression of thymic lymphoma induction by life-long low-dose-rate irradiation accompanied by immune activation in C57BL/6 mice. Radiat Res. 2005;163(2):153-8.
64. Ina Y, Sakai K. Further study of prolongation of life span associated with immunological modification by chronic low-dose-rate irradiation in MRL-lpr/lpr mice: Effects of whole-life irradiation. Radiat Res. 2005 Apr;163(4):418-23.
65. Ina Y, Sakai K. Prolongation of life span associated with immunological modification by chronic low-dose-rate irradiation in MRL-lpr/lpr mice. Radiat Res. 2004 Feb;161(2):168-73.
66. Yonezawa M. Induction of radio-resistance by low dose X-irradiation. Yakugaku Zasshi. 2006 Oct;126(10):833-40.
67. Otsuka K, Koana T, Tauchi H, Sakai K. Activation of antioxidative enzymes induced by low-dose-rate whole-body gamma irradiation: Adaptive response in terms of initial DNA damage. Radiat Res. 2006 Sep;166(3):474-8.
68. Cohen BL. Cancer risk from low-level radiation. AJR Am J Roentgenol. 2002 Nov;179(5):1137-43.
69. Berrington A, Darby SC, Weiss HA, Doll R. 100 years of observation on british radiologists: Mortality from cancer and other causes 1897-1997. Br J Radiol. 2001 Jun;74(882):507-19.
70. Howe GR. Lung cancer mortality between 1950 and 1987 after exposure to fractionated moderate-dose-rate ionizing radiation in the canadian fluoroscopy chart study and a comparison with lung cancer mortality in the atomic bomb survivor study. Radiat.Res. 1995(142):295-305.
71. Davis FG, Boice JD,Jr, Hrubec Z, Monson RR. Cancer mortality in a radiation-exposed cohort of massachusetts tuberculosis patients. Cancer Res. 1989 Nov 1;49(21):6130-6.
72. Tapio S, Jacob V. Radioadaptive response revisited. Radiat Environ Biophys. 2007 Mar;46(1):1-12.
73. Feinendegen LE. Evidence for beneficial low level radiation effects and radiation hormesis. Br J Radiol. 2005 Jan;78(925):3-7.
74. Feinendegen LE. Reactive oxygen species in cell responses to toxic agents. Hum Exp Toxicol. 2002 Feb;21(2):85-90.
75. Sorensen KJ, Attix CM, Christian AT, Wyrobek AJ, Tucker JD. Adaptive response induction and variation in human lymphoblastoid cell lines. Mutat Res. 2002 Aug 26;519(1-2):15-24.
76. Feinendegen LE, Pollycove M, Neumann RD. Whole-body responses to low-level radiation exposure: New concepts in mammalian radiobiology. Exp Hematol. 2007 Apr;35(4 Suppl 1):37-46.
77. Day TK, Zeng G, Hooker AM, Bhat M, Scott BR, Turner DR, et al. Extremely low priming doses of X radiation induce an adaptive response for chromosomal inversions in pKZ1 mouse prostate. Radiat Res. 2006 Nov;166(5):757-66.
78. Cramers P, Atanasova P, Vrolijk H, Darroudi F, van Zeeland AA, Huiskamp R, et al. Pre-exposure to low doses: Modulation of X-ray-induced dna damage and repair? Radiat Res. 2005 Oct;164(4 Pt 1):383-90.

79. Salone B, Grillo R, Aillaud M, Bosi A, Olivieri G. Effects of low-dose (2 cGy) X-ray on cell-cycle kinetics and on induced mitotic delay in human lymphocyte. Mutat Res. 1996 Apr 13;351(2):193-7.
80. Fernet M, Megnin-Chanet F, Hall J, Favaudon V. Control of the G2/M checkpoints after exposure to low doses of ionising radiation: Implications for hyper-radiosensitivity. DNA Repair (Amst). 2010 Jan 2;9(1):48-57.
81. Feinendegen LE. Evidence for beneficial low level radiation effects and radiation hormesis. Br J Radiol. 2005 Jan;78(925):3-7.
82. Ma S, Liu X, Jiao B, Yang Y, Liu X. Low-dose radiation-induced responses: Focusing on epigenetic regulation. Int J Radiat Biol. 2010 Jul;86(7):517-28.
83. Sudprasert W, Navasumrit P, Ruchirawat M. Effects of low-dose gamma radiation on DNA damage, chromosomal aberration and expression of repair genes in human blood cells. Int J Hyg Environ Health. 2006 Nov;209(6):503-11.
84. Klokov D, Criswell T, Leskov KS, Araki S, Mayo L, Boothman DA. IR-inducible clusterin gene expression: A protein with potential roles in ionizing radiation-induced adaptive responses, genomic instability, and bystander effects. Mutat Res. 2004 Dec 2;568(1):97-110.
85. Mayer C, Popanda O, Zelezny O, von Brevern MC, Bach A, Bartsch H, et al. DNA repair capacity after gamma-irradiation and expression profiles of DNA repair genes in resting and proliferating human peripheral blood lymphocytes. DNA Repair (Amst). 2002 Mar 28;1(3):237-50.

Chapter 2

Biological Effects and Adaptive Response from Single and Repeated Computed Tomography Scans in Reticulocytes and Bone Marrow of C57BL/6 Mice

Nghi Phan[1]*, Michael De Lisio[2], Gianni Parise[1,2], and Douglas R. Boreham[1]
[1]Department of Medical Physics and Applied Radiation Sciences, [2]Department of Kinesiology, McMaster University, 1280 Main St. W, Hamilton, Ontario, Canada, L8S 4K1

Manuscript in review: Radiat.Res. 2011; Submitted May, 2011

Author Contributions:

N. Phan and M. De Lisio were responsible for experimental design and data acquisition.
N. Phan was responsible for the interpretation of the results and synthesis of the manuscript.
D. Boreham and G. Parise supervised and guided the research.

ABSTRACT

This study investigated the biological effects and adaptive responses induced by single and repeated *in vivo* computed tomography (CT) scans. We postulated that, through the induction of low level oxidative stress, repeated low-dose CT scans (20 mGy, 2d/wk, 10wk) could protect mice (C57BL/6) from acute effects of high dose radiation (1 Gy, 2 Gy). Micronucleated reticulocyte (MN-RET) count increased linearly following exposure to single CT scans of doses ranging from 20 to 80 mGy ($p=0.033$). Ten weeks of repeated CT scans (total dose 400 mGy) produced a slight reduction in spontaneous MN-RET levels, relative to levels in sham CT scanned mice ($p=0.040$). Decreases of nearly 10% in γH2AX fluorescence level were observed in the repeated CT scanned mice following an *in vitro* challenge dose of 1 Gy ($p=0.017$) and 2 Gy ($p=0.026$). Spontaneous apoptosis levels (caspases 3 and 7 activation) were also significantly lower in the repeated CT scanned mice than the sham controls ($p<0.010$). In contrast, mice receiving only a single CT scan showed a 19% elevation in apoptosis ($p<0.02$), and a 10% increase in γH2AX fluorescence level following a 2 Gy challenge ($p<0.05$), relative to sham-CT scanned mice. Overall, repeated CT scans seemed to confer resistance to larger doses in mice, whereas mice exposed to single CT scans exhibited transient genotoxicity, enhanced apoptosis, and characteristics of radiation sensitization.

INTRODUCTION

In the last decade, the number of computed tomography (CT) scans performed has increased nearly sevenfold worldwide *(1-3)*. In the United States alone, it is estimated that more than 65 million CT scans are performed annually *(2, 4, 5)*. Studies in North America and Europe indicate that these procedures represent only 5-10% of all radiological exams, but account for 30-67% of total radiation exposure in patient populations *(3, 6, 7)*. The estimated average dose range for a single CT examination is between 10-30 mGy, but can be as high as 80 mGy depending on the procedure and size of the individual *(5, 8-10)*. These higher radiation doses have prompted on-going discussions regarding the potential health risks CT scans may pose *(2, 7, 11-17)*. According to the International Commission on Radiological Protection (ICRP) and the United Nations Scientific Committee on the Effects of Atomic Radiation (UNSCEAR), it is important to minimize radiation dose to "as low as reasonably achievable" (ALARA) *(18-21)*; however, CT scans may be critical for immediate medical intervention. Therefore, under certain conditions the benefit of the diagnostic procedure outweighs any small estimated risk from the radiation exposure.

We studied the biological effects of low dose diagnostic X-rays from CT scans. In particular, the effects of single and repeated 20 mGy CT scans were investigated in a C57BL/6 mouse model with respect to three well established biological endpoints: micronucleated reticulocyte (MN-RET) formation, histone H2AX phosphorylation, and apoptosis (Caspases 3/7 activation).

Micronuclei form in dividing cells that contain unstable chromosome aberrations such as acentric chromosome fragments. Micronuclei are useful biological indicators of radiation exposure, and their formation has been used as a means of analyzing *in vivo* chromosomal damage *(22-25)*. The *in vivo* erythrocyte-based micronucleus assay employed in this study has shown a robust dose-response correlation to clastogenic chemicals, as well as to ionizing

radiation exposure at doses up to 1 Gy and dose rates up to 2 Gy/minute *(23, 26-28)*. The broad utility and sensitivity of the MN-RET assay can provide a better understanding of the biological impact of low-dose radiation on hematopoietic stem cell progenies.

In addition to micronuclei analysis, histone H2AX phosphorylation was examined as a surrogate biomarker for radiation-induced DNA double-stranded breaks (DSBs) *(29, 30)*. Histone protein H2AX phosphorylation rapidly forms γH2AX at nascent DNA DSBs sites *(31, 32)*. Thus, the γH2AX assay can be used to measure DNA damage and repair following radiation exposure from CT scans. DNA DSBs can initiate genomic instability, and can potentially lead to cancer after high-dose exposures *(33)*. H2AX phosphorylation analysis provides valuable insight into the response of cells to low-dose diagnostic CT scans and how the effects are processed.

Apoptosis is an evolutionarily conserved form of cell death that has distinctive morphological and biochemical features *(34)*. Organisms activate the apoptotic pathway to eliminate extraneous or genetically damaged cells *(35, 36)*. It is well documented that ionizing radiation can damage DNA and induce apoptosis *(37, 38)*. However, it is not clear if or how the radiation quality and doses of diagnostic CT scans influence the homeostatic balance of cell death. Cell death via apoptosis can be triggered by activation of proteolytic enzymes called caspases. In caspase-dependent pathways of apoptosis, the activation of “executioner” caspases 3 and 7 is an essential step in the apoptotic process *(39, 40)*. In this study, apoptosis, measured by activation of caspases 3 and 7, was investigated to highlight the cytotoxicity of X-rays originating from diagnostic CT imaging procedures.

Having employed the three aforementioned biological endpoints, this study investigated the adaptive response with respect to low dose diagnostic CT scans. Low “priming” doses of ionizing radiation (< 100 mGy) have been shown to alter the biological response of “subsequent”

challenge radiation doses (1-2 Gy) in eukaryotic cells of many difference species, including mice *(41)*, rabbits *(42)*, and humans *(43-46)*. An adaptive response is present when the observed negative biological response is decreased by the priming dose following exposure to the challenge dose. The adaptive response is highly variable across cell types, tissues, systems, and organisms *(37, 47)*. This investigation examined the existence, magnitude, and kinetics of an adaptive response induced by single and repeated *in vivo* CT scans.

Results from this research will further the understanding of the biological effects of low-dose medical diagnostic CT scans. This research is timely and relevant to medical practitioners, policy makers, and regulators who must make informed decisions about the use of ionizing radiation. Its significance cannot be understated in light of the increasingly complex modalities that are being developed to image and manage disease.

MATERIALS & METHODS

Animals

Male C57BL/6 mice (14 weeks old) were purchased from Jackson Laboratory (Bar Harbor, Maine). The mice were allowed to acclimate for two weeks prior to random assignment to the various treatment groups (Table 1). Up to five mice were housed in solid-bottom polycarbonate cages (27 x 12 x 15.5 cm) containing woodchip bedding (Harlan Sani-Chips, 7090). A stainless steel wire-bar hopper held food (Harlan Lab Diets; Indianapolis, USA) and a water bottle for consumption *ad libitum.* The housing room was maintained at a 12:12-h light:dark photoperiod with an inside air temperature of 22±2^{o}C and 40-60% humidity. All protocols were approved by the Animal Research Ethics Board at McMaster University and carried out according to the

regulations of the Canadian Council on Animal Care. Some of the mice from the sham groups were also included in the sham groups for a study performed concurrently by De Lisio *et a*l. *(48)*.

Computed Tomography Protocols

Whole-body CT scans were performed on a Gamma Medica X-SPECT Animal Imaging System (Northridge, California). Mice were placed in pairs into a customized sectioned polycarbonate tube and CT scanned (75 kVp, 215 µA, 1 mm Al filter, half-value layer 4.28 mm Al, 250 projections) for 60 seconds to give a dose of 20 mGy. The mice were not anaesthetized during the CT scans as immobilization for image analysis was not necessary. Mice were treated as follows: A) a single CT scan of either 20-, 40-, 60-, 80-mGy at 25 weeks old; B) repeated 20 mGy CT scans twice a week (Tuesday and Thursday) for 10 consecutive weeks (starting at 16 weeks old); C) a sham single CT scan (i.e. control, age-matched) D) sham repeated CT scans (i.e. control, age-matched) (Table 1).

Computed Tomography Dosimetry

Whole-body dose measurements were obtained using thermoluminescent dosimeter (TLD) chips (Harshaw TLD-100 LiF Chips). TLD chip analyses were performed by a third party specializing in clinical diagnostic radiation measurements (K&S Associates Inc.; Nashville, Tennessee). To measure whole-body absorbed dose in mice, TLD chips were surgically implanted in five locations in a mouse carcass: head, chest, abdomen, above the skin, and under the skin. Measurements were performed on six individual carcasses on two separate occasions (before and during study). The overall uncertainty of the TLD measurement process is 5% at the 95%

confidence interval for a single TLD chip at the measurement location. This uncertainty does not take into account minor variations in the placement of the TLD chips between different mouse carcasses. Consistent dosimetry was confirmed and validated repeatedly throughout the study using a 0.6 cc ionizing chamber (Farmer Dose-meter Model 2570A and PTW Freiburg Model TN30010 Ion Chamber). The calculated mean whole-body dose for a 60-second CT scan at the aforementioned specifications was 19.5±3.6 mGy.

A group of mice were given repeated CT scans twice a week starting at 16 weeks of age to simulate the annual diagnostic CT procedures that may be prescribed to monitor injury or disease status in adult human patients. In order to control for the possible effects of age when assessing the biological differences between single and repeated CT scans, mice were age-matched up until the time of tissue harvest (i.e. 25 weeks old). For the investigation of the effects of repeated CT scans, tissues were harvested five days after the last CT scan time point. This harvesting schedule helped assess the cumulative indirect effects of the repeated CT exposures, instead that of the residual acute effects of the last CT scan. For example, estimates show that reticulocytes have an *in vivo* lifespan of several days *(49, 50)*, and any direct damage from acute radiation exposure is cleared to baseline levels within five days *(26)*.

Acute Radiation Challenge Doses

The effects of *in vivo* and *in vitro* irradiations were investigated. Irradiations performed *in vivo* allow for the investigation of the systems-based biological responses, whereas, *in vitro* irradiations help with understanding cell-specific responses without the influence of systemic factors from the whole animal.

In vivo radiation challenge: Cohorts of mice (Figure 1) were given a whole-body gamma radiation challenge dose of 1 Gy (662 keV - Cs^{137}) at a dose rate of 0.28 Gy per minute. Respective control mice were sham irradiated (i.e. placed in the polycarbonate tubes for an equal amount of time but with no exposure to radiation). All *in vivo* radiation challenges were performed with the same customized polycarbonate tubes used for the CT scans.

In vitro radiation challenge: Bone marrow harvested from euthanized mice (Figure 1) were separated into three aliquots (1×10^6 cells/mL) for *in vitro* γ-radiation challenge of either 0, 1, or 2 Gy at a dose rate of 0.17 Gy per minute (662keV - Cs^{137}). All samples were kept on ice-water slurry (0^oC) during the *in vitro* radiation challenges.

Sample Collection and Cell Preparation

Blood

Mice were anaesthetised using Isofluorane™ and blood was collected at 43 h after *in vivo* radiation challenge via cardiac puncture according to previously published protocols *(26)*. Approximately 50 µL of blood was collected in 1.5 mL microcentrifuge tubes (VWR International, Mississauga, Ontario) containing 350 µL heparin solution (VWR International, Mississauga, Ontario). The heparinised blood was maintained at room temperature before being fixed (within 4 hours). Following blood collection, the mice were euthanized by cervical dislocation.

Bone Marrow

Bone marrow samples were collected by flushing both femurs with a 23 gauge needle containing 1 mL of heparinised RPMI 1640 media (Lonza Inc., Allendale, New Jersey). The disaggregated bone marrow cell suspension was transferred to a1.5 mL microcentrifuge tube (VWR International, Mississauga, Ontario) and then held at 0^{o}C in ice-water slurry until processing (within 1 hour). Bone marrow cells were counted using the Z2 Coulter Particle Count & Size Analyzer (Beckman-Coulter, Miami, Florida). The cell sample was adjusted to a final concentration of $1x10^{6}$ cells/mL in ice-cold RPMI 1640 supplemented with 10% fetal bovine serum (FBS, PAA Laboratories Inc., Etobicoke, Ontario), 1% penicillin-streptomycin (Lonza Inc., Allendale, New Jersey), 1% L-glutamine (Lonza Inc., Allendale, New Jersey). Three 1.5 mL replicate aliquots of the cell sample suspension were made for *in vitro* irradiations at 0, 1, and 2 Gy.

Micronucleated Reticulocyte Assay

Reagents

The reagents used for preparing blood specimens for flow cytometric analysis were from a commercially available kit, Mouse MicroFlowPLUS® (Litron Laboratories, Rochester, NY), and included a heparin-based anticoagulant solution, buffer solution, anti-CD71-FITC, anti-CD61-PE, RNase, and propidium iodide. The kit also provided a flow cytometer calibration standard consisting of fixed *Plasmodium berghei*-infected mouse erythrocytes ("malaria biostandard").

Fixation

Cells were fixed in absolute methanol (CAS no. 67-56-1, Sigma Aldrich, Mississauga, Ontario) at -80^{o}C. Up to six samples were fixed at a time using dry ice. This was done to ensure that the

temperature of the fixative was maintained between -70°C and -80°C. A 180 µL aliquot of diluted blood suspension was forcibly delivered into a 15 mL conical tube (BD Biosciences, Mississauga, Ontario) containing 2 mL of -80°C methanol. The sample tubes were vortexed and struck sharply with a pen-sized plastic tube several times to break up any aggregates. The fixed samples were stored at -80°C for a minimum of 24 hours before staining and flow cytometric analysis.

Staining and flow cytometric analyses

Methanol-fixed blood samples were washed and labelled for flow cytometric analysis according to procedures detailed in the Mouse MicoFlowPLUS Kit manual (vP4.3m) and previously described *(51)*. Briefly, fixed blood cells were washed with 12 mL of kit-supplied buffer solution and the pellets were maintained on ice slurry (0°C) until staining within 4 hours. An 80 uL reagent mixture containing anti-CD71-FITC, anti-CD61-PE, RNase and buffer solution was added to 20 µL aliquot of each fixed blood sample in duplicate. The cells were incubated on ice for 30 minutes followed by 30 minutes at room temperature, and then returned to ice. Immediately before acquisition on the flow cytometer, 1 mL of cold (4°C) propidium iodide (1.25 µg/mL in buffer solution) was added to each tube.

Flow cytometry analysis was performed using a Beckman Coulter EPICS XL flow cytometer (Beckman Coulter, Brea, CA). Cells were analyzed at an average rate of 4000 cells (events) per second. The EPICS XL flow cytometer is equipped with a 488 nm argon laser and four fluorescence detectors. Anti-CD71-FITC, anti-CD61-PE, and propidium iodide fluorescence signals were detected in the FL1 (525±15 nm), FL2 (575±15 nm), and FL3 channels (620±15 nm), respectively. The gating logic used to quantitatively analyse the erythrocyte subpopulations has been previously described *(51)*. Analysis windows were set to quantify the number of reticulocytes (RETs) and MN-RETs for each sample. Representative bivariate graphs illustrating

the resolution of the various erythrocyte populations have been published *(51)*. To ensure adequate sample sizes for statistical significance, the number of RETs was measured in a total of $2x10^5$ erythrocytes. The number of MN-RETs was evaluated based on counting a total of $2x10^4$ total RETs per sample.

γH2AX Fluorescence Assay

Bone marrow cells were adjusted to $1x10^6$ cells/mL, transferred to 15 mL conical tubes (BD Biosciences, Mississauga, Ontario), and irradiated as described above. Following irradiations, 500 µL aliquots were removed from irradiated cell samples and incubated for 30 minutes in a 37^0C water bath. After incubation, 3 mL of 70% ethanol at 0^oC was immediately added to each tube. All sample tubes were maintained on ice-water slurry at 0^oC for 1 hour and stored at -20^oC until analysis.

For analysis, the fixed bone marrow samples were centrifuged at 5^oC (250 g, 8 minutes) and the supernatant was removed. Cells were then washed in 3 mL of Tris-buffered saline (1x TBS; Trizma base + NaCl, Sigma Aldrich, Mississauga, Ontario), centrifuged (250 g, 8 minutes), re-suspended in 1 mL of Tris–saline–triton [TST; TBS + 4% FBS (VWR International, Mississauga, Ontario) + 0.1% Triton X-100 (Sigma Aldrich, Mississauga, Ontario)] and incubated on ice for 10 minutes to permeabilize cells. The cells were again centrifuged (250 g, 8 minutes), the supernatant removed, and cells were re-suspended in 200 µL of a 1:400 dilution of anti-phospho-H2A.X (ser139) antibody (γH2AX; Upstate Cell Signaling, Charlottesville, VA).

Samples containing the primary antibody were incubated on a tube rocker at room temperature for 2 hours in the dark. The cells were then washed with 3 mL of TST, re-suspended in 200 µL of

a 1:500 dilution of AlexaFluor™ 488-conjugated goat anti-rabbit IgG F(ab')2 antibody (Invitrogen Canada, Burlington, Ontario) and incubated at room temperature for 1 hour in the dark. The cells were then washed in 3 mL of TBS and re-suspended in 300 µL TBS + 5 µL propidium iodide (1 mg/mL; Sigma Aldrich). Samples were put on ice and promptly analysed on the Epics XL flow cytometer (Beckman Coulter; Brea, CA). Analysis was based on $5x10^3$ cells from the lymphocyte-rich cell population, as determined by flow cytometric scattering patterns. The level of γH2AX fluorescence was measured by examining the mean fluorescence intensity of cells stained with the AlexaFluor™ 488-conjugated goat anti-rabbit IgG F(ab')2 antibody (Invitrogen Canada, Burlington, Ontario). Each sample was analyzed in duplicate.

Apoptosis Assay

Apoptotic cell death measurements were performed using the Carboxyfluoresein Fluorochrome Inhibitors of Caspases (FLICA) 3, 7 Apoptosis detection kit according to the manufacturer's protocols (Immunochemistry Technologies, LLC, Bloomington, MN). FLICA specific for caspases 3 and 7 (FAM-Asp(OMe)-Glu(OMe)-Val-Asp(OMe)-fluoromethylketone) binds covalently to activated caspase sites, thus allowing the fluorochrome to accumulate in caspase-driven apoptotic cells. Briefly, 10 µL of 30x FLICA solution was added to 300 µL aliquots of irradiated mouse bone marrow cell suspension at a concentration of $1x10^6$ cells/mL. The stained cells in 12x75 mm polypropylene tubes (Sarstedt, Montreal, Quebec) were incubated for 6 hours at 37^oC in 5% CO_2. Aliquots were gently re-suspended every 60 minutes to ensure adequate cellular staining. Cells were washed twice with 2 mL of 1x wash buffer (supplied), and maintained on ice until analysed (within 1 h) on the Epics XL flow cytometer (Beckman Coulter; Brea, CA). Cells identified as dying by apoptosis were defined as FLICA+. The percentage of cells dying by apoptosis was determined from analysis of $5x10^4$ cells.

Statistics

Statistics were performed using Statistical Package for the Social Sciences version 16.0 (Chicago, Illinois). Data is presented as mean ± standard error of the mean with $p \leq 0.05$ considered statistically significant. Dose response significance testing was performed with linear regression or Spearman rank order correlation where appropriate. Student's t-tests were carried out to determine if significant differences existed between groups for micronucleated reticulocyte data. Two-way ANOVA with Bonferroni's post-hoc test was used to determine significance between groups for γH2AX fluorescence levels and apoptosis data.

RESULTS

Biological Effects of Single CT Scans

Induction of Micronucleated Reticulocyte Formation following CT Scans

The induction of MN-RET formation in mouse peripheral blood was assessed following whole-body CT scans of varying doses (20, 40, 60, and 80 mGy). Only three mice per group were needed in order to achieve statistically significant dose separation, because of the high reproducibility and consistency of the MN-RET assay. Inter-day MN-RET levels in unirradiated age-matched control mice were highly stable and minimal variability was observed between mice (data not shown). There was a statistically significant linear dose response for the induction of MN-RETs following exposure to CT scans ($p<0.033$, $R^2=0.9838$) (Figure 2). Significant increases in MN-RET frequencies were detectable for CT scan doses as low as 20 mGy, relative to sham CT scanned mice ($p=0.020$).

CT Scan-Induced Adaptive Response in Micronucleated Reticulocyte Formation

The kinetics of the adaptive response was determined through varying the delay between the priming (CT) and challenge (gamma) doses (Figure 3). A single CT scan increased the MN-RET frequency by 28% above unirradiated sham levels ($p=0.020$), while the un-primed 1 Gy challenge irradiation increased the MN-RET frequency by approximately sevenfold. An adaptive response was observed only with a six hour delay between the priming CT scan and challenge dose ($p=0.039$), as the MN-RET frequency decreased 19% compared to the un-primed 1 Gy challenge dose.

Cellular γH2AX fluorescence levels following a single 20 mGy CT scan

The fluorescence levels of labelled γH2AX in lymphocyte-rich bone marrow cell populations were assessed following a 1 Gy *in vitro* challenge dose given six hours after a priming 20 mGy CT scan (Figure 4). A single CT scan did not change the mean cellular γH2AX levels, relative to the unirradiated sham levels ($p=0.678$). Following a 1 Gy *in vitro* challenge dose, there was no difference in the γH2AX fluorescence levels for sham CT scanned mice and CT scanned mice ($p=0.547$). However, after a larger 2 Gy challenge dose, the γH2AX fluorescence levels were significantly higher in the CT scanned mice than the sham CT scanned mice ($p=0.037$). Both mouse groups demonstrated a significant dose-dependent increase in cellular γH2AX fluorescence levels following *in vitro* challenge doses up to 2 Gy ($p<0.025$).

Apoptosis following a single 20 mGy CT scan

Six hours after a single 20 mGy CT scan, apoptosis levels in the bone marrow cells of CT scanned mice were 8% higher than those in the sham CT scanned mice ($p=0.020$) (Figure 5). This elevated apoptosis level in CT scanned mice persisted following *in vitro* challenge doses of 1 and 2 Gy

($p<0.009$). There was a statistically significant correlation between apoptosis levels and *in vitro* challenge doses for both sham CT scanned mice and CT scanned mice ($p<0.05$); however, the magnitude of the apoptotic processes appeared to plateau after 1 Gy.

Biological Effects of Repeated 20 mGy CT scans

Induction of MN-RET formation following repeated 20 mGy CT scans

The mean percentages of peripheral blood MN-RETs following 10 weeks of repeated CT scans are shown in Figure 6. The MN-RET levels in mice that received repeated CT scans (0.36±0.02%) were slightly reduced, as compared to the sham CT scanned mice (0.41±0.01%) ($p=0.040$). After a 1 Gy *in vivo* challenge dose, there was no significant difference in MN-RET frequencies between repeated CT scanned mice and sham CT scanned mice ($p=0.337$). For both sham and repeated CT scanned mouse groups, the 1 Gy *in vivo* challenge dose produced a sevenfold increase in MN-RET frequencies, relative to the un-challenged mouse groups ($p<0.001$) (Figure 6).

Cellular fluorescence of γH2AX following repeated 20 mGy CT scans

Mean fluorescence levels of labelled γH2AX in lymphocyte-rich bone marrow cell populations were not different between mice CT scanned for 10 weeks and the corresponding sham CT scanned mice ($p=0.30$). However, following *in vitro* challenges of 1 and 2 Gy, mice that received repeated CT scans had approximately 10% lower γH2AX fluorescence levels than that of sham CT scanned mice ($p=0.017$ and $p=0.026$, respectively). There was a significant dose-dependent increase in mean cellular γH2AX fluorescence following the *in vitro* challenge doses for both sham CT scanned mice and repeated CT scanned mice ($p<0.001$) (Figure 7).

Apoptosis following repeated 20 mGy CT scans

Apoptosis levels in bone marrow cell populations of mice given repeated CT scans for 10 weeks were approximately 5% lower compared to sham CT scanned mice at baseline and following a 2 Gy challenge dose ($p<0.010$ and $p=0.034$, respectively). There was no significant difference in apoptosis levels between the two groups of mice following an *in vitro* 1 Gy challenge dose ($p=0.20$). Apoptosis levels increased proportionally to the level of *in vitro* challenge doses for the sham CT scanned mice ($p<0.05$). However, the same correlation was not observed for the repeated CT scanned mice beyond a dose of 1 Gy, as assessed by Spearman's rank order correlation ($p>0.05$) (Figure 8).

DISCUSSION

Research on biological responses to ionizing radiation from diagnostic CT procedures is important; CT scans are becoming increasingly popular and their effects on cells and organisms are of interest. Considering that CT scans contribute up to 67% *(3, 6)* of the dose to the patient population and 14% of the total annual dose to the general population *(52)*, there are good reasons to better understand the biological effects of these diagnostic procedures. The research presented here demonstrated that low doses of single and multiple CT scans can produce significant biological consequences in the hematopoietic system.

Biological Effects of a Single CT scan

Studies assessing cytogenetic effects of X-ray radiation from single CT scans have shown enhanced chromosome aberrations in human lymphocytes *(53-57)*. Cytogenetic events such as increased acentric and dicentric chromosomes, chromosomal fragmentation, chromosomal

translocations, and γH2AX foci formation have been associated with CT radiation *(52-59)*. This study was intended to supplement these findings by examining the genotoxic and cytotoxic effects of single 20 mGy CT scans.

Micronuclei formation has been shown to be a reliable measure of unstable chromosomal aberrations, resulting from ionizing radiation exposures *(26, 60-64)*. In most studies, chromosomal aberrations are observed directly in the treated cells. In this study a flow cytometry-based MN-RET assay was used to measure damage manifested in hematopoietic precursor cells. This provided insight into the processing of upstream damage *(26, 50)*. In this study, a significant linear correlation between MN-RET formation in peripheral blood and CT scan doses as low as 20 mGy was observed (Figure 2). Previous studies investigating both microscopy-based and flow cytometry-based MN-RET formation following acute x-ray and γ-radiation exposures have reported linear dose responses up to 1 Gy *(26, 64)*. However, this is the first report in which a dose less than 50 mGy has been measured using the flow cytometry-based MN-RET assay. The increase in MN-RET formation following a single acute exposure to a 20 mGy CT scan indicates that CT scans can induce change to the division of the hematopoietic system responsible for reticulocyte production and, essentially, erythropoiesis.

A number of studies have investigated the effects of CT scan-induced chromosomal aberrations in human peripheral blood lymphocytes. Stephan *et al.* showed that CT scans (12.9 mGy) in children can significantly elevate the frequencies of dicentrics and excess acentric fragments *(56)*. Similarly, Jost *et al.* reported significant increase in dicentric chromosomes in human lymphocytes exposed *in vitro* to a 20 mGy CT scan *(53, 55)*. If some of these damaged cells escape apoptosis and proceed with cell division, the consequence may be an elevated population of micronucleated cells. Hottayoglu *et al.* demonstrated that measurements of

dicentrics and micronuclei in hematopoietic cells are comparable assessments of radiation-induced genotoxicity *(63)*. In this study, the observed increase in MN-RET frequencies following an *in vivo* single 20 mGy CT scan supports previous documented effects.

When a single 20 mGy CT scan was given six hours before a 1 Gy challenge dose, the MN-RET levels in the CT scanned mice were significantly decreased, relative to sham CT scanned mice challenged with 1 Gy. This response has been described as an adaptive response. However, when mice were CT scanned at 4 hours or 12 hours prior to a 1 Gy challenge dose, there was no apparent adaptive response with this MN-RET endpoint. The adaptive response observed when a CT scan was given six hours prior to a 1 Gy challenge dose may be due to enhanced CT-induced cell killing of prospective micronucleated cells. The increased apoptosis levels detected in bone marrow cells six hours after a single 20 mGy CT scan support this hypothesis (Figure 5). Another explanation for this time-specific adaptive response induction may be cell cycle delay caused by the priming single CT scan. Priming doses as low as 20 mGy have been shown to cause transient cell cycle delay and alter the distribution of cells within the cell cycle *(65-68)*. Sorensen *et al*. found that adaptive responses were highly dependent on the cell cycle stage at the time of challenge irradiation *(44)*.

Using fluorescence microscopy analysis of γH2AX foci formation as a quantitative biomarker for radiation-induced DNA damage in human peripheral blood mononuclear cells, Rothkamm *et al.* reported an 8-10 fold increase following a whole-body *in vivo* CT scan dose of 16.4 mGy (95% confidence level: 15.1, 17.7) *(52)*. Grudzenski *et al.* demonstrated increased γH2AX foci formation in both *in vivo* and *in vitro* CT scans (<20 mGy) *(57)*. Golfier *et al.* reported increases of γH2AX foci formation in human lymphocytes following *in vitro* CT irradiation, with doses as

low as 25 mGy *(53)*. Furthermore, Lobrich *et al.* reported significant increases of γH2AX foci formation in both lymphocytes and fibroblasts after an *in vivo* CT scan (~20 mGy) *(69)*.

In this study, mean cellular γH2AX fluorescence was measured using flow cytometry instead of the standard microscopy-based γH2AX foci formation assay. Pilot projects and previous works demonstrated that the flow cytometry-based γH2AX assay was effective in detecting adaptive responses *(48, 70)*. Although there is a strong correlation between the microscopy-based and flow cytometry-based γH2AX assays *(71-75)*, their detection limits for ionizing radiation exposure may differ. Microscopy-based γH2AX analysis can detect doses less than 5 mGy *(76)*, whereas the minimum reported dose detection limit for flow cytometry-based γH2AX analysis is 100-200 mGy *(72, 73, 77, 78)*. In this study, the reason for the lack of a difference in cellular γH2AX fluorescence levels of sham CT scanned mice and mice that received a single 20 mGy CT scan ($p=0.678$) may be either the kinetics of γH2AX foci induction/disappearance at the sampling time, or the detection limit of the flow cytometry-based γH2AX assay. Phosphorylation of histone protein H2AX is an early response to DNA DSBs. As DNA damage gets repaired, the level of γH2AX foci decreases. Since maximal γH2AX foci induction occurs around 30 minutes following radiation exposure, in this study the six hour wait period following CT scans possibly allowed the initial effects of the CT scan to disappear *(31, 72)*. The six-hour time point was chosen because this time interval between the priming CT scan and the challenge dose was able to induce an adaptive response, albeit with MN-RET formation.

Following a 1 Gy *in vitro* challenge dose, there was no adaptive response observed with respect to mean cellular γH2AX fluorescence levels, in mice that received a single CT scan six hours prior. However, the CT scanned mice showed elevated γH2AX fluorescence levels following a larger 2 Gy challenge dose, relative to the sham CT scanned mice ($p=0.037$). It is possible that the single

20 mGy CT treatment sensitized the bone marrow cell populations, but only the 2 Gy challenge dose was large enough to show this sensitization effect in this endpoint. The biological mechanism(s) of this possible sensitization effect are still unknown, but may involve cell cycle delay. Cramers *et al.* examined γH2AX foci formation in human lymphocytes and suggested that low priming doses can induce perturbations in cell cycle that may affect adaptive responses *(79)*. This study proposes that the 20 mGy CT scan given six hours before the 2 Gy challenge dose caused perturbations in cell cycle kinetics that made lymphocyte-rich bone marrow cells more sensitive to damage from the high-dose challenge, as measured by γH2AX fluorescence levels.

Apoptosis was investigated in the heterogeneous bone marrow cell populations. A single 20 mGy CT scan increased spontaneous levels of apoptosis, and enhanced the cytotoxicity of both 1 and 2 Gy challenge doses. This heightened sensitivity to radiation-induced apoptosis parallels the sensitization effect observed in CT scanned mice with the γH2AX endpoint following a 2 Gy *in vitro* challenge dose. These paralleling sensitization observations could be related. In support of this hypothesis, Lu *et al.* demonstrated that UV radiation-induced γH2AX is required for apoptotic DNA ladder formation *(80)*. Also, the formation of γH2AX was found to be an important step in initiating apoptosis via the Caspase-3/Caspase-activated DNase pathway *(80)*.

Apoptosis is a protective mechanism by which unstable or damaged cells remove themselves from the population *(37)*. Ionizing radiation causes oxidative stress *(81)*, and higher levels of reactive oxygen species have been correlated with increased programmed cell death responses *(82)*. The enhanced apoptosis levels observed in this study following a single acute 20 mGy CT scan support the postulation that radiation from CT scans may trigger apoptosis in a portion of unstable cells, thus potentially changing the overall risk to those cells. Portess *et al*. support this by demonstrating that low-LET radiation (2 mGy) can trigger selective removal of pre-cancerous

(src pre-transformed) cells *(83)*. Also, Belloni *et al*. found that there was a direct relationship between dicentric chromosomes and the triggering of apoptosis following X-ray exposure to human peripheral blood lymphocytes *(84)*.

Apoptosis levels in mouse bone marrow following an *in vivo* 20 mGy CT scan without an *in vitro* challenge dose were higher than levels in sham CT scanned mice following a 1 Gy *in vitro* challenge dose (Figure 5). This observation may be a result of differing kinetics associated with *in vivo* versus in *vitro* irradiations and the timing of when apoptosis analyses were performed. There was a 12 hour period between the time of the *in vivo* single CT scan and the time of apoptosis measurement (i.e. 6 hours between CT scan and *in vitro* radiation challenge dose, plus 6 hours of bone marrow incubation time with caspase markers). In the sham CT scanned mouse group, the radiation-induced apoptosis resulting from the 1 Gy *in vitro* challenge dose only had six hours (bone marrow incubation) to manifest. Thus, the higher apoptosis levels in the former case may be due to when apoptosis was measured, with respect to the two radiation exposures (*in vivo* CT scan and *in vitro* radiation challenge). Further experiments are required to support this postulate. Relatedly, the relatively high spontaneous apoptosis level seen in the sham CT mouse group (24.6%) is likely due to the cellular stress caused by the extraction and six hour *in vitro* incubation of the bone marrow samples, and not a real reflection of *in vivo* basal apoptosis. The significance of this study's apoptosis results is not the absolute apoptosis levels but the demonstration of relative differences in the apoptotic responses following the *in vivo* single CT scans and *in vitro* radiation challenge doses.

Biological Effects of Repeated CT scans

Using a flow cytometry-based micronucleated reticulocyte (MN-RET) assay, this study demonstrated that 10 weeks of repeated 20 mGy CT irradiations (total accumulated dose of 400 mGy) produced a slight reduction in spontaneous MN-RET levels as compared to non-CT scanned mice ($p=0.040$). Further experiments are required to confirm this finding, as this reduction in MN-RET levels was observed only after the data pooling of the second of two independent repeat experiments. Nonetheless, repeated CT scans did not increase spontaneous MN-RET levels.

Reticulocytes are progenies of erythroblasts, which are hematopoietic bone marrow stem cells. A lack of increase in MN-RET levels may indicate that the erythroblast stem cells did not become genomically unstable by the repeated CT irradiations. Using the same flow cytometry-based assay and mouse strain as this study, Hamasaki *et al.* found that one year after an acute *in vivo* 2.5 Gy X-ray dose, spontaneous MN-RET levels in irradiated mice remained significantly higher than the unirradiated controls. Hamasaki *et al*. purported that the higher MN-RET level is evidence of radiation-induced genomic instability caused by the high-dose exposure *(50)*. The lack of elevated spontaneous MN-RET levels following repeated CT scans, when compared to Hamasaki *et al. (50)*, is likely a consequence of the lower total dose (400 mGy vs. 2.5 Gy) and the fractionation of that dose. Moreover, if the observed reduction in spontaneous MN-RET frequencies in the repeated CT scanned mice is real, this may indicate that the population of erythroblasts in these mice may be more stable, and that their clonal expansion and differentiation processes may be improved. However, a similar reduction was not evident in mice treated with repeated CT scans following an *in vivo* 1 Gy challenge ($p=0.337$). The latter result could be because the 1 Gy challenge was too damaging to the erythroblast population,

thus prohibiting the observation of an adaptive response for this particular endpoint, which saturates around 1 Gy *(26)*. Another reason for the lack of an adaptive response may be simply due to the specific kinetics of the adaptive response *(85, 86)*.

It is generally accepted that almost every DNA DSB forms a γH2AX focus. Contention arises, however, when determining if every γH2AX focus represents a DNA DSB *(33, 76, 87)*. Quantitatively, Rothkamm *et al.* demonstrated that detection of γH2AX foci has a strong correlation with DNA DSBs *(76)*. Assuming that cellular γH2AX fluorescence levels correlate well with DNA damage, the fact that there were no significant differences in spontaneous γH2AX fluorescence levels between mice treated with repeated CT scans and sham CT scanned mice may indicate that repeated CT scans did not cause persistent DNA damage. The fact that the dose detection limit of the flow cytometry-based γH2AX assay is relatively insensitive should be considered when interpreting these results *(72, 73, 77, 78)*.

Despite the relatively high dose detection limit for the flow cytometry-based γH2AX assay, an adaptive response was observed in bone marrow cells of repeated CT scanned mice following *in vitro* challenge doses of 1 and 2 Gy (Figure 7). The recurring mild oxidative stress resulting from the repeated CT X-ray treatments may have triggered an adaptive response similar to that reported in a recent study published by Ermakov *et al.*, where oxidative stress was found to be critical for the induction of an adaptive response in human lymphocytes *(81)*.

Similar to the reduction seen with MN-RET formation and cellular γH2AX fluorescence levels, repeated CT treatments significantly lowered spontaneous and radiation-challenged apoptosis levels ($p<0.05$) (Figure 8). The biological mechanism for the observed decreased apoptosis levels is unknown. However, the frequent mild oxidative stress produced by repeated CT scans may have caused an initial elimination of unstable cells, as suggested by the increased apoptosis

results from single CT scans (Figure 5). This increased removal of unstable cells, triggered by the initial CT scan(s), would result in cell populations with fewer chromosomal aberrations and reduced DNA damages. Results of the MN-RET and γH2AX endpoints in mice given repeated CT scans support this postulation. Through a selection process over time, there may be a shift to a homeostatic state wherein the observed lower apoptosis levels reflect a more robust cell population.

The Biological Relationships between Single and Repeated CT scans

Low-dose ionizing radiation from CT scans causes oxidative stress via production of damaging reactive oxygen species. Reactive oxygen species can cause damage to DNA by modification of bases, inter-carbon ruptures in deoxyribose, the appearance of apurinic and aprymidinic sites, single- and double-stranded breaks, DNA-protein cross-links, etc. *(37)*. Damaged cells can attempt to repair or undergo apoptosis if the damage is substantial. A single CT scan will increase DNA damage as demonstrated by increased MN-RET formation (Figure 2), γH2AX foci, and chromosomal aberrations *(52, 53, 55, 56, 59)*. CT radiation-induced oxidative stress will initially cause an increase in apoptosis levels as damaged and/or radiosensitive cells die (supported by the single CT apoptosis results - Figure 5). Ermakov *et al.* suggested that as cells undergo apoptosis, DNA fragments are released into the intercellular space and interact with DNA-binding receptors such as toll-like receptor 9 (TLR9) of neighbouring cells. This interaction activates cellular signalling pathways associated with synthesis of more reactive oxygen species, thus inducing a crucial oxidative stress cascade required in the adaptive response. Repeated CT irradiations would likely continue to increase oxidative stress levels and trigger more unstable/radiosensitive cells to undergo apoptosis. Eventually, most of the unstable or damaged

cells are eliminated, and the remaining cells are more robust and may have fewer chromosomal aberrations. The latter was demonstrated in this study by the slight reduction in MN-RETs and the induction of an adaptive response with respect to mean cellular γH2AX fluorescence levels in mice treated with repeated CT scans. With potentially fewer unstable chromosomal aberrations that would likely trigger apoptosis, the overall effect is lowered apoptosis levels (Figure 8). Results from repeated CT scans support the notion that frequent mild levels of oxidative stress allow for the maintenance of a healthy cell population by fostering the death of unstable and damaged cells.

Summary

The biological effects of single versus repeated CT scans are opposite to but not necessarily unrelated to each other. Many recent research studies have examined only the biological effects following acute single CT scans. This study complements previous works surrounding the biological responses from single CT scan exposures by providing further insight into the biological effects of multiple CT scans. In summary, repeated 20 mGy CT scans do not appear to induce genomic instability in reticulocytes, and confer resistance to larger doses in the bone marrow of mice. Conversely, exposures to single CT scans exhibit transient genotoxicity, enhanced apoptosis, and characteristics of radiation sensitization.

CONFLICT OF INTERESTS

The authors have no conflict of interests to declare.

ACKNOWLEDGEMENTS

Many thanks are deserved by Mary Ellen Cybulski for her technical animal experience; Lisa Laframboise for her dedicated laboratory proficiency; Nicole McFarlane for her expertise and guidance with flow cytometry; Chantal Saab and Rod Rhem for their contribution toward the computed tomography aspects of the study. This research was supported by US Department of Energy, Low Dose Research Program (DE-FG02-07ER64343), Natural Sciences and Engineering Research Council of Canada, CIHR Vanier Post-graduate Scholarship, and CIHR CGS graduate scholarship.

TABLE 1

Experimental groups for the investigation of the biological effects of CT scans.

Experiment 1: CT Scan Dose Response for the Induction of MN-RETs [a]

Treatment	*Specifications*
Sham for Single CT Scan	n= 5*, 25 weeks old
Single 20 mGy CT Scan	n=4**, 25 weeks old
Single 40 mGy CT Scan	n=3, 25 weeks old
Single 60 mGy CT Scan	n=3, 25 weeks old
Single 80 mGy CT Scan	n=3, 25 weeks old

Experiment 2: CT Scan-induced Adaptive Response: MN-RETs [a]

Treatment	*Specifications*
Sham for Single CT Scan	n= 5*, 25 weeks old
Single 20 mGy CT Scan	n=4**, 25 weeks old
1 Gy γ-rays	n=4, 25 weeks old
Single 20 mGy CT Scan + 4 h + 1 Gy γ-rays	n=3, 25 weeks old
Single 20 mGy CT Scan + 6 h + 1 Gy γ-rays	n=3, 25 weeks old
Single 20 mGy CT Scan + 12 h + 1 Gy γ-rays	n=3, 25 weeks old

Experiment 3: Biological Effects of Single and Repeated CT Scans [b]

Treatment	*Specifications*
Sham CT Scan [c]	n = 9, 25 weeks old
Single 20 mGy CT Scan	n = 8, 25 weeks old
Repeat Sham CT Scans [c,d]	twice/week/10weeks (Tues, Thurs) n = 24, starting at 16 weeks old
Repeat 20 mGy CT Scans [d]	twice/week/10weeks (Tues, Thurs) n = 24, starting at 16 weeks old

[a] Experiments were performed on the same day.
* and ** denotes the same mouse groups.

[b] Biological endpoints assessed were MN-RET formation, cellular γH2AX fluorescence, and apoptosis.

[c] Some of the mice from the sham groups were also included in the sham groups for a study performed concurrently by De Lisio *et al*. *(48)*.

[d] Two independent repeat experiments; data was pooled.

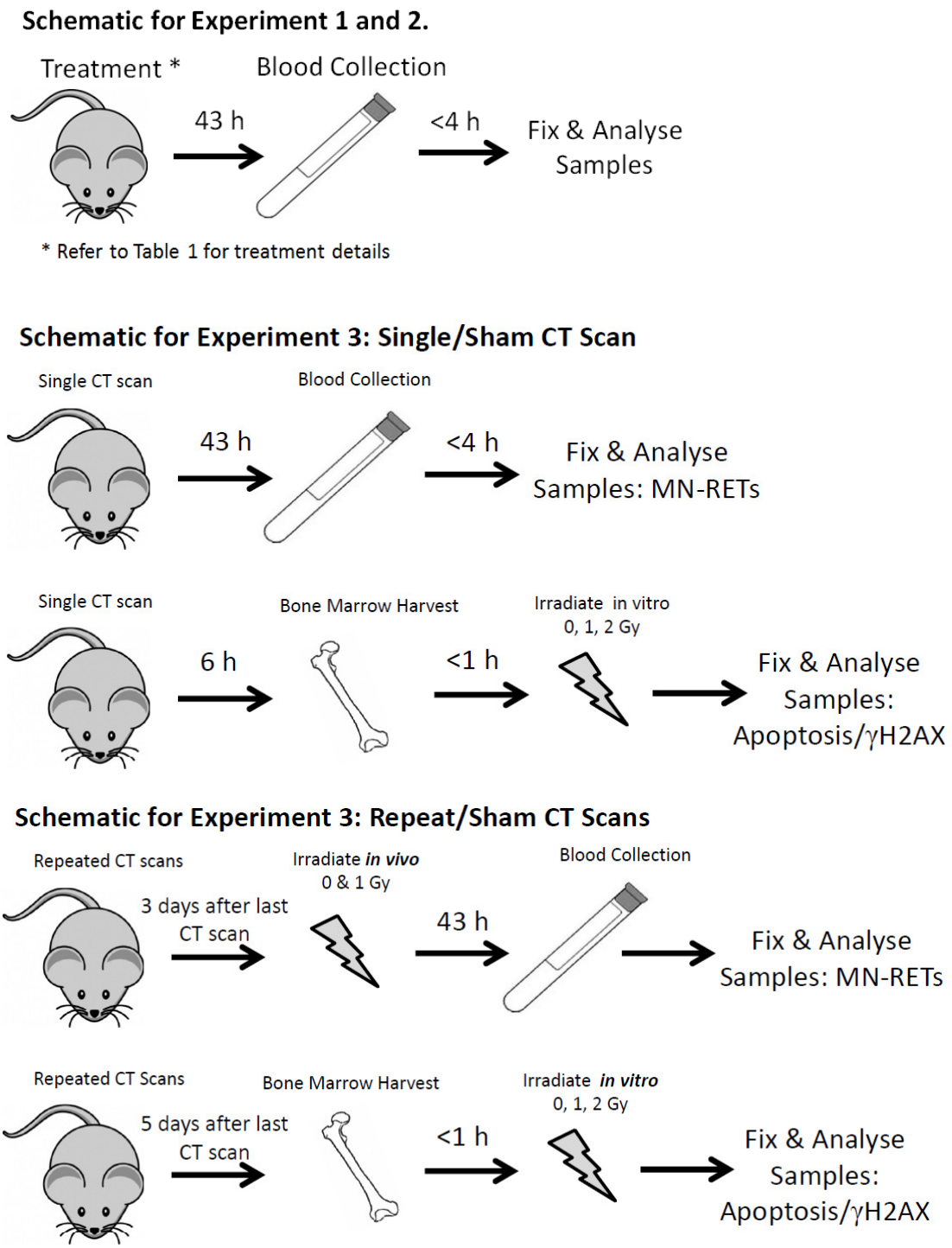

FIG. 1. Schematic of the experimental treatments and collection of tissues for the investigation of Experiment 1) Induction of MN-RET following CT Scans of varying doses; Experiment 2) CT scan-induced adaptive response of MN-RET formation; Experiment 3) Genotoxic and cytotoxic effects of single and repeated CT scans, as measured by MN-RET formation, cellular γH2AX fluorescence, and apoptosis.

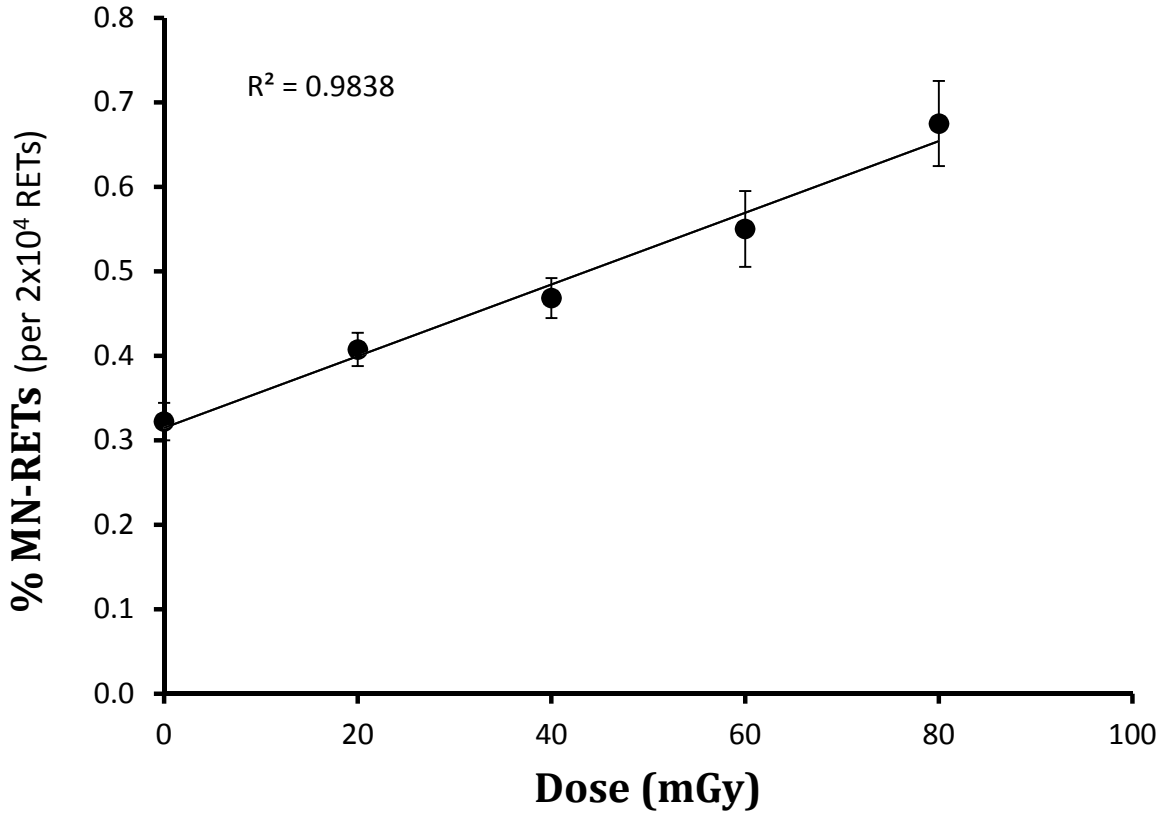

FIG. 2. The induction of MN-RET formation following *in vivo* single CT scans of varying doses; n≥3 mice per dose. Results are sample mean values. Error bars represent standard error of the mean (samples analysed in duplicate).

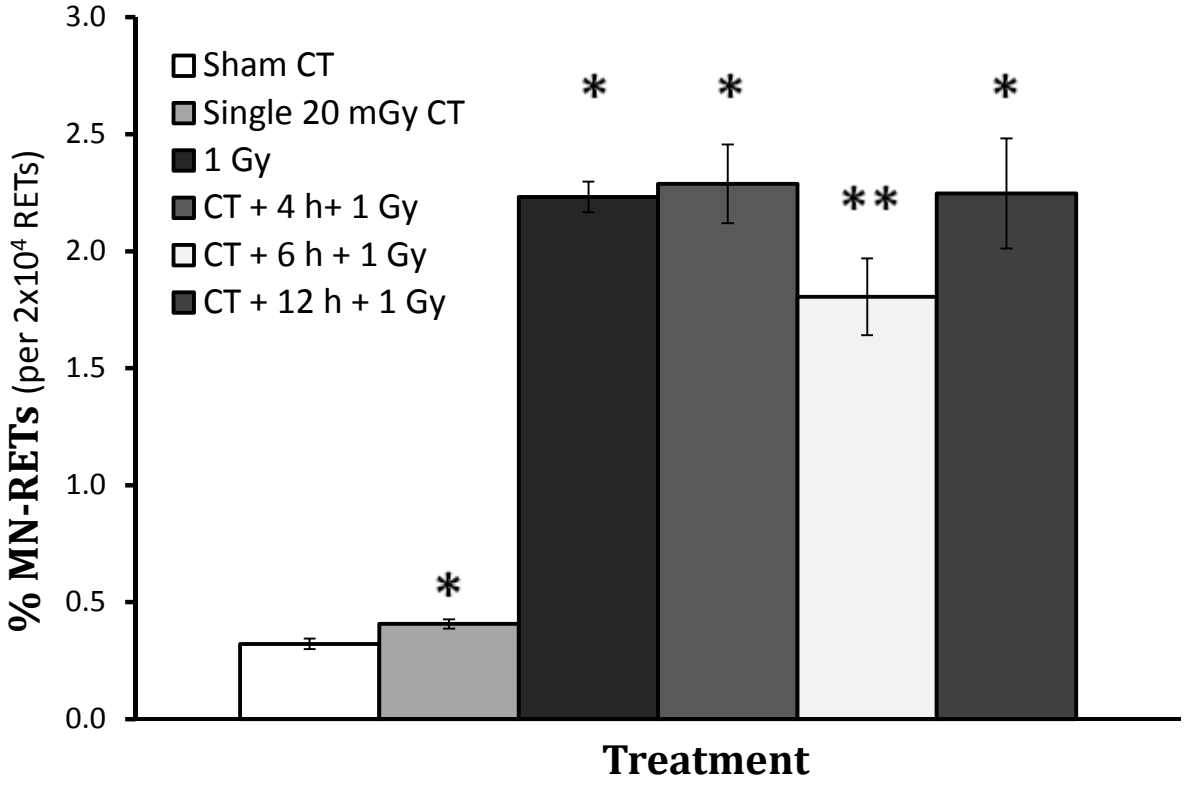

FIG. 3. Adaptive response kinetics for the induction of MN-RET formation for specific time intervals between a priming 20 mGy CT scan and *in vivo* γ-radiation challenge dose (1 Gy); n≥3 mice per treatment. Results are sample mean values. Error bars represent standard error of the mean (samples analysed in duplicate). * denotes $p<0.05$ compared to the controls; ** denotes $p<0.05$ compared to 1 Gy Gamma group.

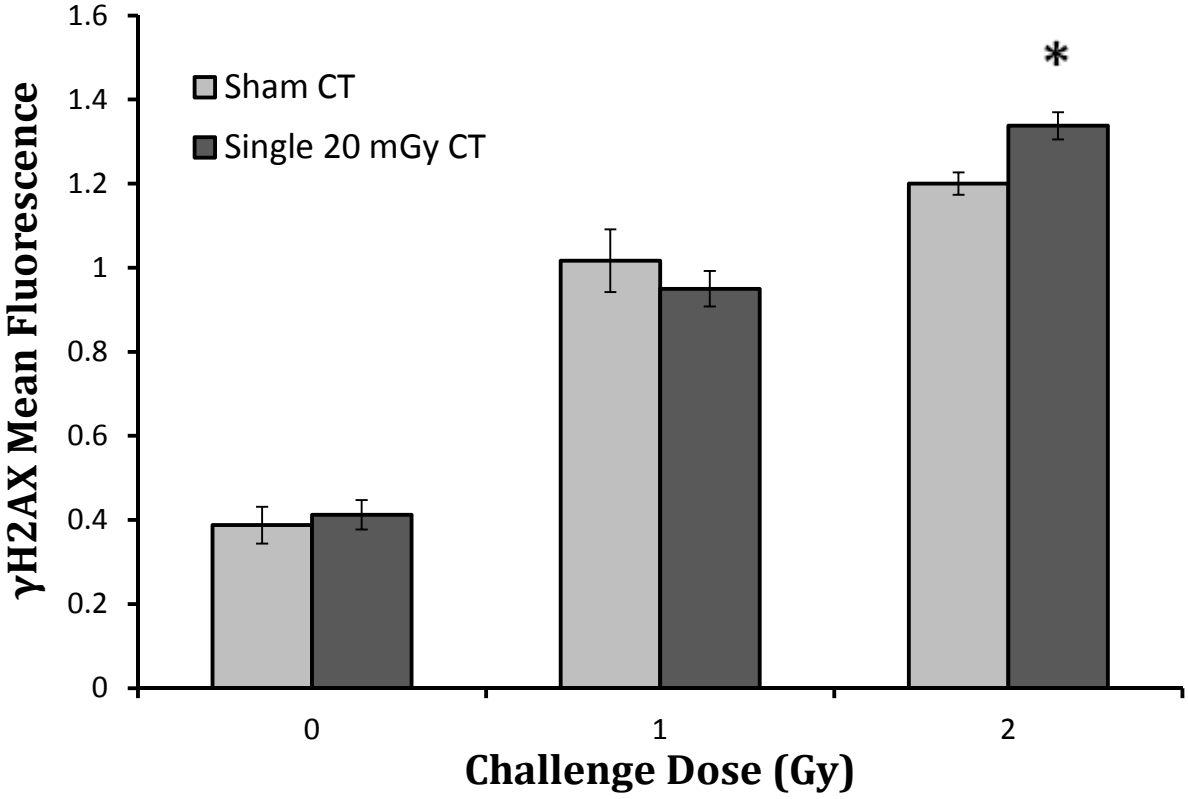

FIG. 4. Mean cellular fluorescence of labelled γH2AX in lymphocyte-rich populations of bone marrow cells after *in vitro* γ-radiation challenge doses of 0, 1 and 2 Gy, six hours following a single 20 mGy CT scan; Sham CT: n=4; Single 20 mGy CT: n=4. Results are sample mean values. Error bars represent standard error of the mean (samples analysed in duplicate). * denotes $p<0.05$ compared to Sham CT following a 2 Gy challenge dose.

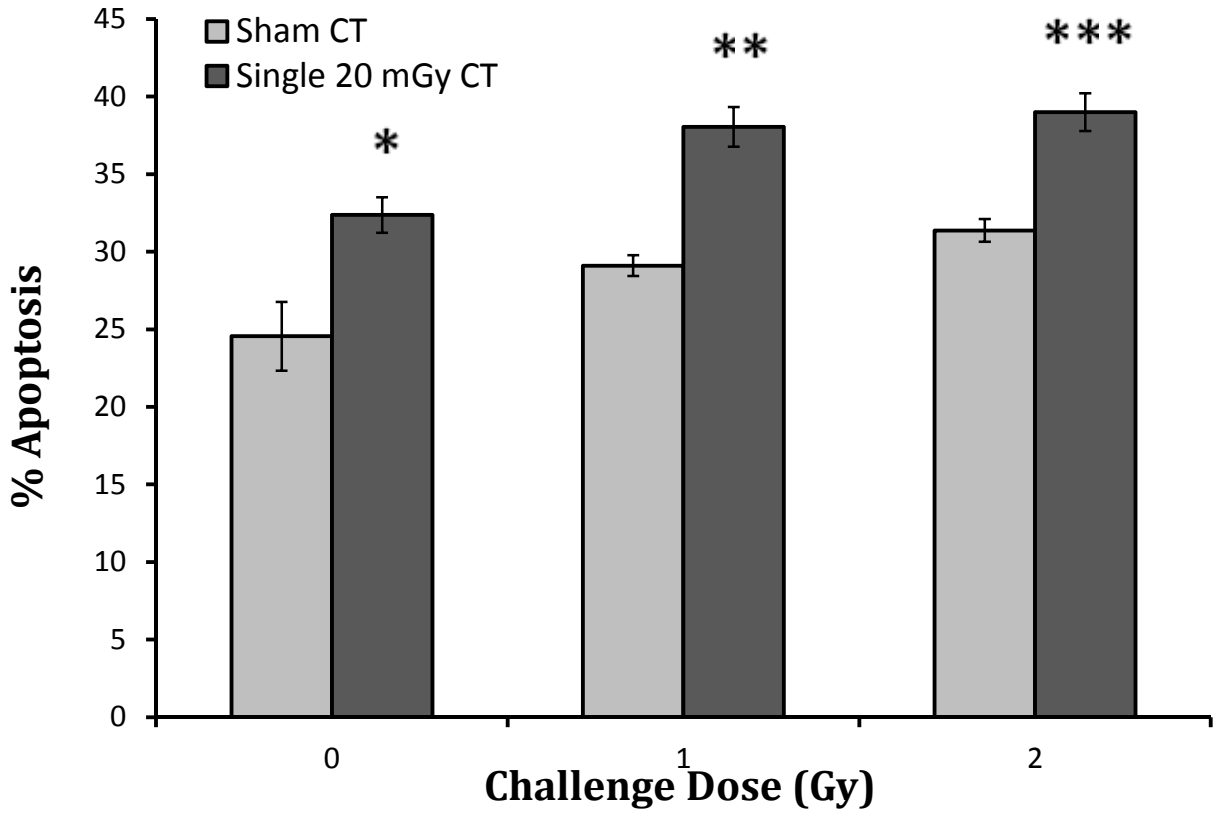

FIG. 5. Apoptosis (caspases 3, 7+) levels in bone marrow cell populations after *in vitro* γ-radiation challenge doses of 0, 1, and 2 Gy, six hours following a single 20 mGy CT scan; Sham CT: n=4; Single 20 mGy CT: n=4. Results are sample mean values. Error bars represent standard error of the mean (samples analysed in duplicate). *, **, *** denote $p<0.05$ compared to Sham CT following 0, 1 and 2 Gy challenge doses, respectively.

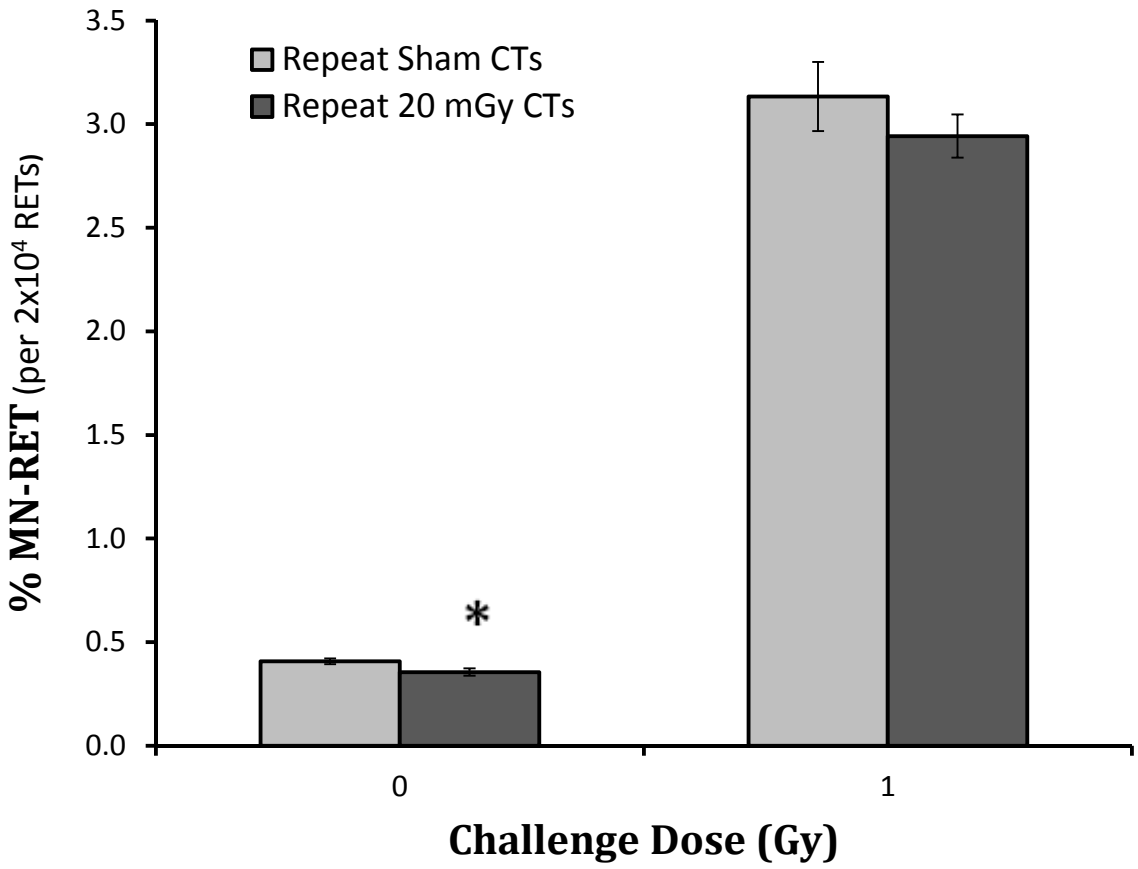

FIG. 6. Comparison of MN-RET percentages in mice treated with 10 weeks of repeated CT scans and the corresponding sham CT mice; Repeat Sham CTs: n=8; Repeat 20 mGy CTs: n=8. Results are pooled sample mean values from two independent experiments. Error bars represent standard error of the mean (samples analysed in duplicate). * denotes $p<0.05$ compared to Repeat Sham CTs at baseline (0 Gy).

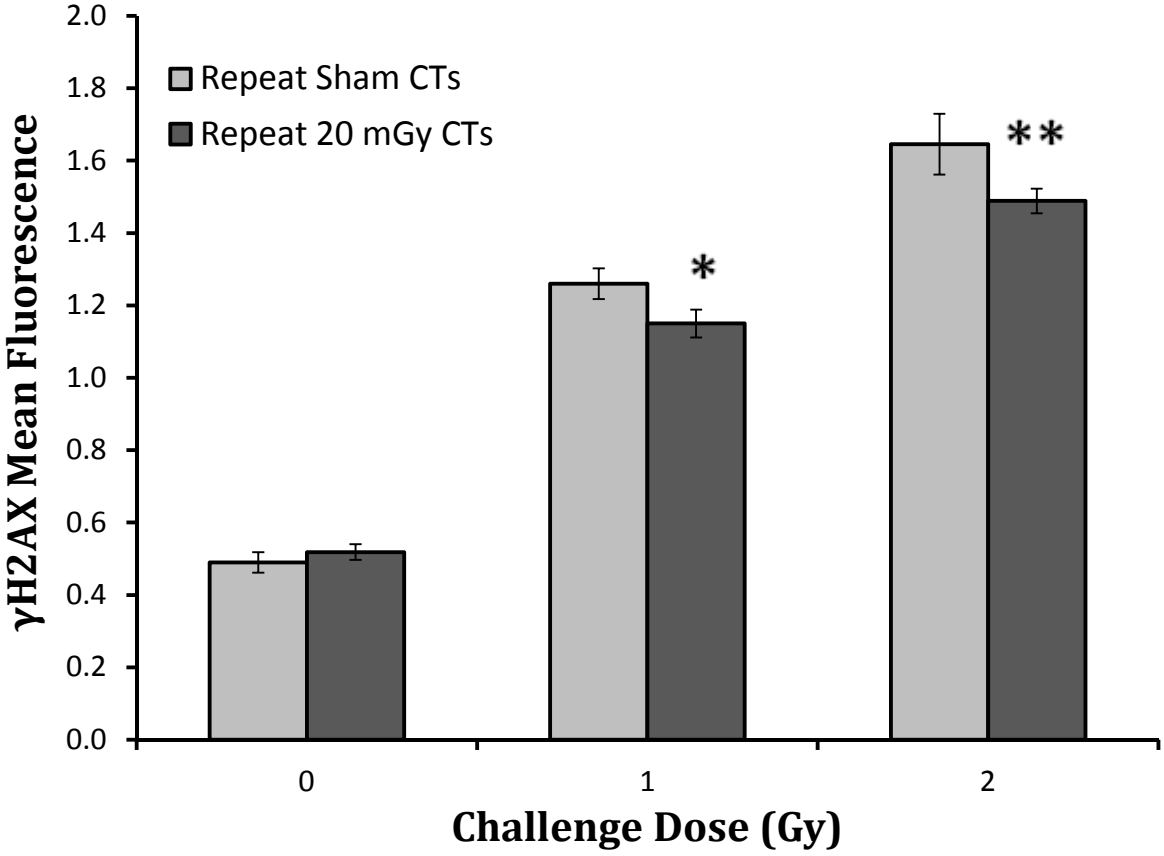

FIG. 7. Mean cellular fluorescence of labelled γH2AX in lymphocyte-rich populations of bone marrow cells after *in vitro* γ-radiation challenge doses of 0, 1 and 2 Gy in mice treated with 10 weeks of repeated CT scans and the corresponding sham CT mice; Repeat Sham CTs: n=8; Repeat 20 mGy CTs: n=8. Results are pooled sample mean values from two independent experiments. Error bars represent standard error of the mean (samples analysed in duplicate). *, ** denotes $p<0.05$ compared to Repeat Sham CTs following 1 and 2 Gy challenge doses, respectively. Error bars represent standard error of the mean.

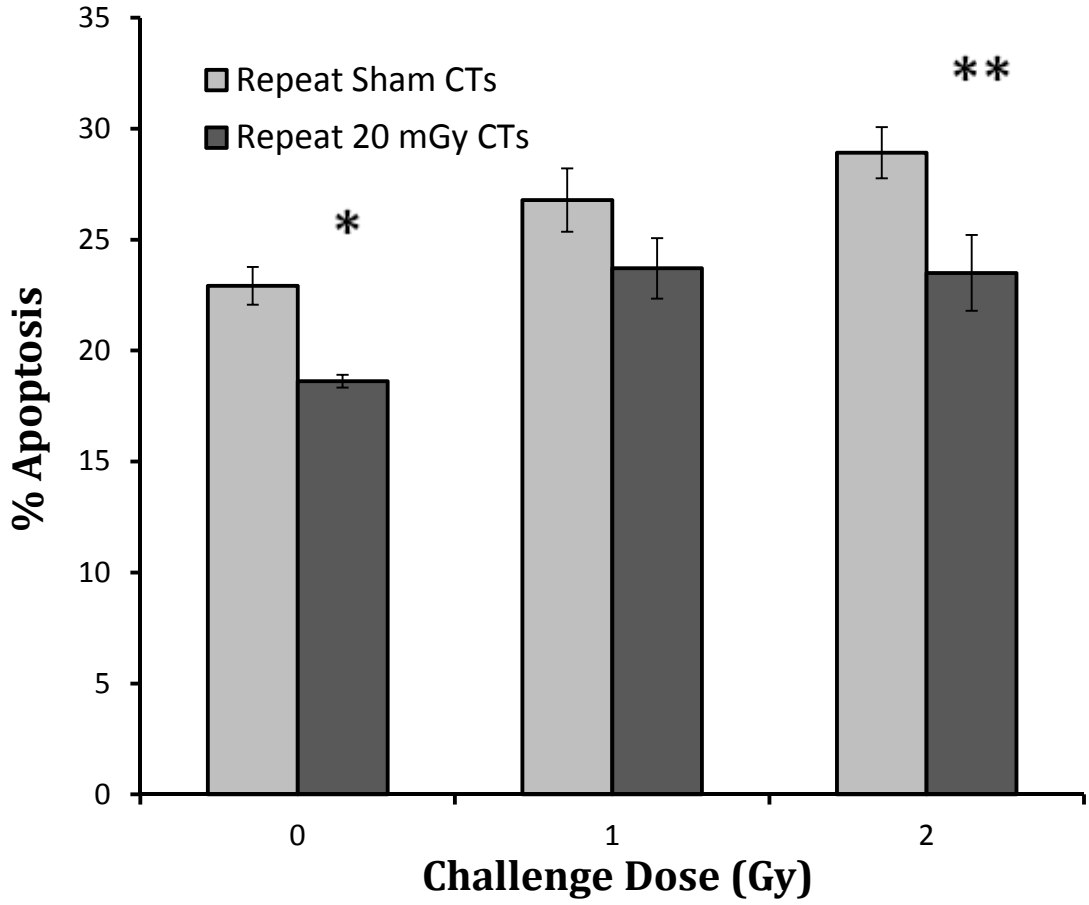

FIG. 8. Apoptosis levels (caspase 3, 7+) in bone marrow cell populations after *in vitro* γ-radiation challenge doses of 0, 1 and 2 Gy in mice treated with 10 weeks of repeated CT scans and the corresponding sham CT mice; Repeat Sham CTs: n=5; Repeat 20 mGy CTs: n=5. Results are sample mean values. Error bars represent standard error of the mean (samples analysed in duplicate). *, ** denotes $p<0.05$ compared to Repeat Sham CTs following 0 and 2 Gy challenge doses, respectively.

References

1. Shah NB, Platt SL. ALARA: Is there a cause for alarm? reducing radiation risks from computed tomography scanning in children. Curr Opin Pediatr. 2008 Jun;20(3):243-7.
2. Brenner DJ, Hall EJ. Computed tomography--an increasing source of radiation exposure. N Engl J Med. 2007 Nov 29;357(22):2277-84.
3. Payne JT. CT radiation dose and image quality. Radiol Clin North Am. 2005 Nov;43(6):953,62, vii.
4. Radiation risks and pediatric computed tomography - national cancer institute [Internet].; cited 11/29/2009]. Available from: http://www.nci.nih.gov/cancertopics/causes/radiation-risks-pediatric-CT.
5. Frush DP, Applegate K. Computed tomography and radiation: Understanding the issues. J Am Coll Radiol. 2004 Feb;1(2):113-9.
6. Imhof H, Schibany N, Ba-Ssalamah A, Czerny C, Hojreh A, Kainberger F, et al. Spiral CT and radiation dose. Eur J Radiol. 2003 Jul;47(1):29-37.
7. Frush DP, Donnelly LF, Rosen NS. Computed tomography and radiation risks: What pediatric health care providers should know. Pediatrics. 2003 Oct;112(4):951-7.
8. Mettler FA,Jr, Wiest PW, Locken JA, Kelsey CA. CT scanning: Patterns of use and dose. J Radiol Prot. 2000 Dec;20(4):353-9.
9. Fujii K, Aoyama T, Yamauchi-Kawaura C, Koyama S, Yamauchi M, Ko S, et al. Radiation dose evaluation in 64-slice CT examinations with adult and paediatric anthropomorphic phantoms. Br J Radiol. 2009 Dec;82(984):1010-8.
10. Shrimpton PC, Hillier MC, Lewis MA, Dunn M. National survey of doses from CT in the UK: 2003. Br J Radiol. 2006 Dec;79(948):968-80.
11. Prokop M. Cancer screening with CT: Dose controversy. Eur Radiol. 2005 Nov;15 Suppl 4:D55-61.
12. Chodick G, Ronckers CM, Shalev V, Ron E. Excess lifetime cancer mortality risk attributable to radiation exposure from computed tomography examinations in children. Isr Med Assoc J. 2007 Aug;9(8):584-7.
13. Brenner DJ, Georgsson MA. Mass screening with CT colonography: Should the radiation exposure be of concern? Gastroenterology. 2005 Jul;129(1):328-37.
14. Baskerville JR. Screening patients with multi-detector computed axial tomography (MDCT): When will we inform patients about the risk of radiation? Emerg Med J. 2008 Jun;25(6):323-4.
15. Preston RJ. Update on linear non-threshold dose-response model and implications for diagnostic radiology procedures. Health Phys. 2008 Nov;95(5):541-6.
16. Tubiana M, Aurengo A, Averbeck D, Masse R. The debate on the use of linear no threshold for assessing the effects of low doses. J Radiol Prot. 2006 Sep;26(3):317-24.
17. Charles MW. LNT--an apparent rather than a real controversy? J Radiol Prot. 2006 Sep;26(3):325-9.

18. BEIR VII.
Health risks from exposure to low levels of ionizing radiation — BEIR VII. Washington, DC: National Academies Press; 2005.
19. UNSCEAR. Sources and effects of ionizing radiation: United nations scientific committee on the effects of atomic radiation: UNSCEAR 2000 report to the general assembly. New York: United Nations; 2000.
20. Semelka RC, Armao DM, Elias J,Jr, Huda W. Imaging strategies to reduce the risk of radiation in CT studies, including selective substitution with MRI. J Magn Reson Imaging. 2007 May;25(5):900-9.
21. International Commission on Radiological Protection.
Managing patient dose in computed tomography. ICRP Publication 87 ed. Elsevier Press; 2001.
22. Boreham DR, Dolling JA, Maves SR, Siwarungsun N, Mitchel RE. Dose-rate effects for apoptosis and micronucleus formation in gamma-irradiated human lymphocytes. Radiat Res. 2000 May;153(5 Pt 1):579-86.
23. Dertinger SD, Bishop ME, McNamee JP, Hayashi M, Suzuki T, Asano N, et al. Flow cytometric analysis of micronuclei in peripheral blood reticulocytes: I. intra- and interlaboratory comparison with microscopic scoring. Toxicol Sci. 2006 Nov;94(1):83-91.
24. Kirsch-Volders M, Fenech M. Inclusion of micronuclei in non-divided mononuclear lymphocytes and necrosis/apoptosis may provide a more comprehensive cytokinesis block micronucleus assay for biomonitoring purposes. Mutagenesis. 2001 Jan;16(1):51-8.
25. Fenech M. In vitro micronucleus technique to predict chemosensitivity. Methods Mol Med. 2005;111:3-32.
26. Dertinger SD, Tsai Y, Nowak I, Hyrien O, Sun H, Bemis JC, et al. Reticulocyte and micronucleated reticulocyte responses to gamma irradiation: Dose-response and time-course profiles measured by flow cytometry. Mutat Res. 2007 Dec 1;634(1-2):119-25.
27. Bryce SM, Bemis JC, Avlasevich SL, Dertinger SD. In vitro micronucleus assay scored by flow cytometry provides a comprehensive evaluation of cytogenetic damage and cytotoxicity. Mutat Res. 2007 Jun 15;630(1-2):78-91.
28. Liu L, Liu Y, Ni G, Liu S. Flow cytometric scoring of micronucleated reticulocytes as a possible high-throughput radiation biodosimeter. Environ Mol Mutagen. 2009 Sep 29.
29. Fillingham J, Keogh MC, Krogan NJ. GammaH2AX and its role in DNA double-strand break repair. Biochem Cell Biol. 2006 Aug;84(4):568-77.
30. Kinner A, Wu W, Staudt C, Iliakis G. Gamma-H2AX in recognition and signaling of DNA double-strand breaks in the context of chromatin. Nucleic Acids Res. 2008 Oct;36(17):5678-94.
31. Ismail IH, Hendzel MJ. The gamma-H2A.X: Is it just a surrogate marker of double-strand breaks or much more? Environ Mol Mutagen. 2008 Jan;49(1):73-82.
32. Kobayashi J, Iwabuchi K, Miyagawa K, Sonoda E, Suzuki K, Takata M, et al. Current topics in DNA double-strand break repair. J Radiat Res (Tokyo). 2008 Mar;49(2):93-103.

33. Srivastava N, Gochhait S, de Boer P, Bamezai RN. Role of H2AX in DNA damage response and human cancers. Mutat Res. 2009 Mar-Jun;681(2-3):180-8.
34. Evan G, Littlewood T. A matter of life and cell death. Science. 1998 Aug 28;281(5381):1317-22.
35. Steller H. Mechanisms and genes of cellular suicide. Science. 1995 Mar 10;267(5203):1445-9.
36. Green DR, Evan GI. A matter of life and death. Cancer Cell. 2002 Feb;1(1):19-30.
37. Feinendegen LE, Pollycove M, Sondhaus CA. Responses to low doses of ionizing radiation in biological systems. Nonlinearity Biol Toxicol Med. 2004 Jul;2(3):143-71.
38. Verheij M, Bartelink H. Radiation-induced apoptosis. Cell Tissue Res. 2000 Jul;301(1):133-42.
39. Nakatsumi H, Yonehara S. Identification of functional regions defining different activity between caspase-3 and caspase-7 within cells. J Biol Chem. 2010 Jun 21.
40. Scott FL, Denault JB, Riedl SJ, Shin H, Renatus M, Salvesen GS. XIAP inhibits caspase-3 and -7 using two binding sites: Evolutionarily conserved mechanism of IAPs. EMBO J. 2005 Feb 9;24(3):645-55.
41. Cai L, Wang P. Induction of a cytogenetic adaptive response in germ cells of irradiated mice with very low-dose rate of chronic gamma-irradiation and its biological influence on radiation-induced DNA or chromosomal damage and cell killing in their male offspring. Mutagenesis. 1995 Mar;10(2):95-100.
42. Liu SZ, Cai L, Sun SQ. Induction of a cytogenetic adaptive response by exposure of rabbits to very low dose-rate gamma-radiation. Int J Radiat Biol. 1992 Aug;62(2):187-90.
43. Olivieri G, Bodycote J, Wolff S. Adaptive response of human lymphocytes to low concentrations of radioactive thymidine. Science. 1984 Feb 10;223(4636):594-7.
44. Sorensen KJ, Attix CM, Christian AT, Wyrobek AJ, Tucker JD. Adaptive response induction and variation in human lymphoblastoid cell lines. Mutat Res. 2002 Aug 26;519(1-2):15-24.
45. Shadley JD. Chromosomal adaptive response in human lymphocytes. Radiat Res. 1994 Apr;138(1 Suppl):S9-12.
46. de Toledo SM, Asaad N, Venkatachalam P, Li L, Howell RW, Spitz DR, et al. Adaptive responses to low-dose/low-dose-rate gamma rays in normal human fibroblasts: The role of growth architecture and oxidative metabolism. Radiat Res. 2006;166(6):849-57.
47. Feinendegen LE, Pollycove M, Neumann RD. Whole-body responses to low-level radiation exposure: New concepts in mammalian radiobiology. Exp Hematol. 2007 Apr;35(4 Suppl 1):37-46.
48. De Lisio M, Phan N, Boreham DR, Parise G. Exercise-induced protection of bone marrow cells following exposure to radiation. Appl Physiol Nutr Metab. 2011 Feb;36(1):80-7.
49. Krzyzanski W, Perez-Ruixo JJ. An assessment of recombinant human erythropoietin effect on reticulocyte production rate and lifespan distribution in healthy subjects. Pharm Res. 2007 Apr;24(4):758-72.

50. Hamasaki K, Imai K, Hayashi T, Nakachi K, Kusunoki Y. Radiation sensitivity and genomic instability in the hematopoietic system: Frequencies of micronucleated reticulocytes in whole-body X-irradiated BALB/c and C57BL/6 mice. Cancer Sci. 2007 Dec;98(12):1840-4.
51. Dertinger SD, Camphausen K, Macgregor JT, Bishop ME, Torous DK, Avlasevich S, et al. Three-color labeling method for flow cytometric measurement of cytogenetic damage in rodent and human blood. Environ Mol Mutagen. 2004;44(5):427-35.
52. Rothkamm K, Balroop S, Shekhdar J, Fernie P, Goh V. Leukocyte DNA damage after multi-detector row CT: A quantitative biomarker of low-level radiation exposure. Radiology. 2007 Jan;242(1):244-51.
53. Golfier S, Jost G, Pietsch H, Lengsfeld P, Eckardt-Schupp F, Schmid E, et al. Dicentric chromosomes and gamma-H2AX foci formation in lymphocytes of human blood samples exposed to a CT scanner: A direct comparison of dose response relationships. Radiat Prot Dosimetry. 2009 Feb;134(1):55-61.
54. Jost G, Golfier S, Pietsch H, Lengsfeld P, Voth M, Schmid TE, et al. The influence of x-ray contrast agents in computed tomography on the induction of dicentrics and gamma-H2AX foci in lymphocytes of human blood samples. Phys Med Biol. 2009 Oct 21;54(20):6029-39.
55. Jost G, Lengsfeld P, Voth M, Schmid E, Pietsch H. The influence of tube voltage and phantom size in computed tomography on the dose-response relationship of dicentrics in human blood samples. Phys Med Biol. 2010 Jun 7;55(11):3237-48.
56. Stephan G, Schneider K, Panzer W, Walsh L, Oestreicher U. Enhanced yield of chromosome aberrations after CT examinations in paediatric patients. Int J Radiat Biol. 2007 May;83(5):281-7.
57. Grudzenski S, Kuefner MA, Heckmann MB, Uder M, Lobrich M. Contrast medium-enhanced radiation damage caused by CT examinations. Radiology. 2009 Dec;253(3):706-14.
58. M'kacher R, Violot D, Aubert B, Girinsky T, Dossou J, Beron-Gaillard N, et al. Premature chromosome condensation associated with fluorescence in situ hybridisation detects cytogenetic abnormalities after a CT scan: Evaluaton of the low-dose effect. Radiat Prot Dosimetry. 2003;103(1):35-40.
59. Kuefner MA, Grudzenski S, Hamann J, Achenbach S, Lell M, Anders K, et al. Effect of CT scan protocols on x-ray-induced DNA double-strand breaks in blood lymphocytes of patients undergoing coronary CT angiography. Eur Radiol. 2010 Dec;20(12):2917-24.
60. Leonard A, Rueff J, Gerber GB, Leonard ED. Usefulness and limits of biological dosimetry based on cytogenetic methods. Radiat Prot Dosimetry. 2005;115(1-4):448-54.
61. Lehnert A, Dorr W, Lessmann E, Pawelke J. RBE of 10 kV X rays determined for the human mammary epithelial cell line MCF-12A. Radiat Res. 2008 Mar;169(3):330-6.
62. Slonina D, Spekl K, Panteleeva A, Brankovic K, Hoinkis C, Dorr W. Induction of micronuclei in human fibroblasts and keratinocytes by 25 kV x-rays. Radiat Environ Biophys. 2003 Apr;42(1):55-61.

63. Hatayoglu SE, Orta T. Relationship between radiation induced dicentric chromosome aberrations and micronucleus formation in human lymphocytes. J Exp Clin Cancer Res. 2007 Jun;26(2):229-34.
64. Kagawa N, Shimura M, Takai A, Endo S, Fujikawa K. Relative biological effectiveness of fission neutrons for induction of micronucleus formation in mouse reticulocytes in vivo. Mutat Res. 2004 Nov 22;556(1-2):93-9.
65. Salone B, Pretazzoli V, Bosi A, Olivieri G. Interaction of low-dose irradiation with subsequent mutagenic treatment: Role of mitotic delay. Mutat Res. 1996 Nov 4;358(2):155-60.
66. Salone B, Grillo R, Aillaud M, Bosi A, Olivieri G. Effects of low-dose (2 cGy) X-ray on cell-cycle kinetics and on induced mitotic delay in human lymphocyte. Mutat Res. 1996 Apr 13;351(2):193-7.
67. Cramers P, Atanasova P, Vrolijk H, Darroudi F, van Zeeland AA, Huiskamp R, et al. Pre-exposure to low doses: Modulation of X-ray-induced dna damage and repair? Radiat Res. 2005 Oct;164(4 Pt 1):383-90.
68. Tapio S, Jacob V. Radioadaptive response revisited. Radiat Environ Biophys. 2007 Mar;46(1):1-12.
69. Lobrich M, Rief N, Kuhne M, Heckmann M, Fleckenstein J, Rube C, et al. In vivo formation and repair of DNA double-strand breaks after computed tomography examinations. Proc Natl Acad Sci U S A. 2005 Jun 21;102(25):8984-9.
70. Lemon JA, Rollo CD, Boreham DR. Elevated DNA damage in a mouse model of oxidative stress: Impacts of ionizing radiation and a protective dietary supplement. Mutagenesis. 2008 Nov;23(6):473-82.
71. Schmid TE, Dollinger G, Beisker W, Hable V, Greubel C, Auer S, et al. Differences in the kinetics of gamma-H2AX fluorescence decay after exposure to low and high LET radiation. Int J Radiat Biol. 2010 Aug;86(8):682-91.
72. MacPhail SH, Banath JP, Yu TY, Chu EH, Lambur H, Olive PL. Expression of phosphorylated histone H2AX in cultured cell lines following exposure to X-rays. Int J Radiat Biol. 2003 May;79(5):351-8.
73. MacPhail SH, Banath JP, Yu Y, Chu E, Olive PL. Cell cycle-dependent expression of phosphorylated histone H2AX: Reduced expression in unirradiated but not X-irradiated G1-phase cells. Radiat Res. 2003 Jun;159(6):759-67.
74. Jucha A, Wegierek-Ciuk A, Koza Z, Lisowska H, Wojcik A, Wojewodzka M, et al. FociCounter: A freely available PC programme for quantitative and qualitative analysis of gamma-H2AX foci. Mutat Res. 2010 Feb 1;696(1):16-20.
75. Hamasaki K, Imai K, Nakachi K, Takahashi N, Kodama Y, Kusunoki Y. Short-term culture and gammaH2AX flow cytometry determine differences in individual radiosensitivity in human peripheral T lymphocytes. Environ Mol Mutagen. 2007 Jan;48(1):38-47.
76. Rothkamm K, Lobrich M. Evidence for a lack of DNA double-strand break repair in human cells exposed to very low x-ray doses. Proc Natl Acad Sci U S A. 2003 Apr 29;100(9):5057-62.

77. Andrievski A, Wilkins RC. The response of gamma-H2AX in human lymphocytes and lymphocytes subsets measured in whole blood cultures. Int J Radiat Biol. 2009 Apr;85(4):369-76.
78. Rothkamm K, Horn S. Gamma-H2AX as protein biomarker for radiation exposure. Ann Ist Super Sanita. 2009;45(3):265-71.
79. Cramers P, Atanasova P, Vrolijk H, Darroudi F, van Zeeland AA, Huiskamp R, et al. Pre-exposure to low doses: Modulation of X-ray-induced dna damage and repair? Radiat Res. 2005 Oct;164(4 Pt 1):383-90.
80. Lu C, Zhu F, Cho YY, Tang F, Zykova T, Ma WY, et al. Cell apoptosis: Requirement of H2AX in DNA ladder formation, but not for the activation of caspase-3. Mol Cell. 2006 Jul 7;23(1):121-32.
81. Ermakov AV, Konkova MS, Kostyuk SV, Egolina NA, Efremova LV, Veiko NN. Oxidative stress as a significant factor for development of an adaptive response in irradiated and nonirradiated human lymphocytes after inducing the bystander effect by low-dose X-radiation. Mutat Res. 2009 Oct 2;669(1-2):155-61.
82. Ryter SW, Kim HP, Hoetzel A, Park JW, Nakahira K, Wang X, et al. Mechanisms of cell death in oxidative stress. Antioxid Redox Signal. 2007 Jan;9(1):49-89.
83. Portess DI, Bauer G, Hill MA, O'Neill P. Low-dose irradiation of nontransformed cells stimulates the selective removal of precancerous cells via intercellular induction of apoptosis. Cancer Res. 2007 Feb 1;67(3):1246-53.
84. Belloni P, Meschini R, Lewinska D, Palitti F. Apoptosis preferentially eliminates irradiated g0 human lymphocytes bearing dicentric chromosomes. Radiat Res. 2008 Feb;169(2):181-7.
85. Sasaki MS. On the reaction kinetics of the radioadaptive response in cultured mouse cells. Int J Radiat Biol. 1995 Sep;68(3):281-91.
86. Shadley JD, Afzal V, Wolff S. Characterization of the adaptive response to ionizing radiation induced by low doses of X rays to human lymphocytes. Radiat Res. 1987 Sep;111(3):511-7.
87. Markova E, Schultz N, Belyaev IY. Kinetics and dose-response of residual 53BP1/gamma-H2AX foci: Co-localization, relationship with DSB repair and clonogenic survival. Int J Radiat Biol. 2007 May;83(5):319-29.

Chapter 3

Computed tomography scans induce protection against high-dose radiation exposures in the hematopoietic system of Trp53 wild-type mice

Nghi Phan, Kristina Taylor, and Douglas R. Boreham
Department of Medical Physics and Applied Radiation Sciences,
McMaster University, 1280 Main St. W, Hamilton, Ontario, Canada, L8S 4K1

Manuscript submission pending: Radiat.Res. 2011

Author Contributions:

N. Phan and K. Taylor were responsible for experimental design and data acquisition.
N. Phan was responsible for the interpretation of the results and synthesis of the manuscript.
D. Boreham supervised and guided the research.

ABSTRACT

Low-dose computed tomography (CT) scans can induce protection against subsequent high-dose radiation exposures in the hematopoietic system of *Trp*53 wild-type mice. A single acute exposure to CT X-rays (0-100 mGy) caused dose-dependent increases in micronuclei formation and γH2AX levels in reticulocytes and bone marrow lymphocytes, respectively ($p<0.01$). A significant increase in apoptosis of peripheral lymphocytes coincided with these cytogenetic effects ($p<0.05$). When single 10 mGy CT scans were given before 1 and 2 Gy challenge doses, there was a 12% reduction in micronucleated reticulocytes (MN-RETs) frequencies and an 11% reduction in γH2AX levels in bone marrow lymphocytes relative to sham CT controls ($p<0.05$). The time interval between the priming CT scan and challenge dose was found to influence the nature of the adaptive response. Weekly 10 mGy CT exposures for ten weeks did not elevate spontaneous MN-RET levels, and conferred resistance to radiation-induced DNA double-stranded breaks (γH2AX levels, $p<0.02$) and DNA oxidative stress damage (8-OHdG levels). Overall, low-dose CT scans, whether through enhanced apoptosis of damaged cells or enhanced protection against oxidative damage, can induce protective adaptations against the genotoxic effects of high-dose radiation exposures.

INTRODUCTION

The health effects of low-dose ionizing radiation are important to understand, particularly within the context of medical diagnostic procedures. Computed tomography (CT) has become an integral part of patient health care over the last decade, and its greater use has resulted in a concurrent increase in ionizing radiation exposure *(1)*. There are many epidemiological studies investigating the possible link between low-dose radiation exposure and increased health risk *(2-5)*. However, these studies encounter challenges such as dose-estimation accuracy, adequate sample size, and heterogeneity in the population. Consequently, the health risks of medical diagnostic CT have come under scrutiny in recent years *(2, 6-8)*.

The typical radiation dose range for a whole-body CT scan is 10 – 30 mGy but can be as high as 80 mGy *(9-11)*. By comparison, the annual natural background exposure is around 2 – 3 mGy in North America *(12)*. Extrapolative risk studies looking at high-dose exposures and data from atomic bomb survivors have suggested that there is a small but statistically significant health risk from CT scans with doses as low as 10 mGy *(2)*. These types of studies are misleading since they ignore a preponderance of evidence which shows that low-dose radiation exposures do not increase risk and can actually have protective effects.

Humans and animals have evolutionarily-conserved cellular processes in place to manage and remove damage from environmental stressors such as low-dose radiation. Extrapolative risk studies that make claims of increased risk at low doses do not take these rudimentary defense mechanisms into account, and assume that both dose and risk are additive. With equal total dose, acute radiation exposures do not yield the same biological consequences as protracted or fractionated exposures *(13)*. When the exposure is spread over time, there are protective

processes that are up-regulated to remove and prevent subsequent damage *(14)*. Therefore, risk is not proportional to the total additive dose, and extrapolating risk estimates from acute high-dose exposures to low- dose exposures is scientifically unsound.

Experiments have shown that low-dose radiation exposures can induce protective responses such as the prevention of radiation damage *(15)*, efficient removal of chromosomal aberrations *(16)*, improved immune functions *(17, 18)*, and selective elimination of precancerous cells *(19, 20)*. The term "adaptive response" is often used to describe a phenomenon whereby a small *priming* radiation dose reduces the biological effects of a subsequent *challenge* radiation dose *(21)*. While many experiments have demonstrated the potential of low-dose radiation to induce adaptive responses, none have been examined within the context of medical diagnostic CT exposures.

In the current study, the biological effects of diagnostic CT radiation were investigated to better understand the cellular processes altered by medical CT procedures. The induction of DNA damage (γH2AX formation) and manifestation of mis-repaired chromosomal aberrations (micronucleated reticulocytes) were assessed following acute exposures to single CT scans. Apoptosis was measured to evaluate the clearance process of the damaged cells. The existence, magnitude, and kinetics of an adaptive response induced by CT scans were also examined. Furthermore, DNA oxidative damage (8-OHdG formation) and cytotoxic effects of repeated CT scans were studied to provide further evidence that risk is not proportional to total additive dose for exposures relevant to medical diagnostic CT procedures.

MATERIALS & METHODS

Animal Breeding and Genotyping

Male *Trp*53 heterozygous (B6.129S2-*Trp*53$^{tm1Tyj/+}$) and female *Trp*53 homozygous (129X1/SvJ *Trp*53+/+) mice, both obtained from Jackson Laboratory (Bar Harbor, Maine), were crossed to yield F1 *Trp*53 wild-type (+/+) and *Trp*53 heterozygous (+/-) mice. Only female *Trp*53 wild-type mice were used in this study. *Trp*53 wild-type status was determined by collecting a small tail snip from mice at five weeks old for PCR-based genotyping (procedure previously described *(22, 23)*). Mouse tail snips were genotyped by a third party specializing in mouse genotyping services (Mouse Genotype.; Carlsbad, California).

Animal Housing

Five or fewer mice were housed in solid-bottom polycarbonate cages (27 x 12 x 15.5 cm) containing woodchip bedding (Harlan Sani-Chips, 7090). A stainless steel wire-bar hopper held food (Harlan Lab Diets; Indianapolis, USA) and a water bottle for consumption *ad libitum.* The specific-pathogen-free housing room was maintained at a 12:12-h light:dark photoperiod with an inside air temperature of 23±2^{o}C and 40-80% humidity. All housing, handling, and experimental procedures were approved by the Animal Research Ethics Board at McMaster University and conducted in accordance to the guidelines of the Canadian Council on Animal Care.

Experimental Design

Dose Responses and CT scan-induced Adaptive Responses

The CT radiation dose responses were investigated in 7-8 weeks old *Trp*53 wild-type mice using flow cytometry-based micronucleated reticulocyte (MN-RET), γH2AX formation, and apoptosis assays. CT scan-induced adaptive responses with respect to the MN-RET and γH2AX endpoints were also examined. Additionally, the effect of age on the spontaneous levels of MN-RETs was studied over a period of 80 weeks. Table 1 outlines the specific design of the various dose response and adaptive response experiments. Gamma radiation dose responses were also assessed for the MN-RET and apoptosis endpoints. The gamma exposure for the apoptosis dose response was performed *in vitro*, whereas all other dose response exposures were performed *in vivo*.

Biological Effects of Repeated CT Scans

The biological effects of repeated CT scans were examined in 11-12 week old female *Trp*53 wild-type mice. Single 10 mGy CT scans were given weekly for ten consecutive weeks. The corresponding control group were sham CT scanned throughout the 10 weeks and handled in the same manner as the CT scanned mice. There were five mice in each experimental group. Five days after the last CT scan time point, all mice were sacrificed and tissues (blood and bone marrow) were harvested for MN-RET, γH2AX, 8-OHdG, and apoptosis analyses. Except for blood used in the MN-RET analyses, tissue samples were given *in vitro* challenge doses of 1 and 2 Gy to further explore possible adaptive responses.

Computed Tomography Protocols

Whole-body CT scans were performed on a Gamma Medica X-SPECT Animal Imaging System (Northridge, California). Mice were placed in pairs into a customized sectioned polycarbonate tube and CT scanned (75kVp, 215µA, 1 mm Al filter, half-value layer 4.28 mm Al) at a dose rate of 18.6 mGy/minute. Mice were not anaesthetized during the CT scanning procedures as immobilization for image analysis was not necessary.

Computed Tomography Dosimetry

Whole-body dose measurements were obtained using thermoluminescent dosimeter (TLD) chips (Harshaw TLD-100 LiF Chips). TLD chip analyses were performed by a third party specializing in clinical diagnostic radiation measurements (K&S Associates Inc.; Nashville, Tennessee). To measure whole-body absorbed dose in mice, TLD chips were surgically implanted at five locations in a mouse carcass: head, chest, abdomen, above the skin, and under the skin. Measurements were performed on two individual carcasses during the study. The overall uncertainty of the TLD measurement process is 5% at the 95% confidence interval for a single TLD chip at the measurement location. This uncertainty does not take into account minor variations in the placement of the TLD chips between different mouse carcasses. Consistent dosimetry was confirmed and validated repeatedly throughout the study using a 0.6 cc ionizing chamber (Farmer Dose-meter Model 2570A and PTW Freiburg Model TN30010 Ion Chamber). The calculated average whole-body dose for a CT scan at the aforementioned specifications was 10.3±1.1 mGy.

γ-*Radiation Exposures*

In vivo Exposures

Mice were placed in pairs into a customized tube and given whole-body γ-radiation exposures (662keV - Cs^{137}) at a dose rate of 18.6 mGy/minute or 0.188 Gy/minute for the 1 Gy challenge dose. Mice assigned as sham controls were sham irradiated (i.e. placed in the polycarbonate tubes for an equal amount of time but with no radiation exposure). All *in vivo* radiation challenges were performed with the same customized polycarbonate tubes used for the CT scans.

In vitro Exposures

Blood and bone marrow were collected and separated into aliquots (1 x 10^6 cells/mL) for *in vitro* irradiation at a dose rate of 0.188 Gy/minute (662keV - Cs^{137}). All samples were kept on ice-water slurry (0^oC) during the *in vitro* radiation exposures.

Sample Collection and Cell Preparation

Blood

Mice were anaesthetised using Isofluorane™ and blood was collected via cardiac puncture or submandibular vein when repeat sampling from the same mice was required (e.g. MN-RETs and age effect investigation). In a previous study, we found that the method of blood sampling did not influence MN-RET formation *(24)*. For MN-RET analysis, approximately 50 µL of blood was collected (43 hours after a radiation exposure) into 1.5 mL microcentrifuge tubes (VWR

International, Mississauga, Ontario) containing 350 µL heparin solution (VWR International, Mississauga, Ontario). For apoptosis analysis, approximately 400 µL of blood was collected in heparinized syringes and kept on ice slurry until further processing according to the apoptosis protocol. Heparinised blood for the MN-RET assay was maintained at room temperature until fixation (within 3 hours).

Bone Marrow

Bone marrow samples for γH2AX and 8-OHdG analyses were collected by flushing both femurs with a 23 gauge needle containing 1 mL of heparinized RPMI 1640 media (Lonza Inc., Allendale, New Jersey). The disaggregated bone marrow cell suspension was transferred to a 1.5 mL microcentrifuge tube (VWR International, Mississauga, Ontario) and held at 0^{o}C on ice slurry until processing (within 1 hour). Bone marrow cells were counted using a Z2 Coulter Particle Count & Size Analyzer (Beckman-Coulter, Miami, Florida). The cell sample was adjusted to a final concentration of $1x10^{6}$ cells/mL in ice-cold RPMI 1640 supplemented with 10% fetal bovine serum (FBS, PAA Laboratories Inc., Etobicoke, Ontario), 1% penicillin-streptomycin (Lonza Inc., Allendale, New Jersey), 1% L-glutamine (Lonza Inc., Allendale, New Jersey). Three 1.5 mL replicate aliquots of the cell sample suspension were made for *in vitro* irradiations at 0, 1, and 2 Gy.

Micronucleated Reticulocyte Assay

Reagents

The reagents used for preparing blood specimens for flow cytometric analysis were all from a commercially available kit, Mouse MicroFlowPLUS® (Litron Laboratories, Rochester, NY), and included a heparin-based anticoagulant solution, buffer solution, anti-CD71-FITC, anti-CD61-PE, RNase, and propidium iodide. Also included was a flow cytometer calibration standard consisting of fixed *Plasmodium berghei*-infected mouse erythrocytes ("malaria biostandard").

Fixation

Cells were fixed in absolute methanol (CAS no. 67-56-1, Sigma Aldrich, Mississauga, Ontario) at -80^{o}C. A maximum of six samples was fixed at a time using dry ice. This was done to ensure that the temperature of the fixative was maintained between -70^{o}C and -80^{o}C. A 180 µL aliquot of diluted blood suspension was forcibly delivered into a 15 mL conical tube (BD Biosciences, Mississauga, Ontario) containing 2 mL of -80^{o}C methanol. The tubes were vortexed and struck sharply with a pen-size plastic tube several times to break up any aggregates. The fixed samples were stored at -80^{o}C for a minimum of 24 hours before staining and flow cytometric analysis.

Staining and flow cytometric analyses

Methanol-fixed blood samples were washed and labelled for flow cytometric analysis according to procedures detailed in the Mouse MicoFlowPLUS Kit manual (vP4.3m) and previously described in *(25)*. Briefly, fixed blood cells were washed with 12 mL of kit-supplied buffer solution and the pellets were maintained on ice slurry (0^{o}C) until staining (within 3 hour). An 80 uL reagent mixture containing anti-CD71-FITC, anti-CD61-PE, RNase and buffer solution was

added to 20 µL aliquot of each fixed blood sample in duplicate. The cells were incubated on ice for 30 minutes followed by 30 minutes at room temperature, and then returned to ice. Immediately before acquisition on the flow cytometer, 1 mL of cold (4^{o}C) propidium iodide (1.25 µg/mL in buffer solution) was added to each tube.

Flow cytometry was performed using a Beckman Coulter EPICS XL flow cytometer (Beckman Coulter, Brea, CA). Cells were analyzed at an average rate of 4000 cells (events) per second. The EPICS XL flow cytometer is equipped with a 488 nm argon laser and four fluorescence detectors. Anti-CD71-FITC, anti-CD61-PE, and propidium iodide fluorescence signals were detected in the FL1 (525±15 nm), FL2 (575±15 nm), and FL3 channels (620±15 nm), respectively. The gating logic used to quantitatively analyse the erythrocyte subpopulations has been described previously *(25)*. The number of reticulocytes (RETs) and MN-RETs were quantified for each sample. Representative bivariate graphs illustrating the resolution of the various erythrocyte populations have been published *(25)(26)*. To ensure adequate sample sizes for statistical significance, the number of RETs was measured in a total of 2x10^{5} erythrocytes. The number of MN-RETs was evaluated based on counting a total of 2x10^{4} total RETs per sample.

γH2AX & 8-OHdG Fluorescence Assays

Bone marrow cells were adjusted to 1x10^{6} cells/mL, transferred to 15 mL conical tubes (BD Biosciences, Mississauga, Ontario), and irradiated as described above. Following irradiations, 500 µL aliquots were removed from irradiated cell samples and incubated for 30 minutes and 120 minutes in a 37^{0}C water bath for the γH2AX and 8-OhdG assays, respectively. After incubation, 3

mL of 70% ethanol at 0^{o}C was immediately added to each tube. All tubes were maintained on ice slurry (0^{o}C) for 1 hour. Samples were stored at -20^{o}C prior to analysis.

For analysis, the fixed bone marrow samples were centrifuged at 5^{o}C (250 g, 8 minutes) and the supernatant was removed. Cells were then washed in 3 mL of Tris-buffered saline (1x TBS; Trizma base + NaCl, Sigma Aldrich, Mississauga, Ontario), centrifuged (250 g, 8 minutes), re-suspended in 1 mL of Tris–saline–triton [TST; TBS + 4% FBS (VWR International, Mississauga, Ontario) + 0.1% Triton X-100 (Sigma Aldrich, Mississauga, Ontario)] and incubated on ice for 10 minutes to permeabilize cells. The cells were again centrifuged (250 g, 8 minutes), the supernatant was removed, and cells were re-suspended in 200 µL of a 1:400 dilution of anti-phospho-H2A.X (ser139) antibody (γH2AX; Upstate Cell Signaling, Charlottesville, VA) or anti-8-OHdG antibody (Chemicon International, Temecula, California).

The cell sample containing the primary antibodies were incubated on a tube rocker at room temperature for 2 hours in the dark. The cells were then washed with 3 mL of TST, re-suspended in 200 µL of a 1:500 dilution of AlexaFluor™ 488-conjugated goat anti-rabbit IgG F(ab')2 antibody (*γH2AX)* or AlexaFluor™ 488-conjugated rabbit anti-goat IgG F(ab')2 antibody (8-OHdG) (Invitrogen Canada, Burlington, Ontario) and incubated at room temperature for 1 hour in the dark. The cells were then washed in 3 mL of TBS and re-suspended in 300 µL TBS + 5 µL propidium iodide (1 mg/mL; Sigma Aldrich). Samples were put on ice and promptly analysed on the Epics XL flow cytometer (Beckman Coulter; Brea, CA). Analysis was based on 5x10^{3} cells from the lymphocyte-rich cell population, as determined by flow cytometric scattering patterns. The levels of γH2AX and 8-OHdG fluorescence were measured by examining the mean fluorescence intensity of cells stained with the AlexaFluor™ 488-conjugated goat anti-rabbit IgG F(ab')2

antibody and AlexaFluor™ 488-conjugated rabbit anti-goat IgG F(ab')2 antibody (Invitrogen Canada, Burlington, Ontario), respectively. Each sample was analyzed in duplicate.

Apoptosis Assay

The protocol for the determination of apoptotic cell death by flow cytometry using Annexin V with 7-amino actinomycin D (7AAD) as a counterstain has been previously described in detail *(27)*. Annexin V is an early marker of apoptosis and 7AAD is a cell viability marker. The reagents were purchased as a commercial kit (Annexin V-FITC-7-AAD; IM3614, Beckman Coulter, Mississauga, Ontario). In the current study, additional anti-CD61-PE (Beckman Coulter, Mississauga, Ontario)and anti-CD45-PE-TexasRed (Invitrogen Canada, Burlington, Ontario) markers were used to identify apoptosis occurring specifically in peripheral blood lymphocytes (CD45+) with the platelet (CD61+) population gated out. Apoptotic lymphocytes were identified as being CD45+, Annexin V+, 7AAD+ and CD61-.

Briefly, each mouse blood sample was divided into three ($1x10^6$ cells/mL) aliquots for 0, 1, and 2 Gy *in vitro* irradiations. Following irradiations on ice-water slurry (0^oC) in 5 mL polypropylene assay tubes (Sarstedt, Montreal, Quebec), the blood (100 µl) was incubated in a CO_2 incubator at 37^oC for 8 hours. The blood was lysed by adding 2 mL of pre-warmed 1x NH_4Cl (37^oC) and incubated at room temperature for 10 minutes. The blood samples were centrifuged (5^oC, 250 g, 5 minutes), the supernatant was removed, and the sample tubes were vortexed gently. The samples were then washed with 2 mL of cold Hank's Buffered Salt Solution (HBSS, 5^oC) (Invitrogen Canada, Burlington, Ontario) and re-suspended in 250 µL of 1x binding buffer

(supplied in kit). To each sample tube, a 100 µL antibody cocktail was added (36 tubes required 3.6 mL of 1x binding buffer, 180 µL of Annexin V, 45 µL of anti-CD45+, 8 µL of anti-CD61+, and 360 µL of 7AAD). Cells were maintained on ice slurry (0^{o}C) and analysed (within 30 minutes) on the Epics XL flow cytometer (Beckman Coulter; Brea, CA). The percentage of cells dying by apoptosis was determined from an analysis of $5x10^{4}$ cells.

Statistical Analyses

Statistical analyses were performed using SigmaPlot version 11.0 (Systat Software Inc., Chicago, Illinois). Data is presented as mean ± standard error (SE) with a p value ≤ 0.05 considered statistically significant. Error bars depicted in all figures are standard errors of the mean. To test for differences in the dose responses between the exposed and unexposed, multiple linear regression analyses were performed. Two-way ANOVA with Bonferroni's post-hoc test was used to determine significance between treatment groups for MN-RET frequency, γH2AX and 8-OHdG fluorescence levels, and apoptosis percentages. Additional Student's t-tests were carried out, where appropriate, to determine if significant differences existed between any two groups.

RESULTS

Dose Responses and Adaptive Responses: Micronucleated Reticulocyte Formation

The induction of MN-RETs following both CT X-rays and gamma radiation exposures was linear from 0 to 100 mGy (r^2=0.993) (Figure 1). The minimum dose that can be detected with either

radiation qualities was 10 mGy (p=0.012). From 0 to 100 mGy, there was no difference in the response of MN-RET formation between CT X-rays and gamma radiation (p=0.142).

To investigate a possible CT-induced adaptive response and its kinetics, various time delays were implemented between when mice received a single 10 mGy CT scan and the subsequent *in vivo* 1 Gy challenge dose (Figure 2). At 4 hours and 6 hours separation between the priming CT scan and the challenge dose, MN-RET levels were significantly lower than the 1 Gy-alone MN-RET levels (12%, p=0.003; and 5%, p=0.043, respectively). At the 9 hours separation, MN-RET levels were significantly higher the 1 Gy-alone levels (6%, p=0.010). When the separation time between the CT scan and challenge dose was 12 hours or longer, there was no difference in MN-RET levels as compared to levels at 1 Gy-alone (p>0.05).

Spontaneous MN-RET levels in a cohort of ten unirradiated mice were monitored over a period of 80 weeks to determine the possible effect of age (Figure 3). After nine periodic assessments, starting when the mice were at 7 weeks old, there were no significant changes in the spontaneous levels of MN-RETs with respect to age (p=0.615).

Dose Responses and Adaptive Responses: γH2AX Fluorescence Levels

The CT X-ray dose response for γH2AX fluorescence levels in bone marrow lymphocytes increased linearly with dose up to 200 mGy (r^2=0.979) (Figure 4). The minimum dose detection limit was 100 mGy (p=0.017), although γH2AX fluorescence levels at lower doses exhibited an upward trend with increasing dose.

To investigate a possible CT-induced adaptive response with respect to γH2AX fluorescence levels, mice were given a single 10 mGy CT scan 24 hours before *in vitro* challenge doses of 1 and 2 Gy. There were no differences in γH2AX levels between CT scanned and non-CT scanned mice at basal level and following the 1 Gy challenge dose (Figure 5). However, following the 2 Gy challenge dose, CT scanned mice had 11% lower γH2AX levels in bone marrow lymphocytes than non-CT scanned mice ($p=0.040$). The γH2AX fluorescence levels increased significantly with the increasing *in vitro* challenge doses ($p<0.001$).

Dose Responses: Apoptosis

Following *in vivo* CT X-ray exposures of 50 and 100 mGy, apoptosis levels in peripheral blood lymphocytes increased significantly ($p<0.05$)(Figure 6). This increase in apoptosis was also seen with *in vitro* gamma radiation exposures of whole blood up 1 Gy ($p<0.05$). Although there were no overlapping doses to compare between the *in vivo* CT X-ray exposures and the *in vitro* gamma exposures, the extrapolated slopes of the two dose response curves are significantly different ($p<0.05$).

Biological Effects of Repeated 10 mGy CT scans

Five days after the last repeated weekly CT scan time point, there were no detectable differences in spontaneous MN-RET frequencies, and basal apoptosis levels relative to sham CT controls ($p>0.05$) (Figure 7a and d). There was, however, a significant 16% reduction in basal 8-OHdG levels in bone marrow lymphocytes of repeated CT scanned mice compared to non-CT

scanned mice (p=0.032) (Figure 7c). When bone marrow was challenged *in vitro* with 1 and 2 Gy, γH2AX fluorescence levels in the bone marrow lymphocytes of the repeated CT scanned mice trended significantly lower than that of non-CT scanned mice (p=0.017). There was a significant 10% reduction in γH2AX fluorescence levels at the 2 Gy challenge dose (p=0.011). When blood was challenged *in vitro* with 1 and 2 Gy, there were no detectable differences in apoptosis levels between the repeated CT scanned mice and their relative sham controls (p>0.05) (Figure 7b and d). (Note: There was no *in vitro* challenge experiment performed with the MN-RET endpoint due to the *in vivo* nature of MN-RET formation *(25)*.) There were significant reductions in 8-OHdG levels in bone marrow lymphocytes of repeated CT scanned mice compared to non-CT scanned mice following the challenge irradiations (p<0.05) (Figure 7c). However, there was no *in vitro* challenge dose response with 8-OHdG fluorescence levels (p=0.775). For the γH2AX and apoptosis endpoints, there were significant positive correlations with *in vitro* challenge doses up to 2 Gy (p<0.05) (Figure 7b and d).

DISCUSSION

Since its inception in the 1970s, the use of computed tomography (CT) in diagnostic medicine has increase rapidly. In recent years, there have been reports that associate increased cancer risk with the radiation doses from CT procedures *(2, 28)*. The evidence to support these claims relies heavily on the extrapolation of risk models at high-dose radiation exposures. In the current study, we investigated the biological effects of CT scans to further understand the underlying cellular processes associated with the potential risk (or lack thereof) of medical diagnostic CT radiation exposures.

The general attributes often associated with ionizing radiation exposures are genotoxicity and cytotoxicity. Here, we used micronucleated reticulocyte (MN-RET) formation and H2AX phosphorylation as measures of genotoxicity, specifically mis-repaired chromosomal damage and DNA double-stranded breaks (DSBs) *(29, 30)*. We examined levels of apoptosis as an indicator of radiation-induced cytotoxicity. *Trp*53 wild-type mice were used to investigate these biological effects to gain insight into the mechanisms of low-dose radiation risk.

Acute Micronucleated Reticulocyte Response

The *in vivo* flow cytometry-based MN-RET assay is a validated cross-species endpoint that is sensitive to clastogenic damage in hematopoietic cells *(30)*. Most of the work performed with this assay is to support the registration of new pharmaceuticals with the U.S. Food and Drug Administration *(31)*. Here, we determined that the radiation sensitivity of the assay for both gamma rays (662 keV) and CT X-rays (75 kVp) is 10 mGy, which is ten-fold lower than the lowest published dose for this assay *(32)*. We investigated doses that are typical of exposures accompanying radiological diagnostic imaging procedures (0 – 100 mGy) *(10, 11)*. The induction of MN-RETs followed a linear dose-dependent response from 0 to 100 mGy for both gamma rays and CT X-rays (Figure 1). Using multiple linear regressions in the tested dose range, the relative biological effectiveness (RBE) value for CT X-rays, with gamma as the reference, was 1. This RBE value is in agreement with the general risk models for low linear-energy-transfer (LET) radiation qualities, although some studies have purported that the RBE value for low energy X-rays should be higher than 1 *(33, 34)*.

The formation of MN-RETs in peripheral blood is a direct dose-dependent manifestation of mis-repaired DNA damage present in hematopoietic progenitors of reticulocytes. The demonstrated increase in MN-RET levels following CT radiation exposure indicates that CT scans, even at 10 mGy, can cause acute genotoxic damage in the hematopoietic system. Although we and others have demonstrated that this increase in MN-RET frequency disappears to basal levels after 115 hours post-irradiation *(24, 25)*, the long-term consequences of this temporary MN-RET increase is largely unknown. It is likely that the transient formation of MN-RET acts as a sensitive biological dosimeter without any real implications on overall risk. In a separate study, we found that the levels of MN-RETs in *Trp*53 heterozygous mice four months after a cancer-inducing 4 Gy exposure were no different than those in unirradiated controls *(35)*. This lack of correlation between MN-RET levels and long-term risk suggests that MN-RET levels may not be reflective of radiation-induced risk.

Although the MN-RET assay may not be used as a surrogate measure for long term radiation risk, it offers information regarding the cellular processing of DNA damage. There are many reports describing adaptive responses induced by low-dose radiation exposures in the context of micronuclei formation (reviewed in *(21, 36)*). Protective effects against high-dose radiation challenges involve the up-regulation of antioxidants, efficient DNA repair, and damage removal by apoptosis *(16, 21, 37, 38)*. Using the MN-RET assay, the adaptive response was investigated by treating mice with a single 10 mGy CT scan before challenging them *in vivo* with 1 Gy. The kinetics of the adaptive response were also examined by varying the time interval between the priming CT scan and challenge dose, as it has been shown to affect the response *(39, 40)*.

The adaptive response was most prominent when there was a separation of 4 hours between the CT scan and the challenge dose (Figure 2). When the separation was 9 hours, the CT scan treatment caused a sensitization effect that increased the damage response of the 1 Gy challenge dose (p=0.010). A separation of 12 hours or longer between the CT scan and challenge dose did not induce an adaptive response, which supports the hypothesis that adaptive response decays if the time interval threshold between the priming and challenge doses is exceeded *(41)*. The observed adaptive response at 4 hours is in agreement with previously published works *(21, 36, 39-41)*. It has been suggested that 4 hours of protein synthesis is required for full expression of an adaptive response *(42)*. The explanation for the sensitization response at 9 hours is not known. We speculate that this modulation in MN-RET response may involve perturbations in cell cycle kinetics caused by the low-dose CT scans. Priming doses as low as 20 mGy have been shown to cause transient cell cycle delay and alter the distribution of cells within the cell cycle *(21, 43-45)*. Sorensen *et al.* found that in ten human lymphoblastoid cell lines the magnitude and direction of the response to a challenge dose, as measured by micronuclei frequency in binucleated cells, were dependent on the cell cycle stage at the time of irradiation *(36)*.

In the present study, the effect of age on the spontaneous formation of MN-RETs was also studied (Figure 3). There are numerous reports that have shown a positive correlation with age and genomic damage in somatic cells (reviewed in *(32, 46)*). Here, we found no significant differences in spontaneous MN-RET levels in *Trp*53 wild-type mice at 7 weeks old through to 80 weeks old (p=0.615). The results are consistent with previous studies in which MN-RET levels did not differ in unirradiated C57BL/6 and BALB/c mice at 10 weeks old through to 52 weeks old *(32,*

47). Although spontaneous MN-RET levels do not appear to change with age, Dertinger *et al.* have shown that the induction of MN-RET levels following radiation exposure is increased significantly with increasing age *(48)*. This observation may reflect a diminished effectiveness in the cellular processing of clastogenic damage with age.

Acute γH2AX Response

DNA double-stranded breaks are biologically significant lesions that can be caused by ionizing radiation. Using the MN-RET assay, we have demonstrated that there are detectable increases in mis-repaired DNA DSBs following *in vivo* CT scans of varying doses (0 to 100 mGy). We complement this data by assessing the *initial* induction of DNA DSBs from low-dose CT scans via the γH2AX endpoint. Similarly to the MN-RET endpoint, we found that *in vivo* CT scans (0 – 200 mGy) induced a statistically significant linear dose response with respect to γH2AX fluorescence levels in lymphocyte-rich bone marrow cell populations. The minimum dose that can be significantly detected above background levels was 100 mGy, which is in agreement with other studies using the flow cytometry-based γH2AX fluorescence assay *(49-51)*. Using the microscopy-based γH2AX assay, the lowest reported dose detected for *in vivo* CT exposure was ~5 mGy *(52)*.

Although the flow cytometry-based γH2AX assay lacks the dose sensitivity to detect DNA DSBs from CT doses below 100 mGy, it was useful in assessing adaptive responses following *in vitro* challenge radiation doses of 1 and 2 Gy. Giving a 2 Gy challenge dose to bone marrow cells 24 hours after mice were CT scanned induced an adaptive response. The adaptive response was an 11% reduction in γH2AX levels in lymphocyte-rich bone marrow cells of CT scanned mice relative

to non-CT scanned mice ($p<0.05$)(Figure 5). This adaptive response observation contrasts the increase in γH2AX levels in our previous study *(53)*; however, the difference may be due to the kinetics of the response. This study examined γH2AX levels 24 hours after a priming CT scan, whereas the previous study examined it after six hours *(53)*. Similarly, there was no adaptive response observed following the 1 Gy challenge dose. We suspect that the magnitude of the radiation challenge at 1 Gy was insufficient to elicit an adaptive response. In support of this speculation, Sasaki *et al.* showed that the magnitude of the challenge dose can influence the observed presence of an adaptive response *(39)*.

Acute Apoptosis Response

When DNA damage in cells becomes too substantial to repair, cells undergo programmed cell death. We have demonstrated that CT scans can cause DNA DSBs that lead to micronuclei formation in hematopoietic cells. Here, we found that levels of apoptosis in lymphocytes were significantly elevated following *in vivo* CT scans of 50 and 100 mGy (Figure 6). This dose-dependent increase in apoptosis is biologically important as it is an evolutionarily-conserved process by which damaged cells are eliminated.

Following *in vitro* gamma exposure to whole-blood, a dose-dependent increase in apoptosis was observed up to 1 Gy. Although there were no overlapping dose points, the rate (level of apoptosis per dose) at which *in vivo* CT scans induced apoptosis was significantly greater than that of the *in vitro* gamma exposures. For instance, a 100 mGy CT scan induced 26% apoptosis in peripheral lymphocytes compared to 24% apoptosis after a 250 mGy *in vitro* gamma exposure

(Figure 6). It may be possible that CT X-rays are more efficient at eliminating damaged cells than gamma rays. However, this difference in apoptosis rate between CT and gamma radiation exposures can be attributed to differences in the dose rates, and the *in vivo*/*in vitro* experimental setup. Further investigation is required to confirm this observation and its significance.

Biological Effects of Repeated 10 mGy CT scans

In a previous study, we found that repeated 20 mGy CT scans given twice a week for ten consecutive weeks resulted in lower spontaneous MN-RET formation, lower γH2AX levels following radiation challenges, and lower spontaneous and radiation-induced levels of apoptosis *(54)*. We also observed that these effects were in contrast to that of single CT exposures. Specifically, single CT scans exhibited characteristics of radiation sensitization with respect to genotoxicity and cytotoxicity; whereas, repeated CT scans did not induce genomic instability and conferred resistance to larger challenge doses. In the current study, we found similar results with treatments of repeated 10 mGy CT scans given once a week for ten consecutive weeks.

Although it has yet to be confirmed whether MN-RET formation is an appropriate surrogate marker for radiation-induced genomic instability, repeated 10 mGy CT scans did not alter the spontaneous levels of MN-RET formation. Hamasaki *et al.* showed that MN-RET levels remained significantly elevated one year after an *in vivo* 2.5 Gy exposure, and claimed that residual radiation-induced MN-RET formation may reflect aberrant DNA damage repair mechanisms and/or genomic instability *(55)*.

The treatment of repeated 10 mGy CT scans induced γH2AX levels in radiation-challenged bone marrow lymphocytes that trended significantly lower in comparison to non-CT scanned mice. This CT-induced reduction in γH2AX levels was most prominent following an *in vitro* 2 Gy challenge dose. Similarly to the adaptive response observed with H2AX formation following a single CT, we suspect that if higher challenge doses were given, we would observe greater differences in the reduction in γH2AX levels between the repeated CT scanned and non-CT scanned mice. Along with Sasaki *et al. (39)*, Cramers and colleagues showed that with certain biological endpoints, larger challenge doses can elicit more obvious adaptive responses *(45, 56)*.

Low-dose ionizing exposure can cause oxidative stress that consequently up-regulate protective antioxidant mechanisms *(57)*. Here, we used 8-OHdG as a biomarker of oxidative stress DNA damage *(58)*. The production of 8-OHdG is derived from hydroxyl radical attack upon the structure of DNA which leads to GC → TA transversions *(59)*.The detection of 8-OHdG in cells can indicate point mutations and possible genomic instability, which in turn can initiate tumorigenesis. Here, we found that repeated CT scans significantly reduced spontaneous and radiation-challenged DNA oxidative stress damages in bone marrow lymphocytes. This data suggests that repeated CT scans do not increase DNA oxidative stress damage, and can confer resistance to persistent oxidative stress-mediated DNA mutations. The lack of an observable dose-dependent increase in 8-OHdG levels two hours after the *in vitro* challenge irradiations may be due to 8-OHdG kinetics. Umegaki *et al.* demonstrated that 8-OHdG levels in mouse bone marrow cells do not start to increase until 3-5 hours after *in vitro* irradiations and then reach a maximum at 24 hours *(60)*.

In contrast to our previous study that found repeated 20 mGy CT scans (twice a week for 10 weeks) reduced spontaneous and radiation-induced apoptosis levels *(53)*, the treatment of repeated 10 mGy CT scans (once a week for 10 weeks) did not. There are some notable variations between these two studies that may explain the discrepancy in the results. Aside from the differences in CT scan doses, the current study examined apoptosis in peripheral blood lymphocytes using Annexin V+ and 7AAD+ in female mice, whereas the previous study assessed apoptosis in bone marrow lymphocytes using Caspases 3+/7+ in male mice. It may be that the repeated treatment of 10 mGy CT scans is below the threshold to induce an adaptive response as seen with the 20 mGy CT scanning treatment. The discrepancy may also be due to differences in the cell population and/or sex of the mice. Additionally, differences in the biomarkers used to detect apoptosis may contribute to the aforementioned discrepancy. This, however, is unlikely, as both methods of apoptosis analyses have been previously validated *(61, 62)*. Additional experiments are required to determine the exact reason(s) for the observed discrepancy.

CONCLUSION

In summary, single CT scans induced acute chromosomal damage that was measurable by MN-RET formation and γH2AX in hematopoietic cells. Single CT scans also induced a dose-dependent increase in apoptosis that is important for the elimination of damaged cells. For both the MN-RET and γH2AX endpoints, a single 10 mGy CT scan was able to induce an adaptive response, albeit under specific priming and challenge conditions. Repeated CT scans over ten weeks did not cause elevated DNA damage or genomic instability. In fact, there was evidence that repeated CT scans conferred resistance to radiation-induced chromosomal aberrations and DNA

oxidative stress damage. Taken together, this data suggests that low-dose CT scans, whether through increased apoptosis of damaged cells or enhanced protection against oxidative damage, can induce protective adaptations against the genotoxic effects of high-dose radiation exposures.

CONFLICT OF INTERESTS

The authors have no conflict of interests to declare.

ACKNOWLEDGEMENTS

Many thanks are deserved by Mary Ellen Cybulski and Jackie Ferreira for their technical animal experience, Lisa Laframboise for her dedicated laboratory proficiency, Nicole McFarlane for her expertise with flow cytometry, and Chantal Saab and Rod Rhem for their contribution toward the computed tomography aspects of the study. This research was supported by US Department of Energy, Low-dose Research Program (DE-FG02-07ER64343), Natural Sciences and Engineering Research Council of Canada, and CIHR Vanier Post-graduate Scholarship.

TABLE 1

Specifications for Dose Response and Adaptive Response Experiments

i) Dose response and CT scan-induced adaptive response: micronucleated reticulocytes

Dose Response: MN-RETs

Treatment*	CT X-rays # of mice	Gamma # of mice
Sham Control	15 [a]	10 [b]
10 mGy	10 [b]	5
20 mGy	8 [b]	5
30 mGy	3	N/A
40 mGy	3	N/A
50 mGy	5	5
80 mGy	5	N/A
100 mGy	5	5

CT Scan-induced [c] Adaptive Response: MN-RETs

Treatment*	# of mice
Sham Control	5
1 CT Scan	5
1 Gy Gamma	5
1 CT + 4 h + 1 Gy	5
1 CT + 6 h + 1 Gy	5
1 CT + 9 h + 1 Gy	5
1 CT + 12 h + 1 Gy	5
1 CT + 24 h + 1 Gy	5
1 CT + 48 h + 1 Gy	5

ii) Age and spontaneous levels of micronucleated reticulocytes

Spontaneous levels of MN-RETs with Age

Age (weeks old)	7	12	15	19	27	36	43	60	80
# of mice	10	10	10	10	10	10	10	10	10

iii) Dose response and CT scan-induced adaptive response: γH2AX.

CT X-rays Dose Response: γH2AX

Treatment*	# of mice
Sham Control	8 [b]
10 mGy	5
20 mGy	5
50 mGy	6 [b]
100 mGy	6 [b]
200 mGy	3

CT Scan-induced [c] Adaptive Response: γH2AX

Treatment*	# of mice
Sham Control	5 [d]
1 CT Scan	5 [d]

iv) Dose response: Apoptosis

Dose Response: Apoptosis

Treatment*	CT X-rays # of mice	Gamma [e] # of mice
Sham Control	5	20 [b]
50 mGy	6	N/A
100 mGy	6	N/A
250 mGy	N/A	10
500 mGy	N/A	10
1000 mGy	N/A	20 [b]

* All mice were female Trp53 wild-type mice at 7-8 weeks old.

a – pooled data from three independent experiments

b – pooled data from two independent experiments

c – a single 10 mGy CT scan was used as a priming exposure

d – bone marrow samples were challenged with 1 and 2 Gy 24 h after a priming/sham CT scan

e – blood samples were irradiated *in vitro*

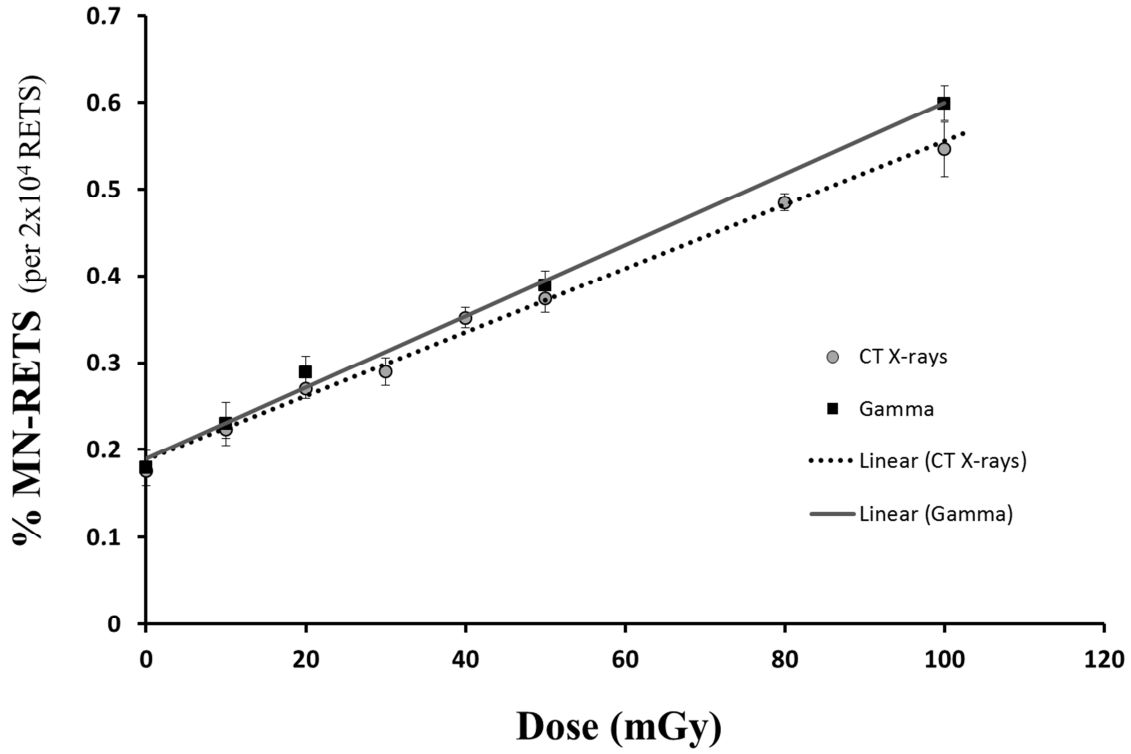

FIG. 1. The induction of MN-RET formation in peripheral blood following in vivo CT scans and in vivo gamma radiation exposures of varying doses; n ≥ 5 mice per dose per radiation quality. Results are sample mean values. Error bars represent standard error of the mean (samples analysed in duplicate).

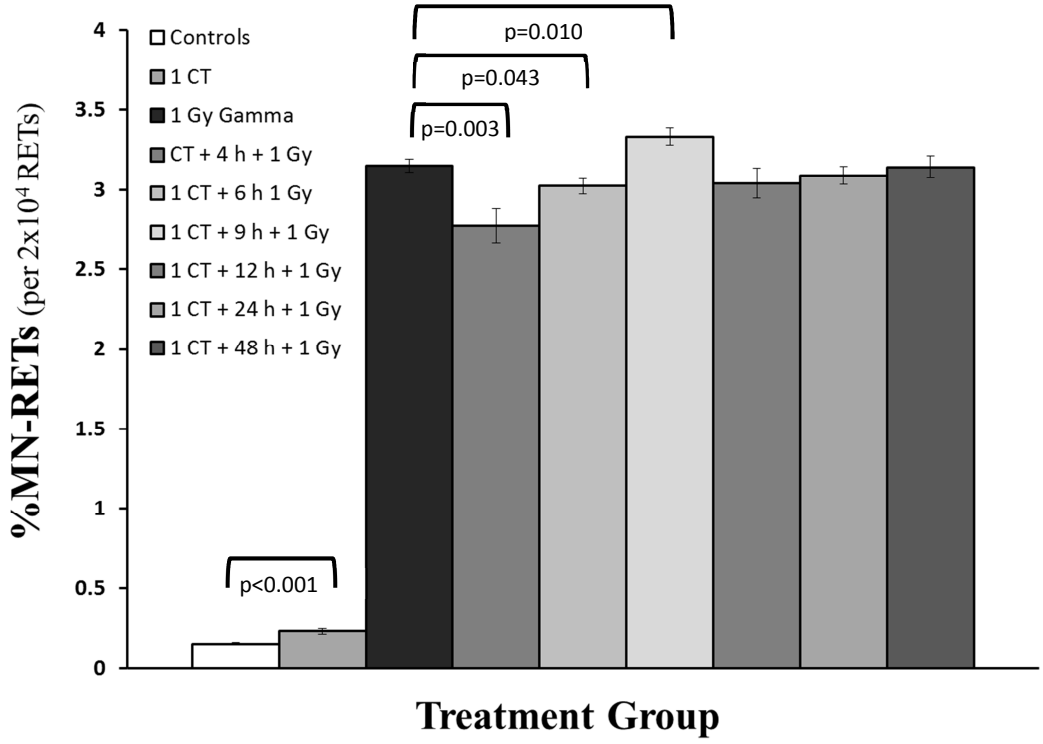

FIG. 2. Adaptive response kinetics for the induction of MN-RET formation after specific time delays between a priming 10 mGy CT scan and *in vivo* γ-radiation challenge dose (1 Gy); n = 3 mice per treatment. Results are sample mean values. Error bars represent standard error of the mean (samples analysed in duplicate).

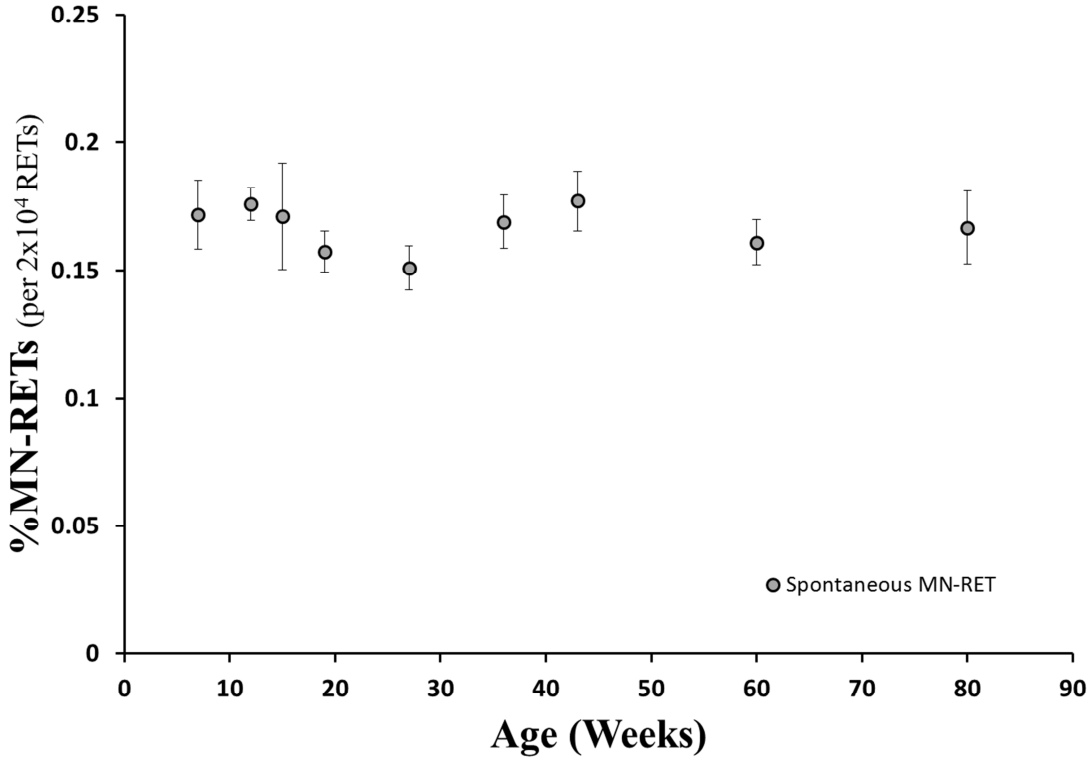

FIG. 3. The spontaneous MN-RET levels in peripheral blood of *Trp*53 wild-type mice assessed at various ages from 7 to 80 weeks old. Each data point represents the mean sample value from a cohort of ten mice followed over a one year period. Error bars represent standard error of the mean (samples analysed in duplicate).

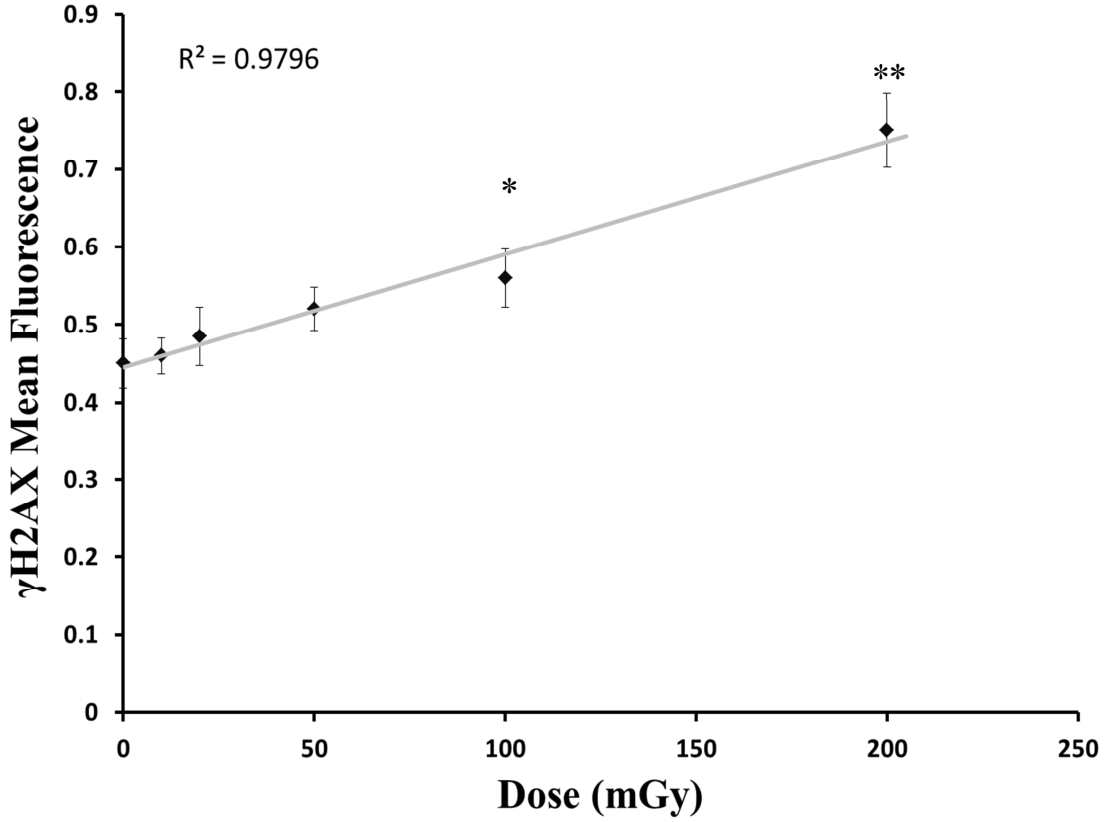

FIG. 4. The mean cellular fluorescence of labelled γH2AX in lymphocyte-rich populations of bone marrow cells following *in vivo* CT scans of varying doses; n ≥ 3 mice per dose. Results are sample mean values. Error bars represent standard error of the mean (samples analysed in duplicate). *, ** denotes $p<0.05$ compared to 0 mGy and 100 mGy, respectively.

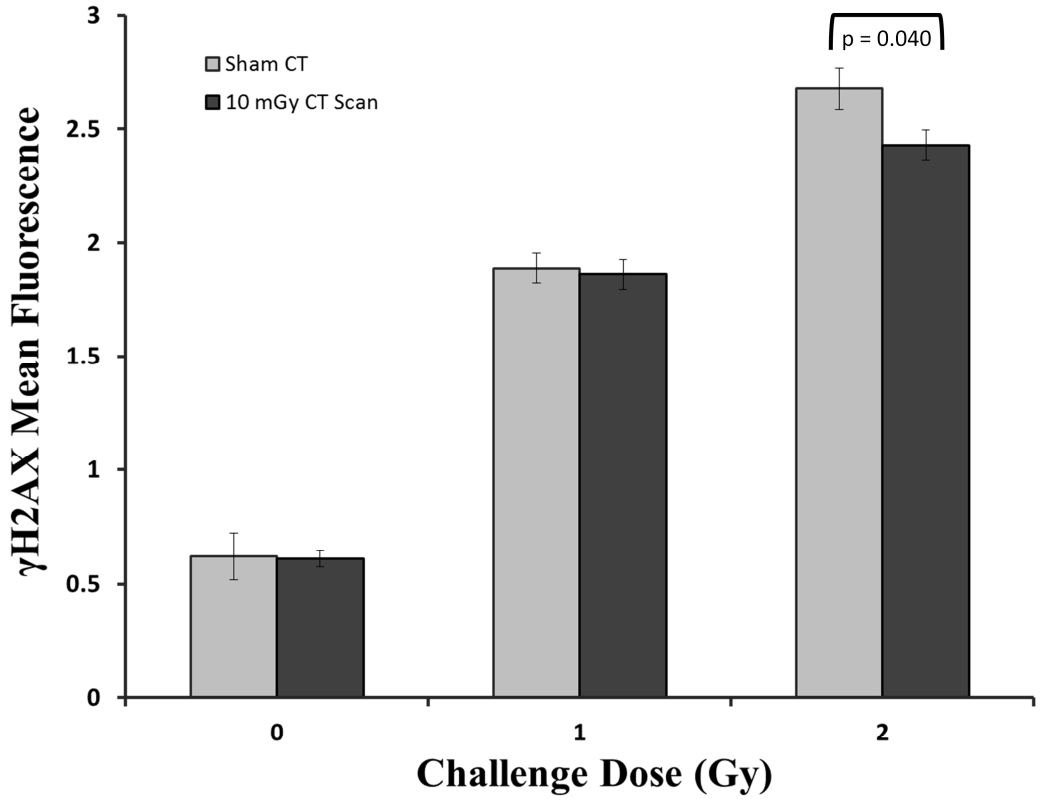

FIG. 5. Mean cellular fluorescence of labelled γH2AX in lymphocyte-rich populations of bone marrow cells after *in vitro* γ-radiation challenge doses of 0, 1 and 2 Gy, 24 hours following a single 10 mGy CT scan; Sham CT: n=5; 10 mGy CT: n=5. Results are sample mean values. Error bars represent standard error of the mean (samples analysed in duplicate).

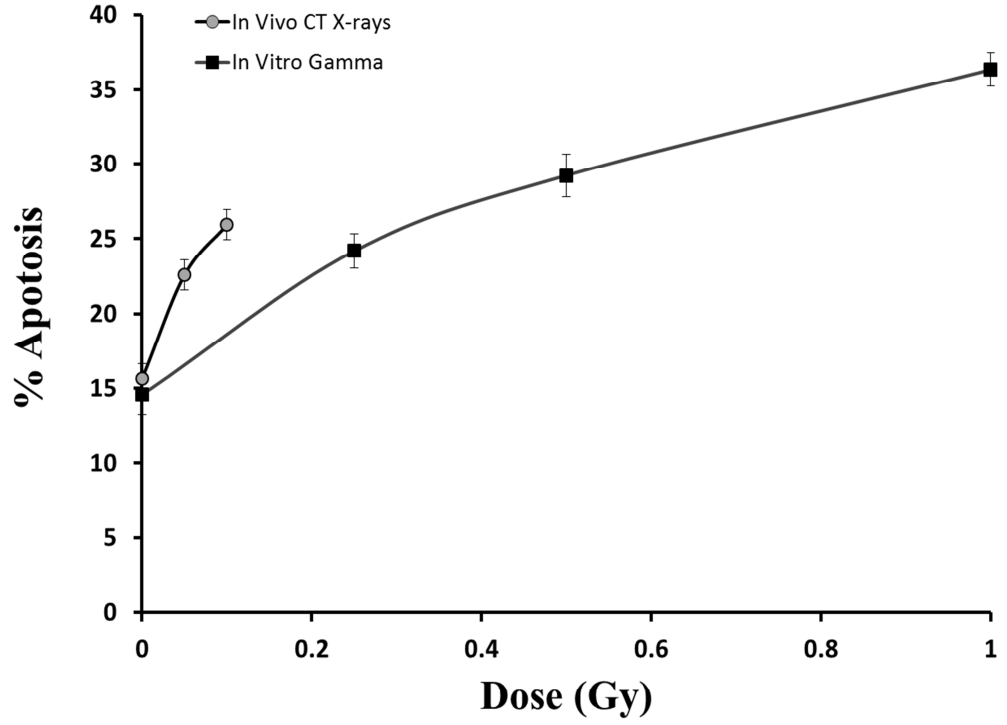

FIG. 6. The induction of apoptosis (Annexin V+, 7AAD+) in peripheral blood CD45+ lymphocytes following *in vivo* CT scans and *in vitro* gamma radiation exposures of varying doses; n ≥ 5 mice per dose per radiation quality. Results are sample mean values. Error bars represent standard error of the mean (samples analysed in duplicate).

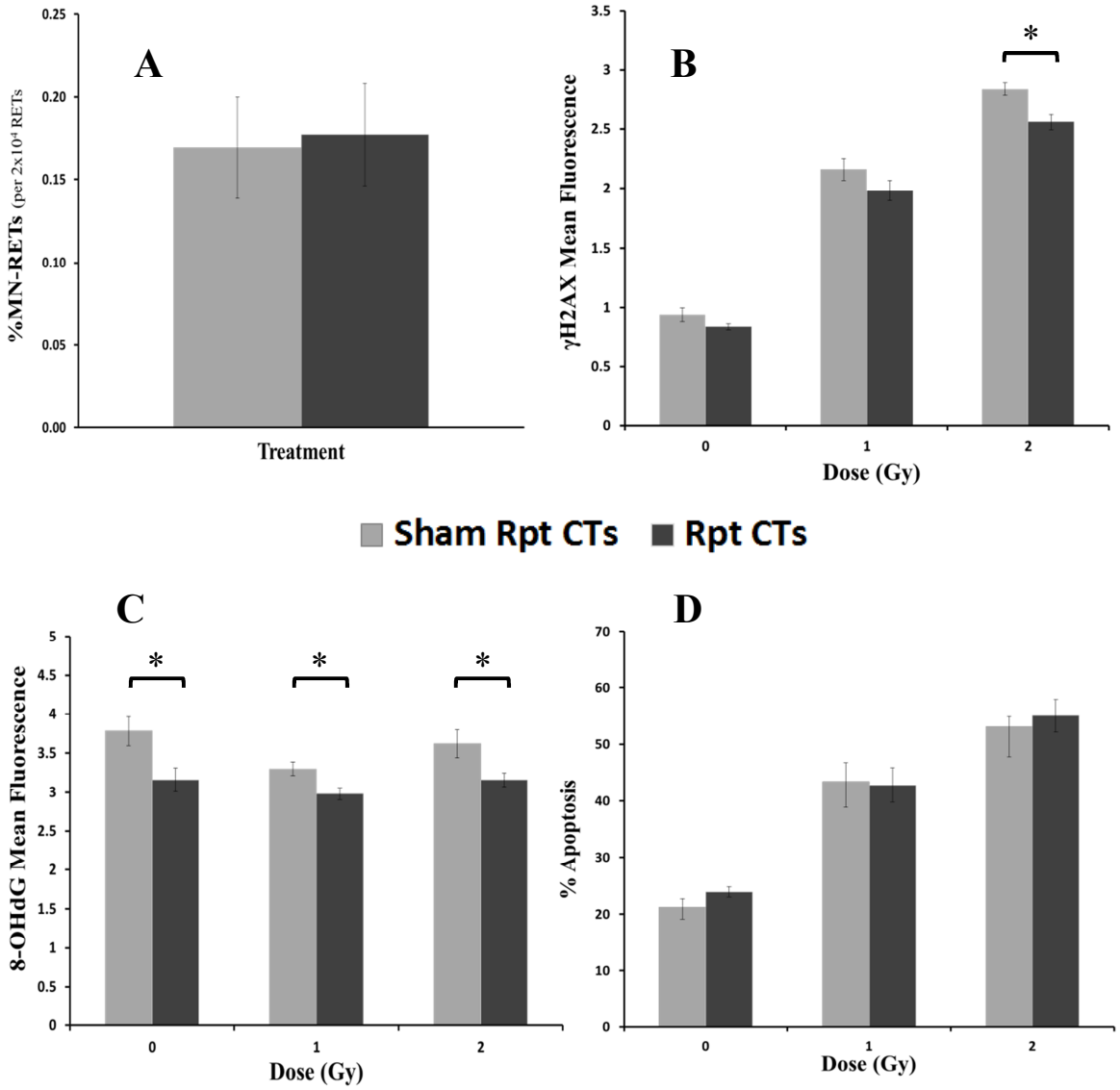

FIG. 7. Acute biological endpoints assessed five days after the last CT scan time point. Sham Rpt CTs: n=5; Rpt CTs: n=5. Results are sample mean values. Error bars represent standard error of the mean (sample analysed in duplicate). * denotes $p<0.05$ **A)** Spontaneous MN-RET levels in peripheral blood. **B)** Mean cellular fluorescence of labelled γH2AX in lymphocyte-rich populations of bone marrow cells after *in vitro* γ-radiation challenge doses of 0, 1 and 2 Gy. **C)** Mean cellular fluorescence of labelled 8-OHdG in lymphocyte-rich populations of bone marrow cells after *in vitro* γ-radiation challenge doses of 0, 1 and 2 Gy. **D)** Apoptosis (Annexin V+, 7AAD+) levels in peripheral blood CD45+ lymphocytes after *in vitro* γ-radiation challenge doses of 0, 1 and 2 Gy.

References

1. Canadian Institute for Health Information. Medical imaging in canada, 2007. Ottawa, ON: CIHI, 2008; 2008.
2. Brenner DJ, Hall EJ. Computed tomography--an increasing source of radiation exposure. N Engl J Med. 2007 Nov 29;357(22):2277-84.
3. Cardis E, Vrijheid M, Blettner M, Gilbert E, Hakama M, Hill C, et al. The 15-country collaborative study of cancer risk among radiation workers in the nuclear industry: Estimates of radiation-related cancer risks. Radiat Res. 2007 Apr;167(4):396-416.
4. Hendry JH, Simon SL, Wojcik A, Sohrabi M, Burkart W, Cardis E, et al. Human exposure to high natural background radiation: What can it teach us about radiation risks? J Radiol Prot. 2009 Jun;29(2A):A29-42.
5. BEIR VII.
Health risks from exposure to low levels of ionizing radiation — BEIR VII. Washington, DC: National Academies Press; 2005.
6. Blecher CM. Alarm about computed tomography scans is unjustified. Med J Aust. 2010 Jun 21;192(12):723-4.
7. Huppmann MV, Johnson WB, Javitt MC. Radiation risks from exposure to chest computed tomography. Semin Ultrasound CT MR. 2010 Feb;31(1):14-28.
8. Smith-Bindman R, Lipson J, Marcus R, Kim KP, Mahesh M, Gould R, et al. Radiation dose associated with common computed tomography examinations and the associated lifetime attributable risk of cancer. Arch Intern Med. 2009 Dec 14;169(22):2078-86.
9. Chen J, Moir D. An estimation of the annual effective dose to the canadian population from medical CT examinations. J Radiol Prot. 2010 Jun;30(2):131-7.
10. Mills DM, Tsai S, Meyer DR, Belden C. Pediatric ophthalmic computed tomographic scanning and associated cancer risk. Am J Ophthalmol. 2006 Dec;142(6):1046-53.
11. Ahmed BA, Connolly BL, Shroff P, Chong AL, Gordon C, Grant R, et al. Cumulative effective doses from radiologic procedures for pediatric oncology patients. Pediatrics. 2010 Oct;126(4):e851-8.
12. Thorne MC. Background radiation: Natural and man-made. J Radiol Prot. 2003 Mar;23(1):29-42.
13. Scott BR. Low-dose radiation risk extrapolation fallacy associated with the linear-no-threshold model. Hum Exp Toxicol. 2008 Feb;27(2):163-8.
14. Feinendegen LE. Evidence for beneficial low level radiation effects and radiation hormesis. Br J Radiol. 2005 Jan;78(925):3-7.
15. Azzam EI, De Toledo SM, Raaphorst GP, Mitchel REJ. Low-dose ionizing radiation decreases the frequency of neoplastic transformation to a level below the spontaneous rate in C3H 10T1/2 cells. Radiat Res. 1996;146(4):369-73.
16. Feinendegen LE, Pollycove M, Sondhaus CA. Responses to low doses of ionizing radiation in biological systems. Nonlinearity Biol Toxicol Med. 2004 Jul;2(3):143-71.

17. Nowosielska EM, Wrembel-Wargocka J, Cheda A, Lisiak E, Janiak MK. Enhanced cytotoxic activity of macrophages and suppressed tumor metastases in mice irradiated with low doses of X- rays. J Radiat Res (Tokyo). 2006 Nov;47(3-4):229-36.
18. Nowosielska EM, Cheda A, Wrembel-Wargocka J, Janiak MK. Anti-neoplastic and immunostimulatory effects of low-dose X-ray fractions in mice. Int J Radiat Biol. 2011 Feb;87(2):202-12.
19. Portess DI, Bauer G, Hill MA, O'Neill P. Low-dose irradiation of nontransformed cells stimulates the selective removal of precancerous cells via intercellular induction of apoptosis. Cancer Res. 2007 Feb 1;67(3):1246-53.
20. Bauer G. Low dose radiation and intercellular induction of apoptosis: Potential implications for the control of oncogenesis. Int J Radiat Biol. 2007 Nov-Dec;83(11-12):873-88.
21. Tapio S, Jacob V. Radioadaptive response revisited. Radiat Environ Biophys. 2007 Mar;46(1):1-12.
22. Mitchel REJ, Jackson JS, Morrison DP, Carlisle SM. Low doses of radiation increase the latency of spontaneous lymphomas and spinal osteosarcomas in cancer-prone, radiation-sensitive Trp53 heterozygous mice. Radiat Res. 2003;159(3):320-7.
23. Jacks T, Remington L, Williams BO, Schmitt EM, Halachmi S, Bronson RT, et al. Tumor spectrum analysis in p53-mutant mice. Curr Biol. 1994 Jan 1;4(1):1-7.
24. Taylor K, Phan N, Boreham DR. Trp53 gene status influences low dose radiation-induced apoptosis and DNA damage in the haematopoietic cells of mice. Mutagenesis. 2011;Submission Pending.
25. Dertinger SD, Tsai Y, Nowak I, Hyrien O, Sun H, Bemis JC, et al. Reticulocyte and micronucleated reticulocyte responses to gamma irradiation: Dose-response and time-course profiles measured by flow cytometry. Mutat Res. 2007 Dec 1;634(1-2):119-25.
26. Dertinger SD, Camphausen K, Macgregor JT, Bishop ME, Torous DK, Avlasevich S, et al. Three-color labeling method for flow cytometric measurement of cytogenetic damage in rodent and human blood. Environ Mol Mutagen. 2004;44(5):427-35.
27. Lemon JA, Rollo CD, McFarlane NM, Boreham DR. Radiation-induced apoptosis in mouse lymphocytes is modified by a complex dietary supplement: The effect of genotype and gender. Mutagenesis. 2008 Nov;23(6):465-72.
28. Richards PJ, George J, Metelko M, Brown M. Spine computed tomography doses and cancer induction. Spine (Phila Pa 1976). 2010 Feb 15;35(4):430-3.
29. Redon CE, Nakamura AJ, Martin OA, Parekh PR, Weyemi US, Bonner WM. Recent developments in the use of gamma-H2AX as a quantitative DNA double-strand break biomarker. Aging (Albany NY). 2011 Feb;3(2):168-74.
30. Chen Y, Tsai Y, Nowak I, Wang N, Hyrien O, Wilkins R, et al. Validating high-throughput micronucleus analysis of peripheral reticulocytes for radiation biodosimetry: Benchmark against dicentric and CBMN assays in a mouse model. Health Phys. 2010 Feb;98(2):218-27.

31. Hayashi M, MacGregor JT, Gatehouse DG, Adler ID, Blakey DH, Dertinger SD, et al. In vivo rodent erythrocyte micronucleus assay. II. some aspects of protocol design including repeated treatments, integration with toxicity testing, and automated scoring. Environ Mol Mutagen. 2000;35(3):234-52.
32. Hamasaki K, Imai K, Hayashi T, Nakachi K, Kusunoki Y. Radiation sensitivity and genomic instability in the hematopoietic system: Frequencies of micronucleated reticulocytes in whole-body X-irradiated BALB/c and C57BL/6 mice. Cancer Sci. 2007 Dec;98(12):1840-4.
33. Lehnert A, Dorr W, Lessmann E, Pawelke J. RBE of 10 kV X rays determined for the human mammary epithelial cell line MCF-12A. Radiat Res. 2008 Mar;169(3):330-6.
34. Lehnert A, Lessmann E, Pawelke J, Dorr W. RBE of 25 kV X-rays for the survival and induction of micronuclei in the human mammary epithelial cell line MCF-12A. Radiat Environ Biophys. 2006 Nov;45(4):253-60.
35. Phan N, Taylor K, Boreham DR. Computed tomography scans modify acute biological effects and tumorigenic consequences of prior high-dose radiation exposures in Trp53 heterozygous mice. Radiat.Res. 2011;submission pending.
36. Sorensen KJ, Attix CM, Christian AT, Wyrobek AJ, Tucker JD. Adaptive response induction and variation in human lymphoblastoid cell lines. Mutat Res. 2002 Aug 26;519(1-2):15-24.
37. Feinendegen LE, Pollycove M, Neumann RD. Whole-body responses to low-level radiation exposure: New concepts in mammalian radiobiology. Exp Hematol. 2007 Apr;35(4 Suppl 1):37-46.
38. Pollycove M, Feinendegen LE. Radiation-induced versus endogenous DNA damage: Possible effect of inducible protective responses in mitigating endogenous damage. Hum Exp Toxicol. 2003 Jun;22(6):290,306; discussion 307, 315-7, 319-23.
39. Sasaki MS. On the reaction kinetics of the radioadaptive response in cultured mouse cells. Int J Radiat Biol. 1995 Sep;68(3):281-91.
40. Shadley JD, Afzal V, Wolff S. Characterization of the adaptive response to ionizing radiation induced by low doses of X rays to human lymphocytes. Radiat Res. 1987 Sep;111(3):511-7.
41. Esposito G, Campa A, Pinto M, Simone G, Tabocchini MA, Belli M. Adaptive response: Modelling and experimental studies. Radiat Prot Dosimetry. 2011 Feb;143(2-4):320-4.
42. Youngblom JH, Wiencke JK, Wolff S. Inhibition of the adaptive response of human lymphocytes to very low doses of ionizing radiation by the protein synthesis inhibitor cycloheximide. Mutat Res. 1989 Dec;227(4):257-61.
43. Salone B, Pretazzoli V, Bosi A, Olivieri G. Interaction of low-dose irradiation with subsequent mutagenic treatment: Role of mitotic delay. Mutat Res. 1996 Nov 4;358(2):155-60.
44. Salone B, Grillo R, Aillaud M, Bosi A, Olivieri G. Effects of low-dose (2 cGy) X-ray on cell-cycle kinetics and on induced mitotic delay in human lymphocyte. Mutat Res. 1996 Apr 13;351(2):193-7.

45. Cramers P, Atanasova P, Vrolijk H, Darroudi F, van Zeeland AA, Huiskamp R, et al. Pre-exposure to low doses: Modulation of X-ray-induced dna damage and repair? Radiat Res. 2005 Oct;164(4 Pt 1):383-90.
46. Morley AA. The somatic mutation theory of ageing. Mutat Res. 1995 Oct;338(1-6):19-23.
47. Dass SB, Ali SF, Heflich RH, Casciano DA. Frequency of spontaneous and induced micronuclei in the peripheral blood of aging mice. Mutat Res. 1997 Nov 19;381(1):105-10.
48. Dertinger SD, Bemis JC, Phonethepswath S, Tsai Y, Nowak I, Hyrien O, et al. Reticulocyte and micronucleated reticulocyte responses to gamma irradiation: Effect of age. Mutat Res. 2009 Apr 30;675(1-2):77-80.
49. MacPhail SH, Banath JP, Yu TY, Chu EH, Lambur H, Olive PL. Expression of phosphorylated histone H2AX in cultured cell lines following exposure to X-rays. Int J Radiat Biol. 2003 May;79(5):351-8.
50. MacPhail SH, Banath JP, Yu Y, Chu E, Olive PL. Cell cycle-dependent expression of phosphorylated histone H2AX: Reduced expression in unirradiated but not X-irradiated G1-phase cells. Radiat Res. 2003 Jun;159(6):759-67.
51. Andrievski A, Wilkins RC. The response of gamma-H2AX in human lymphocytes and lymphocytes subsets measured in whole blood cultures. Int J Radiat Biol. 2009 Apr;85(4):369-76.
52. Rothkamm K, Balroop S, Shekhdar J, Fernie P, Goh V. Leukocyte DNA damage after multi-detector row CT: A quantitative biomarker of low-level radiation exposure. Radiology. 2007 Jan;242(1):244-51.
53. Phan N, De Lisio M, Parise G, Boreham DR. Biological effects and adaptive response from single and repeated computed tomography scans in reticulocytes and bone marrow of C57BL/6 mice. Radiat.Res. 2011;Submitted (in review).
54. Phan N, Boreham DR. Health effects from low dose occupational and medical radiation exposure and the role of adaptive response. Health Phys. 2011 Mar;100(3):286-7.
55. Hamasaki K, Imai K, Hayashi T, Nakachi K, Kusunoki Y. Radiation sensitivity and genomic instability in the hematopoietic system: Frequencies of micronucleated reticulocytes in whole-body X-irradiated BALB/c and C57BL/6 mice. Cancer Sci. 2007 Dec;98(12):1840-4.
56. Karu T, Pyatibrat L, Kalendo G. Irradiation with he--ne laser can influence the cytotoxic response of HeLa cells to ionizing radiation. Int J Radiat Biol. 1994 Jun;65(6):691-7.
57. Ermakov AV, Konkova MS, Kostyuk SV, Egolina NA, Efremova LV, Veiko NN. Oxidative stress as a significant factor for development of an adaptive response in irradiated and nonirradiated human lymphocytes after inducing the bystander effect by low-dose X-radiation. Mutat Res. 2009 Oct 2;669(1-2):155-61.
58. Valavanidis A, Vlachogianni T, Fiotakis C. 8-hydroxy-2' -deoxyguanosine (8-OHdG): A critical biomarker of oxidative stress and carcinogenesis. J Environ Sci Health C Environ Carcinog Ecotoxicol Rev. 2009 Apr;27(2):120-39.

59. Cheng KC, Cahill DS, Kasai H, Nishimura S, Loeb LA. 8-hydroxyguanine, an abundant form of oxidative DNA damage, causes G----T and A----C substitutions. J Biol Chem. 1992 Jan 5;267(1):166-72.
60. Umegaki K, Sugisawa A, Shin SJ, Yamada K, Sano M. Different onsets of oxidative damage to DNA and lipids in bone marrow and liver in rats given total body irradiation. Free Radic Biol Med. 2001 Nov 1;31(9):1066-74.
61. Zhang G, Gurtu V, Kain SR, Yan G. Early detection of apoptosis using a fluorescent conjugate of annexin V. BioTechniques. 1997 Sep;23(3):525-31.
62. Woo M, Hakem R, Soengas MS, Duncan GS, Shahinian A, Kagi D, et al. Essential contribution of caspase 3/CPP32 to apoptosis and its associated nuclear changes. Genes Dev. 1998 Mar 15;12(6):806-19.

Chapter 4

Single computed tomography scans prolong survival by increasing cancer latency in Trp53 heterozygous mice

Nghi Phan, Kristina Taylor, and Douglas R. Boreham
Department of Medical Physics and Applied Radiation Sciences,
McMaster University, 1280 Main St. W, Hamilton, Ontario, Canada, L8S 4K1

Manuscript submission pending: Radiat.Res. 2011

Author Contributions:

N. Phan and K. Taylor were responsible for experimental design and data acquisition.
N. Phan was responsible for the interpretation of the results and synthesis of the manuscript.
D. Boreham supervised and guided the research.

ABSTRACT

Previous studies have demonstrated that low doses of ionizing radiation can have protective effects such as reduced cancer risk and increased lifespan. The aim of this study was to investigate cancer development and longevity of cancer-prone mice exposed to a single 10 mGy exposure from either a diagnostic CT scan or γ-radiation. At 7-8 weeks of age, female Trp53+/- mice were randomly assigned to either the control (n=199), CT scan (n=188), or γ-exposure groups (n=187). All mice were monitored daily for adverse health conditions until the time of death. Histopathology examinations were performed on all mice. The median lifespan of CT scanned mice (502 ± 11.2 days) and γ-exposed mice (499 ± 8.9 days) were greater than that of the control mice (484 ± 7.4 days); however only the lifespan of CT scanned mice was statistically significant ($p=0.004$). There were no differences in the frequency of malignant cancers between the radiation-exposed and control mouse groups ($p>0.05$). Among the groups, sarcoma was the most prevalent cancer (70%), followed by lymphoma (20%) and carcinoma (10%). Treatment with a single CT scan caused a significant increase in the latency of sarcoma and carcinoma ($p<0.05$), but not that of lymphoma ($p=0.429$). We conclude that low-dose radiation exposures, specifically a single 10 mGy CT scan, can prolong lifespan by reducing cancer risk in radiosensitive cancer-prone Trp53+/- mice. The data from this investigation adds to the large body of evidence which shows that risk does not increase linearly with dose in the low dose range.

INTRODUCTION

It is well-established that whole-body exposure to large doses of ionizing radiation decreases survival in many living organisms *(1-4)*. In mammals, longevity has been inversely correlated with dose and dose rate; however, doses below 1 Gy have not always followed this linear relationship *(5, 6)*. At low-dose and low dose-rate exposures there are many published studies reporting prolonged survival and reduced risk of cancer and non-cancer diseases *(5-13)*.

In 1947, Lorenz *et al*. were the first to report radiation-induced lifespan prolongation in mammals *(14)*. Male and female LAF_1 mice irradiated with 1.1 mGy for 8 hours per day, 6 days per week had significantly longer mean survival time than unirradiated controls, by nearly 2 months. In 1955, Lorenz *et al*. repeated the study and found a similar enhancement in longevity *(15)*. Later studies by Grahn in 1970 *(16)* and Spalding *et al*. in 1982 *(13)* confirmed the phenomenon that low doses of ionizing radiation can increase average lifespan. More recently, Ishii *et al*. showed that mice irradiated with 150 mGy X-rays twice a week lived over a month longer than unirradiated controls *(17)*. A detailed review of key initial radiation-prolonged lifespan studies is published by Calabrese and Baldwin *(6)*.

Over the past few years, many more studies have investigated the phenomenon of radiation-induced lifespan prolongation *(5, 10-12, 18, 19)*. Most of these studies have looked at x-rays and γ-exposures with respect to tumourigenesis and immune functions. Mice exposed to a single 100 mGy exposure at a low dose rate exhibited increased latency for myeloid leukemia induced by a 1 Gy challenge dose *(19)*. Immune-compromised mice irradiated at a chronic low dose rate have been shown to live longer than unirradiated mice *(12)*. Although low dose and low dose-rate

exposures have been shown to induce protective effects, the notion that all radiation is bad still persists in radiation protection policies and the general public.

One area that has received much attention surrounding low-dose radiation effects is the radiological diagnostic field in medicine. The use of diagnostic imaging modalities such as computed tomography (CT) have increased exponentially in North America, from 3 million CT procedures in 1980 to over 62 million in 2007 *(20)*. CT scans have become an integral part of physicians' routine assessment of patient health. As such, there have been great interest and concern regarding the radiation risk associated with these diagnostic procedures *(21)*. Radiation risk studies, based on linear extrapolation data from high doses, conclude that exposure to any dose, no matter how low, has an associated health risk *(22, 23)*. The normal average dose range estimate for a single CT examination is between 10 to 30 mGy *(24-27)*. In the current study, we investigated the cancer risk and effects on lifespan in cancer-prone *Trp*53+/- mice exposed whole-body to a single 10 mGy diagnostic CT scan and a single 10 mGy γ-exposure. A cancer-prone mouse model was used to simulate the response of a radiation-sensitive population, and to amplify any potential radiation effects. We postulated that low-dose radiation exposures do not increase risk and can, in fact, induce protective effects such as decreased cancer risk and prolonged lifespan.

MATERIALS & METHODS

Animal Breeding and Genotyping

Male *Trp*53 heterozygous (B6.129S2-*Trp*53$^{tm1Tyj/+}$) mice and female *Trp*53 homozygous (129X1/SvJ *Trp*53+/+), both obtained from Jackson Laboratory (Bar Harbor, Maine), were crossed to yield F1 female *Trp*53 heterozygous (+/-) mice. Heterozygosity of the *Trp*53 gene is due to a mutant allele produced by a targeted neo cassette insertion into the *Trp*53 locus, which removes approximately 40% of the coding capacity of *Trp*53 and completely eliminates p53 protein synthesis *(28)*. The *Trp*53 +/- F1 female mice were genotyped prior to random assignment into the appropriate experimental groups (Table 1). A small tail snip was collected when the mice were five weeks old for PCR-based genotyping (procedure previously described *(5, 28)*). Mouse tail snips were genotyped by a third party specializing in mouse genotyping services (Mouse Genotype.; Carlsbad, California).

Animal Housing

Five or fewer mice were housed in solid-bottom polycarbonate cages (27 x 12 x 15.5 cm) containing woodchip bedding (Harlan Sani-Chips, 7090). A stainless steel wire-bar hopper held food (Harlan Lab Diets; Indianapolis, USA) and a water bottle for consumption *ad libitum.* The specific-pathogen-free housing room was maintained at a 12:12-h light:dark photoperiod with an inside air temperature of 23±2^{o}C and 40-80% humidity. All housing, handling, and experimental procedures were approved by the Animal Research Ethics Board at McMaster University and conducted in accordance to the guidelines of the Canadian Council on Animal

Care. Mice were kept for the duration of their natural life span or until euthanasia was required according to strict and objective criteria determined *a priori* in agreement with previous lifetime mouse studies *(5, 18, 19)*.

In vivo 10 mGy Exposures

At 7-8 weeks old*, Trp*53+/- female mice were randomly assigned to one of three treatment groups: control, single 10 mGy CT scan, or single 10 mGy γ-exposure (662keV - Cs^{137}). CT scans were performed using a Gamma Medica X-SPECT Animal Imaging System (Northridge, California) at the following settings: 75kVp, 215μA, 1 mm Al filter, half-value layer 4.28 mm Al. For both the CT scan and γ-exposure treatments, pairs of mice were irradiated in a customized polycarbonate tube at a dose rate of 18.6 mGy/minute. The control group was handled in the same way as the treatment groups, except for the irradiation procedure. Following treatment, mice were returned to specific-pathogen-free housing and allowed to live for the entirety of their normal lifespans.

Overall Health Assessment

Mice were monitored daily for any indications of poor health. In all cases, treatment status was coded with respect to cage cards, necropsy reports, and histological submissions. Objective criteria in accordance with the guidelines of the Canadian Council on Animal Care were set *a priori* to determine the endpoints for euthanasia. For all mice, selected normal and abnormal tissues were fixed in 10% neutral buffered formalin. Vertebrae and heavily mineralized tissues

were further processed in an EDTA (145 g/L) solution to allow for proper paraffin embedding. The paraffin blocks were sectioned on a Leica RM 2165 microtome at 3 µm thickness and stained with hematoxylin and eosin for histological examination. All pathologies were diagnosed by an experienced animal veterinarian pathologist using information from monitoring tags, necropsy reports, and histopathological examinations. Blinded repeat histological samples were re-submitted to the veterinarian pathologist for quality assurance with a 100% demonstrated precision record. When multiple cancers of the same type were found within a mouse, it was classified as being a single observation of that cancer type as not all primary and metastasized cancers can be uniquely distinguished. Conversely, if a mouse had multiple different types of cancers, each cancer type would be classified separately. The measure of cancer latency in this study was defined as the time after treatment (at 7-8 weeks old) to the time of death/euthanasia (days at risk) in mice with histologically confirmed cancers. In animal studies, obtaining accurate measures of cancer latency is often difficult. For example, internal cancers are diagnosed after death, and they may or may not have been the cause of death. The definition of cancer latency in this study permits the evaluation of cancer risk by measuring the days, following radiation exposure, mice have to develop cancer.

Statistical Analyses

Statistical analyses were performed using SigmaPlot version 11.0 (Systat Software Inc., Chicago, Illinois). Data is presented as median ± standard error (SE) with a p value ≤ 0.05 considered statistically significant. The frequencies of different cancer types in the treatment groups were tested for statistical significance using Fisher's Exact test or Chi-squared test. Survival curve

probabilities were analyzed using Kaplan-Meier analysis. Differences in overall lifespan and cancer latency (calculated as *days at risk* after treatment) were analyzed with the Log Rank test. All statistical tests were corrected for multiple comparisons. Survival analyses, except for all-cause mortalities, accounted for competing causes of death via competing risk censoring.

RESULTS

Lifetime Cancer Study

Effects of Single CT Scans and Single γ-Exposures on Survival and Cancer Frequency

Considering all-cause mortalities, *Trp*53+/- mice treated with either a CT scan or γ-exposure had nominally greater lifespans than control mice (Table 1), although only the median lifespan of CT scanned mice was statistically significant ($p=0.004$). At the 50% survival, CT scanned mice (502 ± 11.2 days) lived 18 days longer than control mice (484 ± 7.4 days). This difference widened in the lower 50% survival level, with CT scanned mice living 34 days longer than control mice at the 25% survival level (Figure 1, $p<0.001$).

The total frequency of malignant cancers were not different between any of the mouse groups ($p>0.140$, Table 1). The ratio of cancers per mouse was greater than 1 for control and radiation-exposed groups, as multiple different cancers often developed within the same animal. In the control group there were 36 mice with lymphoma, 138 mice with one or more sarcomas, and 19 mice with one or more carcinomas. Comparatively, the CT scanned group had 45 mice diagnosed with lymphoma, 135 mice with one or more sarcomas, and 11 mice with one or more carcinomas. In the γ-exposed group, there were 43 mice diagnosed with lymphoma, 126 mice

with one or more sarcomas, and 28 mice with one or more carcinomas. The proportions of lymphoma and sarcoma cancers between the mouse groups were not different ($p>0.451$). However, the incidence of carcinoma in the CT scanned group was statistically lower than the other groups ($p=0.013$). For all groups, certain cancer types were more prevalent than others. Sarcomas were by far the most prevalent (~70%), followed by lymphomas (~20%), and carcinomas (~10%) ($p<0.010$). Pooled across the groups and uncorrected for competing risks, the median post-treatment lifespans of mice diagnosed with lymphoma, sarcoma, and carcinoma were 469 ± 11.7 days, 461 ± 4.6 days, and 471.5 ± 11.3 days) ($p=0.681$).

Effects of Single CT Scans and Single γ-Exposures on Lymphoma Frequency and Latency

Radiation exposures from CT scans or γ-radiation did not influence the frequency of mice developing T-cell or B-cell lymphoma, relative to the control group ($p=0.077$) (Table 1). In all groups, the incidence of B-cell lymphoma was more than double that of T-cell lymphoma ($p<0.05$). When accounting for competing causes of death, neither CT scans nor γ-exposures changed the latency of lymphoma development ($p=0.429$) (Figure 2A).

Effects of Single CT Scans and Single γ-Exposures on Sarcoma Frequency and Latency

The frequencies of the different sarcoma subtypes were not altered by CT scans or γ-exposures ($p=0.647$). Of the various sarcoma subtypes, osteosarcoma was the most prevalent, by at least four-fold, across the mouse groups ($p<0.010$) (Table 1). The treatment of a single 10 mGy CT scan increased the latency of sarcoma development, relative to the control group ($p=0.010$)

(Figure 2B). Correcting for competing risks, the median latency of sarcoma in the CT scan group was 30 days greater than that of the control group (495 ± 10.1 days vs.465 ± 7.5 days). At the 25% survival level, the difference in sarcoma latency was still over 30 days between the CT scanned group and control group. There was no difference in sarcoma latency between the γ-exposed group and the control group (p=0.497).

Effects of Single CT Scans and Single γ-Exposures on Carcinoma Frequency

The frequencies of carcinoma and its subtypes were not different between γ-exposed mice and control mice (p=0.141) (Table 1). Mice treated with a single CT scan had a lower incidence of adenocarcinoma relative to the control and γ-exposed groups (3 compared to 12 and 14, respectively) (p<0.046). When corrected for competing causes of death, CT scans delayed the latency of carcinoma, relative to the other groups (p<0.016) (Figure 2C).

DISCUSSION

A single whole-body exposure to a 10 mGy CT scan at 7-8 weeks of age can significantly increase the median lifespan in cancer-prone *Trp*53+/- female mice by nearly three weeks (p=0.004). A similar prolongation of lifespan, relative to control mice, was observed but not statistically significant for the 10 mGy γ-exposure (p=0.372). In the same mouse model, Mitchel *et al*. also reported a non-significant increase in lifespan following a 10 mGy γ-exposure. With sample sizes of nearly 200 mice per group, the present study had sufficient statistical power (0.8) to detect differences in median lifespans of at least 26 days. Recently, Carlisle *et al*. reported that in

*Trp*53+/- female mice, the life-shortening effect of acute radiation exposure is 38.9 ± 1.9 days per Gy *(4)*. Applying the linear no-threshold hypothesis (i.e. risk of harmful effects increases linearly with dose) to the figure quoted by Carlisle *et al*., the life-shortening effect from a 10 mGy exposure would be less than a day. Although the statistical power in this study was insufficient to detect such a small reduction, a reduction, nonetheless, was to be expected based on this extrapolation. For both CT and γ-radiation exposures, there was no evidence of a reduction in lifespan. Both radiation treatments increased lifespan, although only CT scanning was statistically significant.

While the linear no-threshold hypothesis is generally accepted in radiation risk protection policies, the findings of this paper with respect lifespan do not support it. There are numerous reports that provide evidence to support the biphasic response of radiation exposure. A critical review of past studies on radiation exposure and longevity is published by Calabrese and Baldwin *(6)* and Upton *(7)*.

In the present study, the mechanism(s) responsible for the lifespan extension in CT scanned mice are not fully elucidated. Analysis of cancer latency, as a surrogate measure for cancer risk, in these *Trp*53+/- mice revealed that the observed lifespan extension is due to increased cancer latency, specifically increased sarcoma latency (Figure 2B). Mitchel *et al*. have reported similar findings in this *Trp*53+/- mouse model using a Co^{60} source with a dose rate of 0.5 mGy/minute *(5)*. They showed that a 10 mGy γ-exposure reduced spontaneous cancer risk by increasing the latencies of lymphoma and spinal osteosarcoma. Although the 10 mGy γ-exposure in our study did not replicate these results, the discrepancy may be due to differences in the energy and/or dose rate of the γ-exposures. The γ-radiation energy from a Co^{60} source is ~1.3 MeV compared

to 0.662 MeV for the Cs^{137} source used in our study. The 0.5 mGy/minute dose rate used by Mitchel *et al*. is over 35 times lower than our dose-rate of 18.6 Gy/minute. The influences of radiation energy and dose rate on longevity have been documented previously *(29-33)*.

Many hypotheses have been put forward for the mechanism(s) behind the lifespan extension following both acute *(5, 6, 34)* and chronic exposure *(7, 10, 12, 32, 35)* to low doses of radiation. Two popular hypotheses are radiation-induced stimulation of immune functions and radiation-induced protective effects against neoplastic diseases. Although these are two different hypotheses, they may not be distinctly unrelated. It has been postulated that radiation-enhanced immune responses keeps oncogenic cells under surveillance, and thereby restricting the development of neoplastic diseases *(32, 36-38)*. Nowosielska *et al*. demonstrated that BALB/c mice irradiated *in vivo* with a single 100 mGy exposure of X-rays displayed enhanced anti-tumour reactions mediated by natural killer cells and cytotoxic macrophages when intravenously injected with L1 tumour cells *(37)*. Other researchers have shown similar up-regulation in immune-mediated anti-neoplastic effects following exposures to doses of X-ray as low as 10 mGy *(38, 39)*. In fact, low-dose exposures of non-transformed cells have been shown to stimulate anti-cancer mechanisms to selectively remove precancerous cells *(36)*.

It is known that high doses of acute radiation exposure ablate immune responses. This is most evident in medical procedures involving bone marrow transplants, where marrow transplant patients receive fractionated exposures up to 20 Gy to eliminate host immune responses *(40)*. At low doses and/or low dose rates, there is evidence that immune responses are improved *(32, 33, 35, 41)*. Liu *et al*. found that mice exposed to 75 mGy of X-rays had T-cell function increased by 212%, relative to non-irradiated controls *(35, 41, 42)*. James *et al*. showed mice exposed to 20

days of γ-radiation at doses between 5 and 40 mGy/day can increase the proliferation of splenic T-cells *(43)*. More recently, Ina *et al*. demonstrated that chronic lifetime γ-radiation exposure (0.35 or 1.2 mGy/hour) in immune-compromised MRL-*lpr/lpr* mice significantly increased lifespan, relative to unirradiated controls *(10)*. The prolongation in lifespan was associated with radiation-induced immunological modifications that ameliorated the ensuing autoimmune diseases *(10, 12)*. A follow-up study by the same group found that low dose-rate irradiation in various wild-type mouse strains (C57BL/6, BALB/c, C3H/He, DBA/1, DBA/2 and CBA) stimulated an increase in CD4+ T cells, CD8 molecules expression, and improved response to immunization *(35)*. Sakai and colleagues found that enhanced immune response was associated with the suppression of T-cell lymphoma in C57B/6 mice that were pre-irradiated with 0.075 Gy of X-rays before four cancer-inducing fractions of 1.8 Gy *(11)*. These studies provide support for the hypothesis that low-dose and low dose-rate exposures stimulate various immune responses that help delay disease on-set and prolong survival.

Low-dose radiation exposures have been shown to stimulate DNA repair processes *(44-46)* and reduce endogenous oxidative DNA damage *(47, 48)*. If the correlation between DNA damage and increased risk of neoplastic formation can be assumed, then it follows that low-dose radiation exposure can reduce the risk of tumourigenesis. In the present study, a single 10 mGy CT scan increased lifespan by delaying the onset of cancer. Others have reported similar delay in cancer latency for radiation-induced myeloid leukemia in CBA/H mice *(19)*, and both spontaneous and radiation-induced lymphoma and osteosarcoma in *Trp*53+/- mice *(5, 18)*. In the cancer-prone AKR mouse strain, mice irradiated with 50 or 150 mGy three or two times a week, respectively, had greater survival than unirradiated controls due to a reduction in lymphoma incidence *(17)*.

In the same mouse strain, Shin *et al*. found that mice irradiated with a chronic low dose rate of 0.7 mGy/hour lived significantly longer than unirradiated mice *(32)*. Additionally, the incidence of lymphoma was 10% lower in the irradiated mice than unirradiated mice *(32)*. Similarly, C57BL/6 mice exposed to continuous whole-body γ-radiation for 450 days, starting 35 days before challenging with cancer-inducing exposures totally 7.2 Gy, had nearly 50% less lymphoma than challenge-only mice *(11)*.

In our study with *Trp*53+/- mice, there were no differences in the frequency and proportions of the cancers that developed among the radiation-exposed and control groups. The distribution of mice developing with sarcoma (70%), lymphoma (20%), and carcinoma (10%) are similar to other published studies *(28, 49, 50)*. The lack of effect on cancer frequency but a delay in cancer latency is corroborated by previous studies investigating the same mouse strain *(5, 18)*. Developing upon the idea proposed by Mitchel *et al*. *(18)*, the major effect of a single low-dose exposure in *Trp*53+/-mice is likely due to a delay in the progression, not elimination, of genomic instability associated with endogenous or exogenous cancer-initiating events. Our other concurrent lifetime cancer study, which investigated the effects of repeat CT scans following a 4 Gy exposure, yielded the same lack of difference in cancer frequency but similar delay in cancer latency *(51)*.

The increase in cancer latency was statistically significant for the development of sarcoma and carcinoma in the CT scan mouse group. However, the significance detected for carcinoma latency is questionable since there were only 11 CT scanned mice with carcinoma in the analysis. Sarcomas accounted for 70% of the mice with cancers, thus, there was great statistical power to detect a real difference. The latter is not true for the small cohort of mice diagnosed with

carcinoma. The detected significance for carcinoma latency requires further evaluation to confirm that it is not an artefact of chance (Figure 2C).

CONCLUSION

We conclude that low-dose radiation exposures, under specific conditions, can prolong lifespan by reducing cancer risk in radiosensitive cancer-prone *Trp*53+/- mice. The observed extension in survival is attributed to protective effects induced by exposure to a single whole-body 10 mGy diagnostic CT scan. These CT radiation-induced effects triggered a tissue-specific increase in cancer latency but not a reduction in cancer frequency. This finding is consistent with the hypothesis that single low-dose exposures delay the progression of spontaneously initiated cells becoming genomically unstable. Taken together, these results demonstrate that low-dose diagnostic CT scans do not increase risk and can, in fact, induce protective effects. The data from this investigation adds to the large collection of evidence which shows that the linear no-threshold hypothesis is incorrect at low doses and cannot be systemically applied in the study of radiation biology.

CONFLICT OF INTERESTS

The authors have no conflict of interests to declare.

ACKNOWLEDGEMENTS

Many thanks are deserved by Mary Ellen Cybulski and Jackie Ferreira for their technical animal experience, Lisa Laframboise and Nicole McFarlane for their dedicated laboratory proficiency, and Chantal Saab and Rod Rhem for their contribution toward the computed tomography aspects of the study. We would also like to thank Dr. Dean Percy for the histopathological analysis of samples, acquisition of representative microscopy images and consultation regarding diseases in Trp53+/- mice. This research was supported by US Department of Energy, Low-dose Research Program (DE-FG02-07ER64343), Natural Sciences and Engineering Research Council of Canada, and CIHR Vanier Post-graduate Scholarship.

TABLE 1 – Frequency of Malignant Cancers in Trp53+/- Mice

Group	*Median ± S.E. Survival* [a]	***Lymphoma*** *T-cell:B-cell*	**Sarcoma**				***Carcinoma***				***Others***	***Total Cancers*** *(per mouse)* [c]
			Osteo	*Hemangio*	*Fibro*	*Others*	*Adeno*	*Squamous Cell*	*Basal Cell*	*Basosquamous Cell*		
Control *(n = 199)*	*484±7.4*	*11:25*	*104*	23	10	16	*12*	*2*	*2*	*4*	*2*	***211*** *(1.06)*
10 mGy CT Scan *(n = 188)*	*502±11.2* *(p=0.004)* [b]	*8:37*	*113*	23	10	14	*3*	*4*	*1*	*4*	*2*	***219*** *(1.16)*
10 mGy Gamma *(n = 187)*	*499±8.9*	*8:35*	*92*	23	14	16	*14*	*2*	*1*	*0*	*3*	***208*** *(1.11)*

[a] For all-causes of death, no correction required for competing risks.

[b] Statistically significant relative to the control group.

[c] No significant differences in cancer frequencies and proportions were detected between the groups (p>0.05).

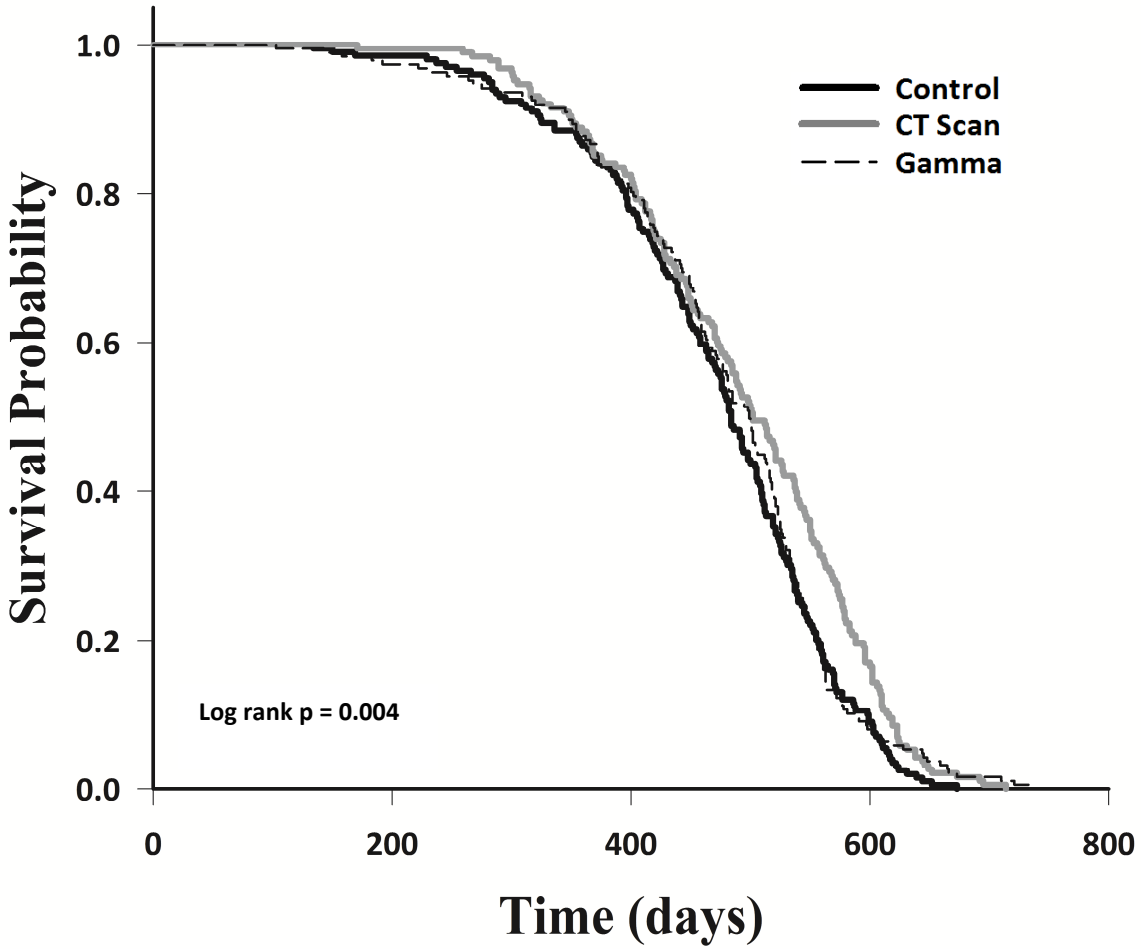

FIG. 1. Comparison of overall survival (all-cause mortality) of control mice (n=199), and mice exposed to either a single 10 mGy CT scan (n=188) or a single 10 mGy γ-exposure (n=187).

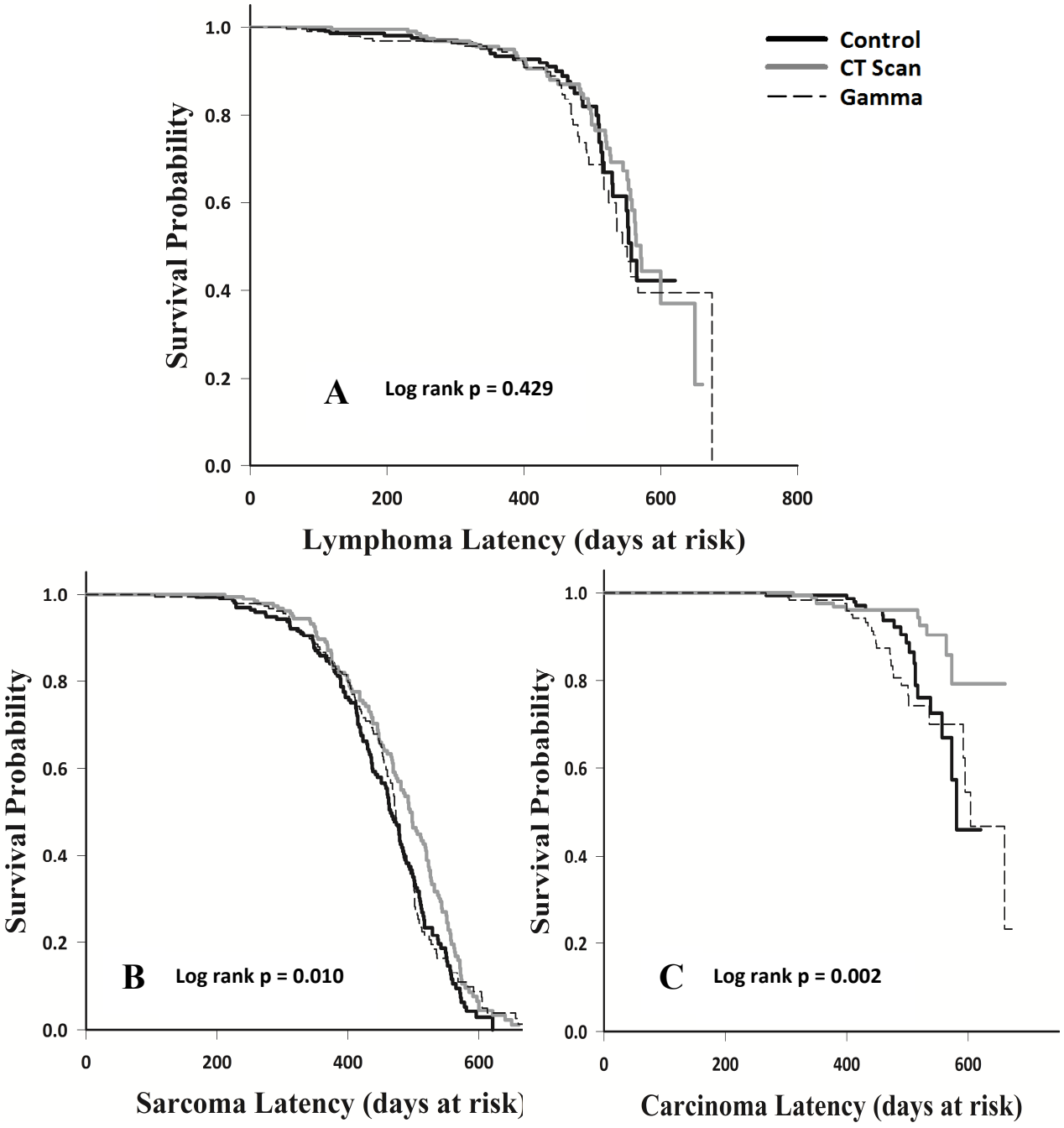

FIG. 2. Comparisons of cancer type-specific latency in Trp53+/- mice of control mice (n=199), and mice exposed to either a single 10 mGy CT scan (n=188) or a single 10 mGy γ-exposure (n=187). Survival probabilities were corrected for competing causes of death. **A)** Latency of mice developing lymphoma. **B)** Latency of mice developing sarcoma. **C)** Latency of mice developing carcinoma.

References

1. Thomson JF, Williamson FS, Grahn D, Ainsworth EJ. Life shortening in mice exposed to fission neutrons and gamma rays I. single and short-term fractionated exposures. Radiat Res. 1981 Jun;86(3):559-72.
2. Thomson JF, Grahn D. Life shortening in mice exposed to fission neutrons and gamma rays. VIII. exposures to continuous gamma radiation. Radiat Res. 1989 Apr;118(1):151-60.
3. Grahn D, Lombard LS, Carnes BA. The comparative tumorigenic effects of fission neutrons and cobalt-60 gamma rays in the B6CF1 mouse. Radiat Res. 1992 Jan;129(1):19-36.
4. Carlisle SM, Burchart PA, Mitchel RE. Cancer and non-cancer risks in normal and cancer-prone Trp53 heterozygous mice exposed to high-dose radiation. Radiat Res. 2010 Jan;173(1):40-8.
5. Mitchel REJ, Jackson JS, Morrison DP, Carlisle SM. Low doses of radiation increase the latency of spontaneous lymphomas and spinal osteosarcomas in cancer-prone, radiation-sensitive Trp53 heterozygous mice. Radiat Res. 2003;159(3):320-7.
6. Calabrese EJ, Baldwin LA. The effects of gamma rays on longevity. Biogerontology. 2000;1(4):309-19.
7. Upton AC. Radiation hormesis: Data and interpretations. Crit Rev Toxicol. 2001 Jul;31(4-5):681-95.
8. Caratero A, Courtade M, Bonnet L, Planel H, Caratero C. Effect of a continuous gamma irradiation at a very low dose on the life span of mice. Gerontology. 1998;44(5):272-6.
9. Courtade M, Caratero A, Jozan S, Pipy B, Caratero C. Influence of continuous, very low-dose gamma-irradiation on the mouse immune system. Int J Radiat Biol. 2001 May;77(5):587-92.
10. Ina Y, Sakai K. Prolongation of life span associated with immunological modification by chronic low-dose-rate irradiation in MRL-lpr/lpr mice. Radiat Res. 2004 Feb;161(2):168-73.
11. Ina Y, Tanooka H, Yamada T, Sakai K. Suppression of thymic lymphoma induction by life-long low-dose-rate irradiation accompanied by immune activation in C57BL/6 mice. Radiat Res. 2005;163(2):153-8.
12. Ina Y, Sakai K. Further study of prolongation of life span associated with immunological modification by chronic low-dose-rate irradiation in MRL-lpr/lpr mice: Effects of whole-life irradiation. Radiat Res. 2005 Apr;163(4):418-23.
13. Spalding JF, Thomas RG, Tietjen GL. Life span of C57 mice as influenced by radiation dose, dose rate, and age at exposure. . 1982;LA-9528(UC-48).
14. LORENZ E, HESTON WE. Biological studies in the tolerance range. Radiology. 1947 Sep;49(3):274-85.
15. Lorenz E, Jacobson LO, Heston W, Shimkin M, Eschenbrenner AB, Deringer MK, et al. Effects of long-continued total-body gamma irradiation of mice, guinea pigs, and rabbits. III. effects of life span, weight, blood picture, and carcinogenesis and the role of the intensity of radiation. Zirkle RE (ed) Biological Effects of External X and Gamma Radiation. 1954:24–248.
16. Grahn D. Biological effects of protracted low dose radiation of man and animal. Fry RJM, Grahn D, Griem ML and Rust JH (eds) Late Effects of Radiation. 1970:101-110.

17. Ishii K, Hosoi Y, Yamada S, Ono T, Sakamoto K. Decreased incidence of thymic lymphoma in AKR mice as a result of chronic, fractionated low-dose total-body X irradiation. Radiat Res. 1996 Nov;146(5):582-5.
18. Mitchel RE, Jackson JS, Carlisle SM. Upper dose thresholds for radiation-induced adaptive response against cancer in high-dose-exposed, cancer-prone, radiation-sensitive Trp53 heterozygous mice. Radiat Res. 2004 Jul;162(1):20-30.
19. Mitchel REJ, Jackson JS, McCann RA, Boreham DR. The adaptive response modifies latency for radiation-induced myeloid leukemia in CBA/H mice. Radiat Res. 1999;152(3):273-9.
20. Brenner DJ, Hall EJ. Computed tomography--an increasing source of radiation exposure. N Engl J Med. 2007 Nov 29;357(22):2277-84.
21. Blecher CM. Alarm about computed tomography scans is unjustified. Med J Aust. 2010 Jun 21;192(12):723-4.
22. Brenner DJ, Sachs RK. Estimating radiation-induced cancer risks at very low doses: Rationale for using a linear no-threshold approach. Radiat Environ Biophys. 2006 Mar;44(4):253-6.
23. Preston RJ. Update on linear non-threshold dose-response model and implications for diagnostic radiology procedures. Health Phys. 2008 Nov;95(5):541-6.
24. Mettler FA,Jr, Wiest PW, Locken JA, Kelsey CA. CT scanning: Patterns of use and dose. J Radiol Prot. 2000 Dec;20(4):353-9.
25. Frush DP, Applegate K. Computed tomography and radiation: Understanding the issues. J Am Coll Radiol. 2004 Feb;1(2):113-9.
26. Fujii K, Aoyama T, Yamauchi-Kawaura C, Koyama S, Yamauchi M, Ko S, et al. Radiation dose evaluation in 64-slice CT examinations with adult and paediatric anthropomorphic phantoms. Br J Radiol. 2009 Dec;82(984):1010-8.
27. Shrimpton PC, Hillier MC, Lewis MA, Dunn M. National survey of doses from CT in the UK: 2003. Br J Radiol. 2006 Dec;79(948):968-80.
28. Jacks T, Remington L, Williams BO, Schmitt EM, Halachmi S, Bronson RT, et al. Tumor spectrum analysis in p53-mutant mice. Curr Biol. 1994 Jan 1;4(1):1-7.
29. Maisin JR, Wambersie A, Gerber GB, Mattelin G, Lambiet-Collier M, De Coster B, et al. Life-shortening and disease incidence in C57Bl mice after single and fractionated gamma and high-energy neutron exposure. Radiat Res. 1988 Feb;113(2):300-17.
30. Maisin JR, Gerber GB, Vankerkom J, Wambersie A. Survival and diseases in C57BL mice exposed to X rays or 3.1 MeV neutrons at an age of 7 or 21 days. Radiat Res. 1996 Oct;146(4):453-60.
31. Thomson JF, Williamson FS, Grahn D. Life shortening in mice exposed to fission neutrons and gamma rays. V. further studies with single low doses. Radiat Res. 1985 Dec;104(3):420-8.
32. Shin SC, Kang YM, Kim HS. Life span and thymic lymphoma incidence in high- and low-dose-rate irradiated AKR/J mice and commonly expressed genes. Radiat Res. 2010 Sep;174(3):341-6.

33. Shin SC, Lee KM, Kang YM, Kim K, Lim SA, Yang KH, et al. Differential expression of immune-associated cancer regulatory genes in low- versus high-dose-rate irradiated AKR/J mice. Genomics. 2011 Jan 23.
34. Calabrese EJ. Overcompensation stimulation: A mechanism for hormetic effects. Crit Rev Toxicol. 2001 Jul;31(4-5):425-70.
35. Ina Y, Sakai K. Activation of immunological network by chronic low-dose-rate irradiation in wild-type mouse strains: Analysis of immune cell populations and surface molecules. Int J Radiat Biol. 2005 Oct;81(10):721-9.
36. Portess DI, Bauer G, Hill MA, O'Neill P. Low-dose irradiation of nontransformed cells stimulates the selective removal of precancerous cells via intercellular induction of apoptosis. Cancer Res. 2007 Feb 1;67(3):1246-53.
37. Nowosielska EM, Wrembel-Wargocka J, Cheda A, Lisiak E, Janiak MK. Enhanced cytotoxic activity of macrophages and suppressed tumor metastases in mice irradiated with low doses of X- rays. J Radiat Res (Tokyo). 2006 Nov;47(3-4):229-36.
38. Cheda A, Wrembel-Wargocka J, Lisiak E, Nowosielska EM, Marciniak M, Janiak MK. Single low doses of X rays inhibit the development of experimental tumor metastases and trigger the activities of NK cells in mice. Radiat Res. 2004 Mar;161(3):335-40.
39. Cheda A, Nowosielska EM, Wrembel-Wargocka J, Janiak MK. Production of cytokines by peritoneal macrophages and splenocytes after exposures of mice to low doses of X-rays. Radiat Environ Biophys. 2008 Apr;47(2):275-83.
40. Wong JY, Liu A, Schultheiss T, Popplewell L, Stein A, Rosenthal J, et al. Targeted total marrow irradiation using three-dimensional image-guided tomographic intensity-modulated radiation therapy: An alternative to standard total body irradiation. Biol Blood Marrow Transplant. 2006 Mar;12(3):306-15.
41. Lacoste-Collin L, Jozan S, Cances-Lauwers V, Pipy B, Gasset G, Caratero C, et al. Effect of continuous irradiation with a very low dose of gamma rays on life span and the immune system in SJL mice prone to B-cell lymphoma. Radiat Res. 2007 Dec;168(6):725-32.
42. Liu SZ, Liu WH, Sun JB. Radiation hormesis: Its expression in the immune system. Health Phys. 1987 May;52(5):579-83.
43. James SJ, Makinodan T. T cell potentiation in normal and autoimmune-prone mice after extended exposure to low doses of ionizing radiation and/or caloric restriction. Int J Radiat Biol Relat Stud Phys Chem Med. 1988 Jan;53(1):137-52.
44. Feinendegen LE, Pollycove M, Neumann RD. Whole-body responses to low-level radiation exposure: New concepts in mammalian radiobiology. Exp Hematol. 2007 Apr;35(4 Suppl 1):37-46.
45. Tapio S, Jacob V. Radioadaptive response revisited. Radiat Environ Biophys. 2007 Mar;46(1):1-12.

46. Otsuka K, Koana T, Tauchi H, Sakai K. Activation of antioxidative enzymes induced by low-dose-rate whole-body gamma irradiation: Adaptive response in terms of initial DNA damage. Radiat Res. 2006 Sep;166(3):474-8.
47. Pollycove M, Feinendegen LE. Radiation-induced versus endogenous DNA damage: Possible effect of inducible protective responses in mitigating endogenous damage. Hum Exp Toxicol. 2003 Jun;22(6):290,306; discussion 307, 315-7, 319-23.
48. Feinendegen LE, Pollycove M, Sondhaus CA. Responses to low doses of ionizing radiation in biological systems. Nonlinearity Biol Toxicol Med. 2004 Jul;2(3):143-71.
49. Flores ER, Sengupta S, Miller JB, Newman JJ, Bronson R, Crowley D, et al. Tumor predisposition in mice mutant for p63 and p73: Evidence for broader tumor suppressor functions for the p53 family. Cancer Cell. 2005 4;7(4):363-73.
50. Baskar R, Ryo H, Nakajima H, Hongyo T, Li L, Syaifudin M, et al. Spontaneous and radiation-induced tumorigenesis in p53-deficient mice. Int Congr Ser. 2002 7;1236:115-8.
51. Phan N, Taylor K, Boreham DR. Computed tomography scans modify acute biological effects and tumorigenic consequences of prior high-dose radiation exposures in Trp53 heterozygous mice. Radiat.Res. 2011;submission pending.

Chapter 5

Computed tomography scans modify acute biological effects and tumorigenic consequences of prior high-dose radiation exposures in Trp53 heterozygous mice

Nghi Phan, Kristina Taylor, and Douglas R. Boreham
Department of Medical Physics and Applied Radiation Sciences,
McMaster University, 1280 Main St. W, Hamilton, Ontario, Canada, L8S 4K1

Manuscript submission pending: Radiat.Res. 2011

Author Contributions:

N. Phan and K. Taylor were responsible for experimental design and data acquisition.
N. Phan was responsible for the interpretation of the results and synthesis of the manuscript.
D. Boreham supervised and guided the research.

ABSTRACT

We have investigated the potential of computed tomography (CT) scans to modify the consequences of a prior high-dose radiation exposure to cancer-prone mice. Female *Trp*53+/- mice were exposed to an acute whole-body 4 Gy dose of γ-radiation. After four weeks, weekly CT scans (10 mGy/scan, 75 kVp) were given for ten consecutive weeks. The acute biological responses and subsequent lifetime cancer risk were investigated. Five days after the last CT scan, there were no detectable differences in the spontaneous levels of micronucleated reticulocytes and histone H2AX phosphorylation in mice given CT scans post-4 Gy compared to 4 Gy alone or unirradiated controls. CT scanned mice had constitutive levels of DNA oxidative stress (8-OHdG) and apoptosis (Annexin V + 7AAD) that were significantly lower (~9% and ~20%, respectively) than non-CT scanned mice ($p<0.05$). Mice in the lifetime investigation were monitored daily to assess the risk of radiation-induced tumorigenesis (i.e. cancer frequency, latency, and mortality). The overall lifespan of mice treated with repeated CT scans post-4 Gy was increased by ~8% compared to mice exposed to 4 Gy-alone ($p=0.017$). Repeated CT scans increased lymphoma latency significantly (~16%, $p=0.040$) but not the latencies of sarcoma or carcinoma. We conclude that repeated CT scans can modify the acute biological responses of a prior high-dose radiation exposure, and delay the progression of specific types of radiation-induced cancers in *Trp*53+/- mice.

INTRODUCTION

Following the detonation of the atomic bombs in Japan over half a century ago, the effects of ionizing radiation have been extensively explored within various biological systems at different levels of organization. From molecules, to cells, to tissues and whole organisms, the research indicates that there are important differences between the consequences of low-dose and high-dose radiation exposure. Acute high-dose radiation has been reported to cause significant increases in chromosomal aberrations, genomic instability, cell death, tissue damage, tumorigenesis, and mortality rates *(1-6)*. Conversely, there is substantial evidence that low-dose and/or low-dose rate exposure can induce an adaptive response that protects against an array of damaging agents, including harmful high-doses of radiation *(7-12)*. The radiation-induced adaptive response is conventionally described as a reduction in the damaging effect(s) associated with a high 'challenge' dose of radiation when preceded by a low 'priming' dose. Here, we broaden the scope of this radiation-induced adaptive response to include protective effects induced by low-dose radiation, both prior to and *following* a high dose exposure.

In this study, we investigated the potential modifying effects of low-dose exposures delivered *after* an acute *in vivo* high-dose radiation exposure in a cancer-prone *Trp*53 (+/-) heterozygous mouse model. Low-dose exposures were delivered via weekly single 10 mGy CT scans for ten consecutive weeks commencing four weeks after a 4 Gy γ-radiation exposure. This experimental schedule was designed to determine the latent genotoxic and cytotoxic effects of a cancer-inducing radiation exposure, and to assess the subsequent modifying responses produced by weekly CT scans. In *Trp*53+/- cancer-prone mice, radiation-induced tumorigenesis is associated with the loss of p53 function and is suggested to be initiated within weeks of a high-dose

radiation exposure. Donehower and colleagues showed that inactivation of p53 two weeks after high-dose irradiation led to the promotion of lymphoma development *(13)*. Reporting complementary results, Evans and colleagues found that activating p53 function two weeks after a high-dose radiation exposure suppressed lymphoma development in mice *(14)*. Presuming that high-dose radiation exposure abrogates p53 function *(15)*, we postulated that a four week period following an acute 4 Gy exposure is sufficient to initiate tumorigenesis in cancer-prone *Trp*53+/- mice. Under this premise, we aimed to investigate the cancer-modifying effects of low-dose fractionated exposures via repeated CT scans.

The rationale behind this experimental design came from cases wherein cancer patients undergo routine CT scans to monitor disease status and progression. Reports by Beyan *et al. (16)* and Pierobon *et al. (17)* found that cumulative diagnostic CT doses can be considerable in patients with lymphoma (median effective dose as high as 518 mSv over a median follow-up period of 7.5 years). Radiation doses in this range have raised concerns of increasing the risk of developing secondary malignancies *(16, 18)*. In the present study, we endeavoured to address these concerns and postulated that repeated diagnostic CT scans may not increase risk, and can potentially provide protective effects such as delaying disease progression and extending overall survival.

The late cancer effects of repeated low-dose radiation exposures following a high-dose radiation challenge have not been investigated previously. There are numerous reports of acute and chronic low-dose exposures reducing cancer incidence *(19-21)*, increasing cancer latency *(22-24)*, and increasing overall survival in various animal models *(19, 20, 25)*. Mitchel *et al.* demonstrated that a single 10 mGy γ-exposure can significantly increase the latency of lymphoma and

osteosarcoma in cancer-prone mice *(22)*. Ina *et al.* reported prolonged lifespan in immune compromised MRL-Ipr/Ipr mice exposed to 1.2 mGy/h for three weeks *(19, 25)*. Similarly, a study by Shin *et al.* showed chronic low-dose rate exposure to AKRJ mice reduced the incidence of lymphoma and extended overall survival, as compared to unirradiated controls *(20)*. Although these studies and many others were able to demonstrate a radiation-induced adaptive response at the whole-animal level, few investigated concurrently the biological mechanisms responsible for the protective phenomenon.

To gain an insight into the biological mechanisms involved in radiation-induced tumorigenesis and the subsequent modifying effects of low-dose CT scans, biological endpoints associated with persistent unstable chromosomal aberrations, residual DNA damage, DNA oxidative stress damage, and apoptosis were examined. One of the best-validated methods for measuring chromosomal damage following radiation exposure is the enumeration of micronuclei formation *(4, 26, 27)*. Micronuclei form in dividing cells that contain unstable chromosome aberrations such as acentric chromosome fragments *(28, 29)*. In most studies, the formation of micronuclei is observed directly in treated cells. Here, we used a flow cytometry-based micronucleated reticulocyte (MN-RET) assay which measures damage manifested in hematopoietic precursor cells, thus providing insight into the processing of upstream damage.

Radiation-induced DNA damage was assessed using histone H2AX phosphorylation as a surrogate biomarker for DNA double-stranded breaks (DSBs) *(30)*. Histone protein in H2AX becomes rapidly phosphorylated to form γH2AX at nascent DNA DSBs sites. Although γH2AX foci are not always indicative of DNA DSBs, Rothkamm *et al.* have quantitatively demonstrated that the detection of γH2AX foci is strongly correlated with the presence of DNA DSBs *(31)*.Measuring

γH2AX levels long after radiation exposure can reveal aberrant DNA repair mechanisms and genomic instability. Elevated levels of γH2AX formation have been noted in tumour cells *(32)*; thus, evaluating γH2AX levels can help discern the DNA related processes involved with radiation-induced tumorigenesis.

Radiation exposure can perturb oxidative stress metabolism within cells *(33)*. Persistently high levels of oxidative stress can deregulate redox homeostasis mechanisms and promote tumour formation through aberrant induction of signalling networks *(34)*. Several different malignancies such as lymphoma and carcinoma have been associated with significantly elevated levels of oxidative stress *(35-37)*. A widely used biomarker of oxidative stress related to DNA damage is 8-hydroxy-2'-deoxyguanosine (8-OHdG) *(38)*. The production of 8-OHdG is derived from hydroxyl radical attack upon the structure of DNA which leads to GC → TA transversions *(39)*. The detection of 8-OHdG in cells can indicate point mutations and possible genomic instability, which in turn can initiate and promote tumorigenesis *(38)*. In the present study, 8-OHdG levels were assessed to determine the link between the modifying effects of low-dose CT scans on DNA oxidative stress damage and radiation-induced tumorigenesis.

When cells become overly damaged and cannot repair themselves effectively, an evolutionary conserved process known as apoptosis is activated. Apoptosis has been shown to be preferentially triggered in cells bearing unstable chromosomal aberrations such as dicentrics, relative to those with balanced translocations *(40)*. This self-regulatory mechanism is beneficial in preventing the accumulation of replication errors and genetic damage from clastogens such as ionizing radiation *(41, 42)*. However, fractionated radiation exposures have been shown to lower basal apoptosis levels, presumably because the remaining cell population is healthier and less

burdened with genetic damage *(43)*. Apoptosis analysis permits the assessment of self-regulatory processes that may be modulated by repeated low-dose CT scans and possibly correlated with radiation-induced tumorigenesis.

In conjunction with acute genotoxic and cytotoxic endpoints, overall lifetime cancer risk measures (e.g. cancer frequency, latency, and mortality) were also assessed. By incorporating acute biological effects with lifetime cancer risk data, this study is poised to explore the cellular processes involved in radiation-induced tumorigenesis. The novelty of this research is that it investigates the modifying effects of low-dose radiation exposures of CT scans after a high-dose cancer-inducing radiation dose. Furthermore, it is clinically insightful, as it investigates concerns of increased secondary malignancy risk due to repeated radiological diagnostic CT procedures.

MATERIALS & METHODS

Animal Breeding and Genotyping

Male *Trp*53 heterozygous (B6.129S2-*Trp*53$^{tm1Tyj/+}$) mice and female *Trp*53 homozygous (129X1/SvJ *Trp*53+/+), both obtained from Jackson Laboratory (Bar Harbor, Maine), were crossed to yield F1 female *Trp*53 heterozygous (+/-) mice. Heterozygosity of the *Trp*53 gene is due to a mutant allele produced by a targeted neo cassette insertion into the *Trp*53 locus, which removes approximately 40% of the coding capacity of *Trp*53 and completely eliminates p53 protein synthesis *(44)*. The *Trp*53 +/- F1 female mice were genotyped prior to random assignment into the appropriate experimental groups (Table 1). A small tail snip was collected when the mice were 5 weeks old for PCR-based genotyping (procedure previously described *(22,*

44)). Mouse tail snips were genotyped by a third party specializing in mouse genotyping services (Mouse Genotype.; Carlsbad, California).

Animal Housing

Five or fewer mice were housed in solid-bottom polycarbonate cages (27 x 12 x 15.5 cm) containing woodchip bedding (Harlan Sani-Chips, 7090). A stainless steel wire-bar hopper held food (Harlan Lab Diets; Indianapolis, USA) and a water bottle for consumption *ad libitum.* The specific-pathogen-free housing room was maintained at a 12:12-h light:dark photoperiod with an inside air temperature of 23±2^{o}C and 40-80% humidity. All housing, handling, and experimental procedures were approved by the Animal Research Ethics Board at McMaster University and conducted in accordance to the guidelines of the Canadian Council on Animal Care. Mice assigned to the lifetime groups were kept for the duration of their natural life span or until euthanasia was required according to strict and objective criteria determined *a priori* in agreement with previous lifetime mouse studies *(22-24)*. The experimental designs of the study are shown in Figure 1.

In vivo Radiation Challenge

Cohorts of mice (7-8 weeks old) were placed in pairs into a customized polycarbonate tube and given a whole-body γ-radiation challenge dose of 4 Gy (662keV - Cs^{137}) at a dose rate of 0.349 Gy/minute (Table 1). The control and CT scan-only groups were sham irradiated (i.e. placed in the polycarbonate tubes for an equal amount of time but with no exposure to radiation).

Following 4 Gy exposure, mice assigned to the lifetime investigation were returned to specific-pathogen-free housing and allowed to live for the entirety of their normal lifespans.

Computed Tomography Protocols

Four weeks after the 4 Gy *in vivo* radiation challenge, assigned groups were given weekly whole-body CT scans for ten consecutive weeks on the same day each week (Wednesday) (Table 1). CT scans were performed on a Gamma Medica X-SPECT Animal Imaging System (Northridge, California). Mice were placed in pairs into the aforementioned customized polycarbonate tubes and given a CT scan (75kVp, 255µA, 1 mm Al filter, half-value layer 4.28 mm Al, 185 projections) with a whole-body absorbed dose of ~10 mGy. Mice were not anaesthetized during the CT scanning procedure as immobilization for image analysis was not necessary.

Computed Tomography Dosimetry

Whole-body dose measurements were obtained using thermoluminescent dosimeter (TLD) chips (Harshaw TLD-100 LiF Chips). TLD chip analyses were performed by a third party specializing in clinical diagnostic radiation measurements (K&S Associates Inc.; Nashville, Tennessee). To measure whole-body absorbed dose in mice, TLD chips were surgically implanted at five locations in a mouse carcass: head, chest, abdomen, above the skin, and under the skin. Measurements were performed on two individual carcasses during the study. The overall uncertainty of the TLD measurement process is 5% at the 95% confidence interval for a single TLD chip at the measurement location. This uncertainty does not take into account minor

variations in the placement of the TLD chips between different mouse carcasses. Consistent dosimetry was confirmed and validated repeatedly throughout the study using a 0.6 cc ionizing chamber (Farmer Dose-meter Model 2570A and PTW Freiburg Model TN30010 Ion Chamber). The calculated average whole-body dose for a CT scan at the aforementioned specifications was 10.3±1.1 mGy, with a dose rate of 18.6 mGy/minute.

In vitro Radiation Challenge

Tissues from mice assigned to the acute biological endpoint investigation were harvested five days after the final CT scan time-point. Blood and bone marrow were collected and separated into three aliquots (1 x 10^6 cells/mL) for *in vitro* radiation challenge of either 0, 1, or 2 Gy at a dose rate of 0.188 Gy/minute (662keV - Cs^{137}). All samples were kept on ice-water slurry (0^oC) during the *in vitro* radiation challenges.

Sample Collection and Cell Preparation

Blood

Blood was collected via cardiac puncture from mice anaesthetized with Isofluorane™. Approximately 500 µL of blood was collected in heparinized syringes, of which 50 µL was immediately aliquoted into 1.5 mL microcentrifuge tubes (VWR International, Mississauga, Ontario) containing 350 µL heparin solution (VWR International, Mississauga, Ontario) for micronucleated reticulocyte (MN-RET) analysis. The remaining blood was kept on ice slurry for

apoptosis analyses. Heparinised blood for the MN-RET assay was maintained at room temperature until fixation (within 3 hours). Following blood collection, mice were euthanized by cervical dislocation.

Bone Marrow

Bone marrow samples were collected by flushing both femurs with a 23 gauge needle containing 1 mL of heparinized RPMI 1640 media (Lonza Inc., Allendale, New Jersey). The disaggregated bone marrow cell suspension was transferred to a 1.5 mL microcentrifuge tube (VWR International, Mississauga, Ontario) and held at 0^{o}C on ice slurry until processing (within 1 hour). Bone marrow cells were counted using a Z2 Coulter Particle Count & Size Analyzer (Beckman-Coulter, Miami, Florida). The cell sample was adjusted to a final concentration of 1×10^{6} cells/mL in ice-cold RPMI 1640 supplemented with 10% fetal bovine serum (FBS, PAA Laboratories Inc., Etobicoke, Ontario), 1% penicillin-streptomycin (Lonza Inc., Allendale, New Jersey), 1% L-glutamine (Lonza Inc., Allendale, New Jersey). Three 1.5 mL replicate aliquots of the cell sample suspension were made for *in vitro* irradiations at 0, 1, and 2 Gy.

Micronucleated Reticulocyte Assay

Reagents

The reagents used for preparing blood specimens for flow cytometric analysis were all from a commercially available kit, Mouse MicroFlowPLUS® (Litron Laboratories, Rochester, NY), and included a heparin-based anticoagulant solution, buffer solution, anti-CD71-FITC, anti-CD61-PE,

RNase, and propidium iodide. Also included was a flow cytometer calibration standard consisting of fixed *Plasmodium berghei*-infected mouse erythrocytes ("malaria biostandard").

Fixation

Cells were fixed in absolute methanol (CAS no. 67-56-1, Sigma Aldrich, Mississauga, Ontario) at -80^{o}C. Up to six samples was fixed at a time using dry ice. This was done to ensure that the temperature of the fixative was maintained between -70^{o}C and -80^{o}C. A 180 µL aliquot of diluted blood suspension was forcibly delivered into a 15 mL conical tube (BD Biosciences, Mississauga, Ontario) containing 2 mL of -80^{o}C methanol. The tubes were vortexed and struck sharply with a pen-size plastic tube several times to break up any aggregates. The fixed samples were stored at -80^{o}C for a minimum of 24 hours before staining and flow cytometric analysis.

Staining and flow cytometric analyses

Methanol-fixed blood samples were washed and labelled for flow cytometric analysis according to procedures detailed in the Mouse MicoFlowPLUS Kit manual (vP4.3m) and previously described in *(45)*. Briefly, fixed blood cells were washed with 12 mL of kit-supplied buffer solution and the pellets were maintained on ice slurry (0^{o}C) until staining (within 4 hour). An 80 uL reagent mixture containing anti-CD71-FITC, anti-CD61-PE, RNase and buffer solution was added to 20 µL aliquot of each fixed blood sample in duplicate. The cells were incubated on ice for 30 minutes followed by 30 minutes at room temperature, and then returned to ice. Immediately before acquisition on the flow cytometer, 1 mL of cold (4^{o}C) propidium iodide (1.25 µg/mL in buffer solution) was added to each tube.

Flow cytometry was performed using a Beckman Coulter EPICS XL flow cytometer (Beckman Coulter, Brea, CA). Cells were analyzed at an average rate of 4000 cells (events) per second. The EPICS XL flow cytometer is equipped with a 488 nm argon laser and four fluorescence detectors. Anti-CD71-FITC, anti-CD61-PE, and propidium iodide fluorescence signals were detected in the FL1 (525±15 nm), FL2 (575±15 nm), and FL3 channels (620±15 nm), respectively. The gating logic used to quantitatively analyse the erythrocyte subpopulations has been described previously *(45)*. Analysis windows were set to quantify the number of reticulocytes (RETs) and MN-RETs for each sample. Representative bivariate graphs illustrating the resolution of the various erythrocyte populations have been published *(45)(46)*. To ensure adequate sample sizes for statistical significance, the number of RETs was measured in a total of $2x10^5$ erythrocytes. The number of MN-RETs was evaluated based on counting a total of $2x10^4$ total RETs per sample.

γH2AX & 8-OHdG Fluorescence Assays

Bone marrow cells were adjusted to $1x10^6$ cells/mL, transferred to 15 mL conical tubes (BD Biosciences, Mississauga, Ontario), and irradiated as described above. Following irradiations, 500 µL aliquots were removed from irradiated cell samples and incubated for 30 minutes and 120 minutes in a 37^0C water bath for the γH2AX and 8-OhdG assays, respectively. After incubation, 3 mL of 70% ethanol at 0^oC was immediately added to each tube. All tubes were maintained on ice slurry (0^oC) for 1 hour. Samples were stored at -20^oC prior to analysis.

For analysis, the fixed bone marrow samples were centrifuged at 5^oC (250 g, 8 minutes) and the supernatant was removed. Cells were then washed in 3 mL of Tris-buffered saline (1x TBS; Trizma base + NaCl, Sigma Aldrich, Mississauga, Ontario), centrifuged (250 g, 8 minutes), re-

suspended in 1 mL of Tris–saline–triton [TST; TBS + 4% FBS (VWR International, Mississauga, Ontario) + 0.1% Triton X-100 (Sigma Aldrich, Mississauga, Ontario)] and incubated on ice for 10 minutes to permeabilize cells. The cells were again centrifuged (250 g, 8 minutes), the supernatant was removed, and cells were re-suspended in 200 µL of a 1:400 dilution of anti-phospho-H2A.X (ser139) antibody (γH2AX; Upstate Cell Signaling, Charlottesville, VA) or anti-8-OHdG antibody (Chemicon International, Temecula, California).

The cell sample containing the primary antibodies were incubated on a tube rocker at room temperature for 2 hours in the dark. The cells were then washed with 3 mL of TST, re-suspended in 200 µL of a 1:500 dilution of AlexaFluor™ 488-conjugated goat anti-rabbit IgG F(ab')2 antibody (*γH2AX)* or AlexaFluor™ 488-conjugated rabbit anti-goat IgG F(ab')2 antibody (8-OHdG) (Invitrogen Canada, Burlington, Ontario) and incubated at room temperature for 1 hour in the dark. The cells were then washed in 3 mL of TBS and re-suspended in 300 µL TBS + 5 µL propidium iodide (1 mg/mL; Sigma Aldrich). Samples were put on ice and promptly analysed on the Epics XL flow cytometer (Beckman Coulter; Brea, CA). Analysis was based on $5x10^3$ cells from the lymphocyte-rich cell population, as determined by flow cytometric scattering patterns. The levels of γH2AX and 8-OHdG fluorescence were measured by examining the mean fluorescence intensity of cells stained with the AlexaFluor™ 488-conjugated goat anti-rabbit IgG F(ab')2 antibody and AlexaFluor™ 488-conjugated rabbit anti-goat IgG F(ab')2 antibody (Invitrogen Canada, Burlington, Ontario), respectively. Each sample was analyzed in duplicate.

Apoptosis Assay

The protocol for the determination of apoptotic cell death by flow cytometry using Annexin V with 7-amino actinomycin D (7AAD) as a counterstain has been previously described in detail *(47)*. Annexin V is an early marker of apoptosis and 7AAD is a cell viability marker. The reagents were purchased as a commercial kit (Annexin V-FITC-7-AAD; IM3614, Beckman Coulter, Mississauga, Ontario). In the current study, additional anti-CD61-PE (Beckman Coulter, Mississauga, Ontario)and anti-CD45-PETR (Invitrogen Canada, Burlington, Ontario) markers were used to identify apoptosis occurring specifically in peripheral blood lymphocytes (CD45+) with the platelet (CD61+) population gated out. Apoptotic lymphocytes were identified as being CD45+, Annexin V+, 7AAD+ and CD61-.

Briefly, each mouse blood sample was divided into three (1 x 10^6 cells/mL) aliquots for 0, 1, and 2 Gy *in vitro* irradiations. Following irradiations on ice-water slurry (0^{o}C) in 5 mL polypropylene assay tubes (Sarstedt, Montreal, Quebec), the blood (100 µl) was incubated in a CO_2 incubator at 37^{o}C for 8 hours. The blood was lysed by adding 2 mL of pre-warmed 1x NH_4Cl (37^{o}C) and incubated at room temperature for 10 minutes. The blood samples were centrifuged (5^{o}C, 250 g, 5 minutes), the supernatant was removed, and the sample tubes were vortexed gently. The samples were then washed with 2 mL of cold Hank's Buffered Salt Solution (HBSS, 5^{o}C) (Invitrogen Canada, Burlington, Ontario) and re-suspended in 250 µL of 1x binding buffer (supplied in kit). To each sample tube, a 100 µL antibody cocktail was added (36 tubes required 3.6 mL of 1x binding buffer, 180 µL of Annexin V, 45 µL of anti-CD45+, 8 µL of anti-CD61+, and 360 µL of 7AAD). Cells were maintained on ice slurry (0^{o}C) and analysed (within 30 minutes) on

the Epics XL flow cytometer (Beckman Coulter; Brea, CA). The percentage of cells dying by apoptosis was determined from an analysis of $5x10^4$ cells.

Overall Health Assessment

Mice in the lifetime cancer risk investigation were monitored and checked daily for any indications of poor health. In all cases, mouse treatment status was coded and undisclosed with respect to cage cards, necropsy reports, and histological submissions. Objective criteria in accordance with the guidelines of the Canadian Council on Animal Care were set *a priori* to determine the endpoints for euthanasia. For all mice, selected normal and abnormal tissues were fixed in 10% neutral buffered formalin. Vertebrae and heavily mineralized tissues were further processed in an EDTA (145 g/L) solution to allow for proper paraffin embedding. The paraffin blocks were sectioned on a Leica RM 2165 microtome at 3 µm thickness and stained with hematoxylin and eosin for histological examination. All pathologies were diagnosed by an experienced animal veterinarian pathologist using information from monitoring tags, necropsy reports, and histopathological examinations. Blinded repeat histological samples were re-submitted to the veterinarian pathologist for quality assurance with a 100% demonstrated precision record. When multiple cancers of the same type were found within a mouse, it was classified as being a single observation of that cancer type, as not all primary and metastasized cancers can be uniquely distinguished. Conversely, if a mouse had multiple different types of cancers, each cancer type would be classified separately. The measure of cancer latency in this study was defined as the time between the 4 Gy exposure to the time of death/euthanasia (days at risk) in mice with histologically confirmed cancers. Although this definition of latency does not

follow the strict conditions often assumed for cancer latency (i.e. time between exposure and clinical onset of cancer), it permits the determination of the days at risk of developing cancer following radiation exposure.

Statistical Analyses

Statistical analyses were performed using SigmaPlot version 11.0 (Systat Software Inc., Chicago, Illinois). Data is presented as mean ± standard error (SE) with a p value ≤ 0.05 considered statistically significant. Error bars depicted in all figures are standard errors of the mean. Dose response significance testing was performed with multiple linear regression analysis. Student's t-tests were carried out to determine if significant differences existed between groups for MN-RET data. Two-way ANOVA with Bonferroni's post-hoc test was used to determine significance between groups for γH2AX and 8-OHdG fluorescence levels, and apoptosis data. The frequencies of different cancer types in the lifetime groups were tested for statistical significance using Fisher's Exact test or Chi-squared test. Survival curve probabilities were analyzed using Kaplan-Meier analysis. Differences in overall lifespan and cancer latency (calculated as *days at risk* after 4 Gy exposure) were analyzed with the Log Rank test. All statistical tests were corrected for multiple comparisons. Survival analyses, except for all-cause mortalities, accounted for competing causes of death via competing risk censoring.

RESULTS

Acute Biological Endpoint Investigation

Micronucleated Reticulocyte

We enumerated MN-RETs in mouse peripheral blood, fifteen weeks after a single acute 4 Gy exposure, to investigate genomic instability. We also explored the potential of repeated 10 mGy CT scans in modifying both spontaneous and radiation-induced MN-RET formation (Figure 2A). We found that exposure to 4 Gy and/or repeated CT scans did not alter MN-RET frequencies from control levels ($p>0.30$).

γH2AX

Five days after the last CT scan time-point, the spontaneous γH2AX fluorescence levels in bone marrow lymphocytes were not significantly different between the various treatment groups ($p=0.421$) (Figure 2B). However, when the bone marrow were given *in vitro* challenge doses of 1 and 2 Gy, mice that received only the repeated CT scans had nearly 10% lower γH2AX fluorescence levels than that of non-CT scanned mice ($p<0.015$). Repeated CT scans after a 4 Gy exposure did not produce the same reduction, relative to 4 Gy alone ($p=0.870$) (Figure 2B). All treatment groups demonstrated a significant positive correlation between mean cellular γH2AX fluorescence levels and *in vitro* γ-radiation doses up to 2 Gy ($p<0.010$).

8-OHdG

As a biomarker for oxidative stress damage to DNA, fluorescence levels of 8-OHdG were measured in bone marrow lymphocyte-rich cell populations to examine the impact of a 4 Gy

exposure and/or repeated CT scans. Mice treated with weekly CT scans showed a significant reduction (> 9%) in spontaneous 8-OHdG fluorescence levels, relative to non-CT scanned mice ($p=0.027$) (Figure 2C). Exposure to 4 Gy alone did not change the spontaneous levels of 8-OHdG, relative to controls ($p=0.723$). When bone marrow was challenged *in vitro* with 1 Gy, there was no modifying effect of the repeated CT scans. However, following an *in vitro* 2 Gy challenge dose, bone marrow from repeatedly CT scanned mice exhibited a reduction in 8-OHdG levels relative to non-CT scanned mice ($p = 0.032$). There was no significant correlation between 8-OHdG mean fluorescence levels and the *in vitro* challenge doses ($p=0.677$) (Figure 2C).

Apoptosis

Apoptotic cell death in peripheral blood CD45+ lymphocytes was measured to assess persistent cytotoxicity following an *in vivo* 4 Gy exposure and subsequent repeated CT scans. Mice exposed exclusively to 4 Gy at 7-8 weeks old did not exhibit differences in apoptotic response, relative to control mice, when measured at 22-23 weeks old ($p>0.05$)(Figure 2D). Mice treated with weekly CT scans exhibited a significant 20% reduction in spontaneous apoptosis levels, compared to non-CT scanned mice ($p=0.038$). When their peripheral blood was challenged *in vitro* with 1 and 2 Gy *in vitro*, the same reduction in apoptosis was observed, relative to non-CT scanned mice ($p<0.05$). The lower apoptosis levels induced by repeated CT scans were not influenced by a prior 4 Gy exposure (i.e. no difference between Rpt CTs vs. 4 Gy + Rpt CTs groups at all doses). There was a significant positive correlation between apoptosis levels and *in vitro* challenge doses up to 2 Gy ($p<0.010$) (Figure 2D).

Lifetime Cancer Risk Investigation

Effects of Repeated CT Scans on Survival and Total Cancer Frequency following 4 Gy Exposure

Considering all-cause mortalities, *Trp*53+/- mice exposed to 4 Gy at 7-8 weeks old had a median lifespan of 246 ± 6.1 days. The median lifespan of mice given ten weekly CT scans post-4 Gy was 258 ± 5.2 days, which is a gain of 12 days (p=0.023) (Figure 3). The frequencies of malignant cancers in the 4 Gy group and the 4 Gy + Rpt CTs group were not statistically different, 256 and 268, respectively. The ratio of cancers per mouse was over 1 for both treatment groups, as multiple different cancers often developed within the same animal in *Trp*53+/- mice *(44, 48)*, especially from subtypes of sarcomas and carcinomas (Table 2). In the 4 Gy-alone group there were 122 mice with lymphoma, 78 mice with one or more sarcomas, and 24 mice with one or more carcinomas. Comparatively, the 4 Gy + Rpt CTs group had 109 mice diagnosed with lymphoma, 84 mice with one or more sarcomas, and 28 mice with one or more carcinomas. The differences in cancer frequencies between the 4 Gy-alone and 4 Gy + Rpt CTs group were not significant (p>0.32). However, within the treatment groups there was a significant difference in the types of cancer that mice developed. In both treatment groups, lymphomas were the most prevalent (~60% of mice), followed by sarcomas (~40% of mice), and carcinomas (~10% of mice) (p < 0.014). Pooled across both treatment groups and uncorrected for competing risks, the median survival post-4 Gy of mice that were diagnosed with lymphoma was ~60 days (173 ± 3.5 days) shorter than the median survival of mice with either sarcoma (233 ± 4.1 days) or carcinoma (232 ± 12.0 days) (p<0.001). There was no difference between the median survival of mice diagnosed with sarcoma and carcinoma (p=0.515).

Effects of Repeated CT Scans on Lymphoma Frequency and Latency following 4 Gy Exposure

The treatment of repeated CT scans following 4 Gy did not influence the frequency of mice developing T-cell or B-cell lymphoma, relative to the 4 Gy-alone group ($p=0.747$) (Table 2). In both groups, the incidence of T-cell lymphoma was three times higher than that of B-cell lymphoma ($p<0.05$). When accounting for competing causes of death, repeated CT scans given after 4 Gy significantly increased lymphoma latency, as reflected by the survival of mice with lymphomas compared to mice exposed to 4 Gy alone ($p=0.040$) (Figure 4A). With non-lymphoma deaths censored, CT scanned mice that were diagnosed with lymphoma had a median latency that was 30 days (~16%) greater than non-CT scanned mice with lymphoma (233 ± 8.0 days vs. 203 ± 6.3 days, $p<0.05$).

Effects of Repeated CT Scans on Sarcoma Frequency and Latency following 4 Gy Exposure

The frequencies of the various sarcoma subtypes were not altered by the treatment of repeated CT scans following the 4 Gy exposure ($p>0.05$). In the group that received only 4 Gy there were 63 mice that had only one sarcoma, 14 mice that had exactly two distinct sarcomas, and one mouse that had three distinct sarcomas. Similarly, in the CT scanned group there were 61 mice that had only one sarcoma, 20 mice that had two distinct sarcomas, and three mice that had three distinct sarcomas. In both treatment groups the most prevalent sarcoma subtypes were osteosarcoma, hemangiosarcoma, and fibrosarcoma. Approximately 50% of mice diagnosed with sarcoma had osteosarcoma, which is a higher proportion than mice diagnosed with either hemangiosarcoma (34%) or fibrosarcoma (33%) ($p<0.05$). The treatment of repeated CT scans

following 4 Gy did not alter the latency of sarcoma development, relative to the 4 Gy alone group (p=0.194) (Figure 4B). Correcting for competing risks, the median latency of sarcoma was similar between the CT scanned group and the 4 Gy-alone group (240 ± 5.9 days vs. 249 ± 3.7 days, p>0.05). There were no significant differences in cancer latency between the treatment groups when stratification analyses were performed on the various sarcoma subtypes (p>0.05).

Effects of Repeated CT Scans on Carcinoma Frequency and Latency following 4 Gy Exposure

The frequencies of overall carcinoma cases and its subtypes were not different between mice that were CT scanned following 4 Gy and mice that were exposed to only 4 Gy (p>0.05). When corrected for competing causes of death there were no differences in the latency of carcinoma between the two mouse groups (p=0.475). With non-carcinoma deaths censored, the median latency for CT scanned mice with carcinoma was 293 ± 11.2 days, compared to 289 ± 7.1 days for non-CT scanned mice with carcinoma (Figure 4C).

DISCUSSION

The genotoxic and cytotoxic effects of high-dose radiation exposure have been well described in mice for a variety of biological endpoints *(4, 49, 50)*. There have also been several studies investigating the tumorigenic effects and survival measures in wild-type and cancer-prone mouse models exposed *in vivo* to different radiation doses and qualities *(5, 6, 51-57)*. Although there are obvious limitations to using a non-human model, similarities between mice and

humans at the cellular level make the findings of this research valuable to the understanding of the biological responses and cancer risk of diagnostic CT radiation at low doses.

At high-dose rates and doses above 500 mGy there is convincing evidence to support that risk is proportional to dose *(2, 2, 58-60)*. However, the biological and health consequences of doses ≤ 100 mGy are still under investigation. One of the earliest investigations of low-dose exposure took place in 1909, and showed that mice given low levels of radiation were protected against bacterial disease *(61)*. Since then, there have been many experiments conducted to elucidate the diverse effects of low-dose radiation *(9, 62-66)*. The induction of a protective response, also known as an adaptive response, following low-dose or low-dose-rate exposures has been reported at the molecular, cellular and organismal level *(21, 25, 66-70)*. In the current study, using *Trp*53 heterozygous cancer-prone mice, we explored the potential effects of repeated low-dose CT scans in modifying the biological responses as well as the late cancer effects of a prior high-dose 4 Gy γ-exposure delivered during adolescence (7-8 weeks old). By examining biological endpoints associated with unstable chromosomal aberrations, persistent genomic instability, DNA oxidative stress damage, and apoptosis, we sought to gain deeper insight into the mechanistic developments associated with radiation-induced tumorigenesis and the possible modifying effects of fractionated low-dose exposure via repeated CT scans.

Acute Biological Responses

The assessment of the biological effects of 4 Gy and/or repeated CT scans was conducted five days after the last CT scan time-point to allow for the overall assessment of the repeated CT

treatment and not the immediate effects of the last CT scan. Radiation-induced genomic instability, genotoxicity, oxidative stress, and cytotoxicity were investigated via micronucleated reticulocyte (MN-RET) formation, H2AX phosphorylation, 8-OHdG oxidative stress, and apoptosis, respectively.

Micronucleated reticulocytes are manifestations of unstable chromosomal aberrations in hematopoietic stem cells. They are enumerated as a measure of acute genotoxicity or induced genomic instability. The average lifespan of reticulocytes *in vivo* is only a few days *(71, 72)*. Thus, examining MN-RET frequency in peripheral blood five days after the last CT scan, which is 15 weeks after the 4 Gy exposure, allowed for the assessment of indirect radiation damage resulting from radiation-induced genomic instability in precursor stem cells. In the current study, *Trp*53+/- mice that were exposed to 4 Gy and/or repeated CT scans did not have differing MN-RET frequencies relative to age-matched unirradiated controls. This observation contrasts with a study performed by Hamasaki *et al*. in which it was reported that one year after a single 2.5 Gy X-ray exposure BALB/c and C57BL/6 mice had significantly elevated MN-RET frequencies *(72)*. However, the elevated MN-RET levels in BALB/c and C57Bl/6 were statistically different. Therefore, the discrepancy between Hamasaki's study and the present one may be associated with differences in mouse strains. Another possible explanation for this discrepancy is the age at which MN-RETs were assessed. Mice in Hamasaki's study were over one year old and mice in our study were 22-23 weeks old. It may be possible that older mice have a diminished capacity to suppress radiation-induced genomic instability, while younger mice still have efficient surveillance mechanisms to limit the manifestation of such damage. This latter postulation is

supported by Dertinger *et al*. who showed that a 1 Gy exposure induces more MN-RET in older mice than younger ones *(73)*.

DNA DSBs, which are marked by the induction of H2AX phosphorylation to produce γH2AX foci, are prevalent consequences of radiation exposures *(11, 74, 75)*. Following an acute exposure to γ-radiation, levels of γH2AX formation reach a maximum at 30 minutes and decrease to background levels within two days (half-life of ~4 hrs) *(76, 77)*. In the current study, γH2AX fluorescence levels were measured in lymphocyte-rich bone marrow cell populations five days after the last CT scan time-point. This timing is important, as elevated levels of γH2AX fluorescence would represent residual DNA DSBs and genomic instability, instead of initial direct radiation damage. Consistent with the observed MN-RET response, spontaneous levels of γH2AX mean fluorescence were not different among the various treatment and control groups. One interpretation of this result is that mice that were exposed to 4 Gy radiation at 7-8 weeks of age did not develop genomic instability after 15 weeks. Rube *et al.* reported that residual DNA damage depends decisively on the underlying cell ability to repair DNA DSBs *(78)*. The lack of an increase in levels of γH2AX may be due to the fact that the relatively young mice still had effective repair capacity to remove radiation-induced DNA damages and limit genomic instability. The same interpretation can be applied to mice exposed to repeated CT scans alone or a 4 Gy exposure prior to those CT scans. Some caution should be taken however, when interpreting these results, since the minimum reported dose detection limit for the employed flow cytometry-based γH2AX assay is approximately 100 mGy *(31, 31, 74, 79, 80)*.

To further explore the existence of an adaptive response, mouse bone marrow cells were challenged *in vitro* with 1 and 2 Gy of γ-radiation. There was a significant reduction in γH2AX

fluorescence levels in mice that received only repeated CT scans, relative to control mice (Figure 2B). This reduction was not observed when 4 Gy preceded the CT scanning regimen. We suspect that the treatment of an *in vivo* 4 Gy exposure ablated the potential for low-dose CT scans to adapt cells with respect to phosphorylation of histone H2AX at this particular analysis time point. Further investigation into the latent impact of a 4 Gy exposure on DNA repair mechanisms and antioxidant pathways is required to explain this phenomenon. It has been suggested that high-dose radiation exposures may induce significant oncogenic stress in proliferating cells (i.e. bone marrow cells) that can keep γH2AX levels relatively static to change, and presumably also to adaption *(81)*.

Ionizing radiation exposure produces reactive oxygen species (ROS) and can perturb oxidative stress metabolism in cells *(82)*. Excessive oxidative stress can cause damage to cell structures, including proteins, lipids, and DNA *(34)*. The most frequent DNA mutations caused by oxidative stress triggered by ionizing radiation are the formations of 8-hydroxy-2'-deoxyguanosine (8-OHdG) *(38, 83)*. There is evidence that persistent elevation of oxidative stress regularly exists in the progeny of irradiated cells whose genomes are unstable *(84, 85)*. In the current study, 8-OHdG levels were assessed following a high-dose 4 Gy exposure and/or repeated low-dose CT scans in lymphocyte-rich bone marrow cell populations of mice. The involvement of repeated CT scans in activating a possible adaptive response associated with oxidative stress was examined. Mice treated with repeated CT scans had lower baseline levels of 8-OHdG than non-CT scanned mice ($p=0.027$) (Figure 2 C). This data suggests that repeated CT scans do not increase DNA oxidative stress damage, and can confer resistance to persistent oxidative stress-mediated DNA mutations in bone marrow lymphocyte progenitor cells.

The main proposed mechanisms to explain the phenomenon of an adaptive response are increased efficiency in DNA repair and/or induction of antioxidant enzymes *(86)*. Several studies have demonstrated that mice given antioxidant drugs and diets were protected against radiation damage and lived significantly longer than untreated controls *(37, 87, 88)*. It is possible that fractionated exposures of ionization radiation associated with repeated CT scans can up-regulate antioxidant enzymes that decrease baseline level of oxidative stress damage (Figure 2C). Supporting this postulation is the fact that fractionated low-dose radiation exposures have been shown to reduce 8-OHdG levels in mice with prion-infection and significantly prolonged their survival *(89)*.

To further examine the protective effects associated with oxidative stress, 8-OHdG levels in mouse bone marrow cells were analysed two hours after an *in vitro* 1 and 2 Gy challenge dose. An adaptive response was only observed in bone marrow of CT scanned mice following the 2 Gy dose. There was a lack of a dose-dependent increase in 8-OHdG levels following the *in vitro* challenge irradiations (Figure 2C). This result questions the interpretive value of the *in vitro* challenge irradiation data for this endpoint. The appearance of 8-OHdG following *in vitro* irradiation has been shown to be highly time dependent. Umegaki *et al.* demonstrated that 8-OHdG levels in mouse bone marrow cells do not start to increase until 3-5 hours after *in vitro* irradiations, and reach a maximum at 24 hours *(83)*. Thus, the lack of a dose-dependent increase in 8-OHdG levels observed two hours after the *in vitro* irradiations may be due to 8-OHdG kinetics and not necessarily an absence of increasing oxidative stress damage following acute radiation exposure.

The CT-induced reduction in basal DNA oxidative stress damage (8-OHdG levels) in lymphocyte-rich bone marrow cells complements the observed apoptosis reduction in peripheral lymphocyte of mice that were repeatedly CT scanned (Figure 2D). Apoptosis is an evolutionary conserved self-regulatory mechanism activated to eliminate cells that are "unfit" or overly burdened with damages *(41, 90, 91)*. Our previous study demonstrated that a single CT scan can increase chromosomal aberrations initially *(43)*. This increase in CT-induced chromosomal damages later disappeared following repeated CT scans, with evidence trending towards a reduction in damages below baseline control levels *(43)*. Redpath *et al.* and Portess *et al*. have published data to support the hypothesis that damaged or pre-transformed cells are stimulated to readily undergo apoptosis following an initial low-dose exposure (e.g. CT scan) *(92-95)*. We postulate that repeated exposures via CT scans would likely maintain the purging of genomically unstable and unfit cells until the majority are eliminated. The remaining cell populations would then be more robust and have fewer chromosomal aberrations. This proposal is supported in the current study by the decrease in γH2AX levels following *in vitro* challenge doses and also the persistent lower baseline 8-OHdG levels in mice that were CT scanned, relative to controls (Figure 2B & 2C). Assuming that these biomarkers reflect reduced genomic instability and DNA oxidative stress damage, the observed apoptosis reduction in peripheral lymphocytes of CT scanned mice is justified. This adaptive apoptosis response was also evident following *in vitro* challenge doses of 1 and 2 Gy for mice given repeated CT scans.

The present study demonstrates that repeated low-dose radiation exposures do not contribute to genomic instability and can confer protection against persistent chromosomal aberrations, DNA oxidative stress damage, and radiation-induced cytotoxicity. In the next section, we draw

correlations between these acute biological effects and the modifying effects of repeat CT scans on high-dose radiation-induced tumorigenesis.

Radiation-induced Cancer Late Effects

High-dose radiation exposures can increase tumorigenesis in many organisms, including humans *(2, 5, 52, 54, 96-99)*. Tumorigenesis is a multistep process that can be initiated or accelerated by genetic lesions caused by high-dose radiation *(51, 100, 101)*. Lately, there have been growing concerns of increased cancer risk from low-dose diagnostic CT scans, especially development of secondary malignancies among cancer patients from follow-up scans *(16, 17)*. In the current study, an *in vivo* 4 Gy exposure was given at 7-8 weeks old to initiate and/or accelerate the tumorigenic effects in cancer-prone *Trp*53+/- mice. A waiting period of four weeks was allowed for the initiation of neoplastic transformation to occur before the repeated 'follow-up' CT scans. We aimed to determine if repeated low-dose CT scans increase cancer risk, and hypothesized that repeated low-dose CT exposures could, in fact, delay the onset of cancer by interrupting the progression stage of tumorigenesis.

The accumulation and persistent elevation of radiation-induced DNA damage due to mis-repair or aberrant apoptotic pathways can lead to mutagenesis and consequently transformation *(60, 78, 102, 103)*. Low-dose exposures have been shown to protect cells against neoplastic transformation following a subsequent large acute challenge dose *(67, 104)*. Acute and chronic low-dose exposures have also been reported to increase cancer latency and overall lifespan in cancer-prone *(22)*, radiation-challenged *(103, 105, 106)*, and immune-compromised mice *(20,*

25, 107). Moreover, low-dose radiation exposures (<150 mGy per fraction) have been used on a clinical trial-basis to treat cancers in humans *(108)*. In the current study, treatment of repeated CT scans significantly extended the overall lifespan of mice post-4 Gy exposure (Figure 3). The CT scanning regimen did not increase the total frequency of malignancies or the frequencies of the various cancer subtypes common to this mouse strain (Table 2). This observation supports the postulation that fractionated low-dose CT exposures do not influence the initiation step of radiation-induced tumorigenesis, but rather the progression stage. In agreement with this interpretation, Mitchel *et al.* reported that the frequencies of the cancer subtypes were not changed by various adapting low-dose radiation treatments in *Trp*53+/- mice, even though cancer latency was extended significantly *(24)*. Mitchel hypothesized that low-dose exposures can modify mechanisms associated with genomic instability and consequently alter the progression rate of initiated cells becoming fully malignant. The present study provides acute biological evidence to support this contention via the observed adaptive response in γH2AX formation, 8-OHdG oxidative stress, and apoptosis in mice treated with CT scans.

It is plausible that weekly low-dose CT X-rays can induce protective mechanisms that are associated with efficient DNA repair. When lymphocyte-rich bone marrow cells were challenged *in vitro* with 1 and 2 Gy, reduced γH2AX levels were observed exclusively in CT scanned mice. This result is presumably due to less DNA damage-induced genomic instability (Figure 2B). We further postulate that repeat CT scans can up-regulate protective antioxidant pathways, and thereby lower DNA oxidative stress damage. The reduction in spontaneous levels of 8-OHdG in bone marrow cells of CT scanned mice supports this argument (Figure 2C). Persistently high levels of oxidative stress can initiate tumorigenesis and accelerate cancer progression *(1, 37, 60)*.

Since there was significant reduction in 8-OHdG levels, we propose that low-dose CT scans can delay tumorigenesis by limiting excessive oxidative stress damage, and ultimately apoptosis, as there would be less damaged cells to eliminate. Extrapolating these protective CT-induced biological responses to the whole animal, it is reasonable to assume that treatments of repeated CT scans can confer resistance against late cancer effects of high-dose radiation at the whole-animal level.

The overall lifespan in CT scanned mice were significantly extended by nearly two weeks following a 4 Gy exposure; however, the main effect was driven by a delay in cancer latency of mice with lymphoma (Figure 4A). The median cancer latency of CT scanned mice that were diagnosed with lymphoma (233 days) was 30 days greater than non-CT scanned mice with lymphoma (203 days) ($p<0.05$). The increase in cancer latency was only seen for lymphoma, not sarcoma or carcinoma malignancies (Figure 4B & 4C). This observation is possibly due to an upper-dose threshold for protective effects that is dependent on tissue type. Mitchel *et al.* found that 100 mGy alone was able to significantly extend lymphoma latency but not the latency of osteosarcoma, whereas 10 mGy alone was able to extend both cancer subtype latencies *(12, 22)*. Thus, it is arguable that the total dose of repeated CT scans (100 mGy) is beyond the protective upper dose threshold for sarcoma and carcinoma malignancies. Additionally, the intrinsic late development of sarcoma and carcinoma relative to lymphoma may limit the potential of low-dose radiation to increase their latencies (Figure 4) *(24)*. We hypothesize that mice with early-onset cancers (e.g. radiation-induced lymphoma) have greater potential to benefit from any protective biological modifications induced by repeated CT scans than mice with late-onset cancers (e.g. sarcoma and carcinoma). The premise for this hypothesis is that increasing the

latency of late-developing cancers is biologically more challenging, as it contends with the limitations of the natural lifespan.

CONCLUSION

We conclude that repeated low-dose CT scans (total dose of 100 mGy) given four weeks after a high-dose 4 Gy exposure do not increase risk of secondary malignancy and can reduce cancer risk in radiation-challenged cancer-prone *Trp*53+/- mice. This protective effect is likely associated with anti-oncogenic mechanisms associated with DNA repair, antioxidant up-regulation, and apoptosis. Assessment of key biological endpoints revealed that mice treated with repeated CT scans demonstrated: 1) no observable measures of genomic instability, 2) resistance to radiation-induced chromosomal aberrations, 3) persistently low levels of DNA oxidative stress damage, and 4) decreased cytotoxicity. Although the CT scans were unable to counteract the initiation processes of radiation-induced tumorigenesis, the fractionated low-dose exposures did delay the progression of cancer type-specific malignancies. From this study, it is evident that fractionated low-dose exposures via CT scans can be an effective post-exposure measure for up-regulating biological responses that are protective against radiation-induced tumorigenesis.

CONFLICT OF INTERESTS

The authors have no conflict of interests to declare.

ACKNOWLEDGEMENTS

Many thanks are deserved by Mary Ellen Cybulski and Jackie Ferreira for their technical animal experience, Lisa Laframboise for her dedicated laboratory proficiency, Nicole McFarlane for her expertise with flow cytometry, and Chantal Saab and Rod Rhem for their contribution toward the computed tomography aspects of the study. We would also like to thank Dr. Dean Percy for the histopathological analysis of samples, acquisition of representative microscopy images and consultation regarding diseases in Trp53+/- mice. This research was supported by US Department of Energy, Low-dose Research Program (DE-FG02-07ER64343), Natural Sciences and Engineering Research Council of Canada, and CIHR Vanier Post-graduate Scholarship.

TABLE 1 – Treatment Groups

	Group[a]		**Treatment** *
Acute Biological Endpoint Study	*Control*	(n=5)	No radiation exposure
	Rpt CTs	(n=5)	Weekly CT scans for 10 weeks (starting @ 11-12 w.o.)
	4 Gy	(n=5)	4 Gy acute exposure (7-8 w.o.)
	4 Gy + Rpt CTs	(n=10)	4 Gy acute exposure (7-8 w.o.) + 10 weekly CT scans (starting @ 11-12 w.o.)
Lifetime Cancer Study	*4 Gy*	(n=203)	4 Gy acute exposure (7-8 w.o.)
	4 Gy + Rpt CTs	(n=198)	4 Gy acute exposure (7-8 w.o.) + 10 weekly CT scans (starting @ 11-12 w.o.)

** Except for the lifetime study groups, all groups were age-matched at time of respective treatments and at the time of tissue collection (22-23 w.o.). Tissue collection (and in vitro irradiations) occurred five days after the last CT scan time point.*

TABLE 2 – Frequency of Malignant Cancers in Trp53+/- Mice Exposed

Group	*Median ± S.E. Survival* [a]	***Lymphoma*** *T-cell:B-cell*	**Sarcoma** *Osteo*	*Hemangio*	*Fibro*	*Others*	***Carcinoma*** *Adeno*	*Squamous Cell*	*Basal Cell*	*Basosquamous Cell*	***Others***	***Total Cancers*** *(per mouse)* [c]
4 Gy *(n = 203)*	*246±6.1*	*97:26*	*36*	21	26	11	*7*	*8*	*5*	*5*	*14*	***256*** *(1.26)*
4 Gy + Rpt CTs *(n = 198)*	*258±5.2* *(p=0.023)* [b]	*84:25*	*41*	33	27	9	*8*	*4*	*8*	*10*	*18*	***268*** *(1.35)*

[a] For all-causes of death, no correction required for competing risks.

[b] Statistically significant relative to the '4 Gy' group.

[c] No significant differences in cancer frequencies and proportions were detected between the '4 Gy' and the '4 Gy + Rpt CTs' groups ($p > 0.05$).

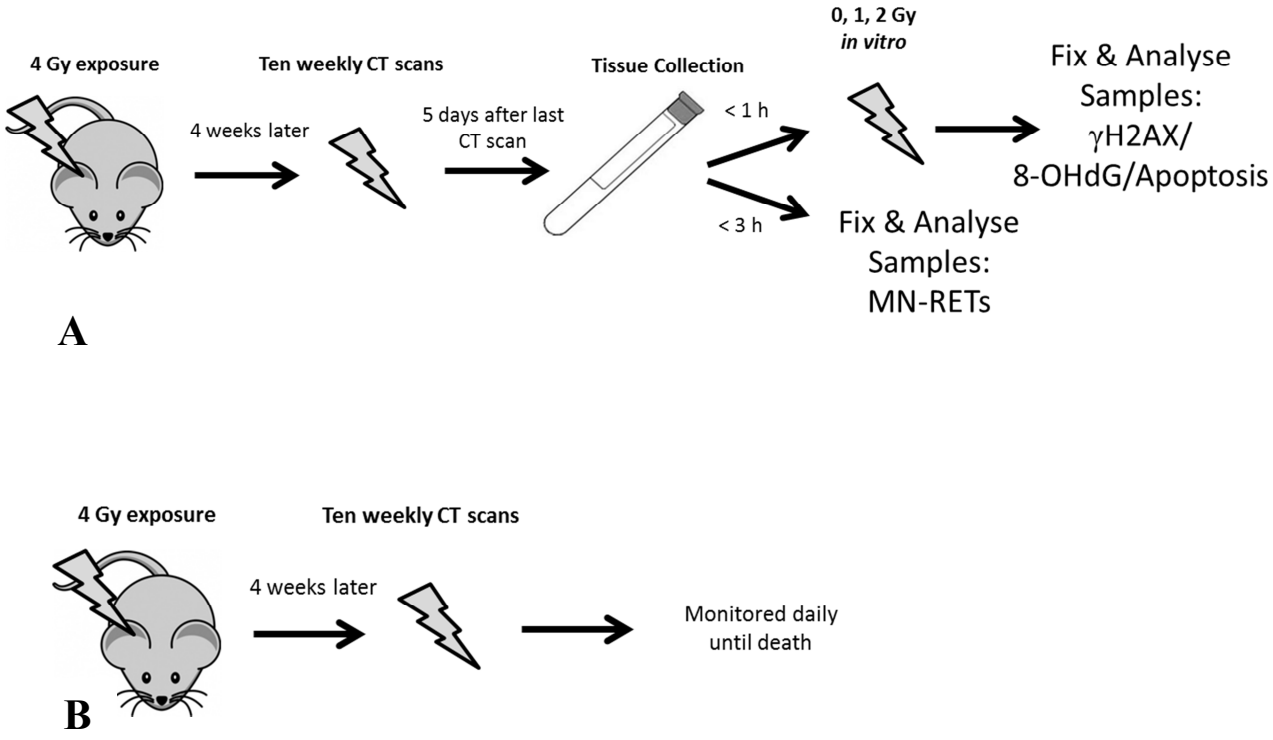

FIG. 1. Experimental designs for A) acute biological endpoint investigation B) lifetime cancer risk investigation. Mice were 7-8 weeks old when exposed to 4 Gy. Mice were 22-23 weeks old when blood and bone marrow were collected for biological endpoint analyses.

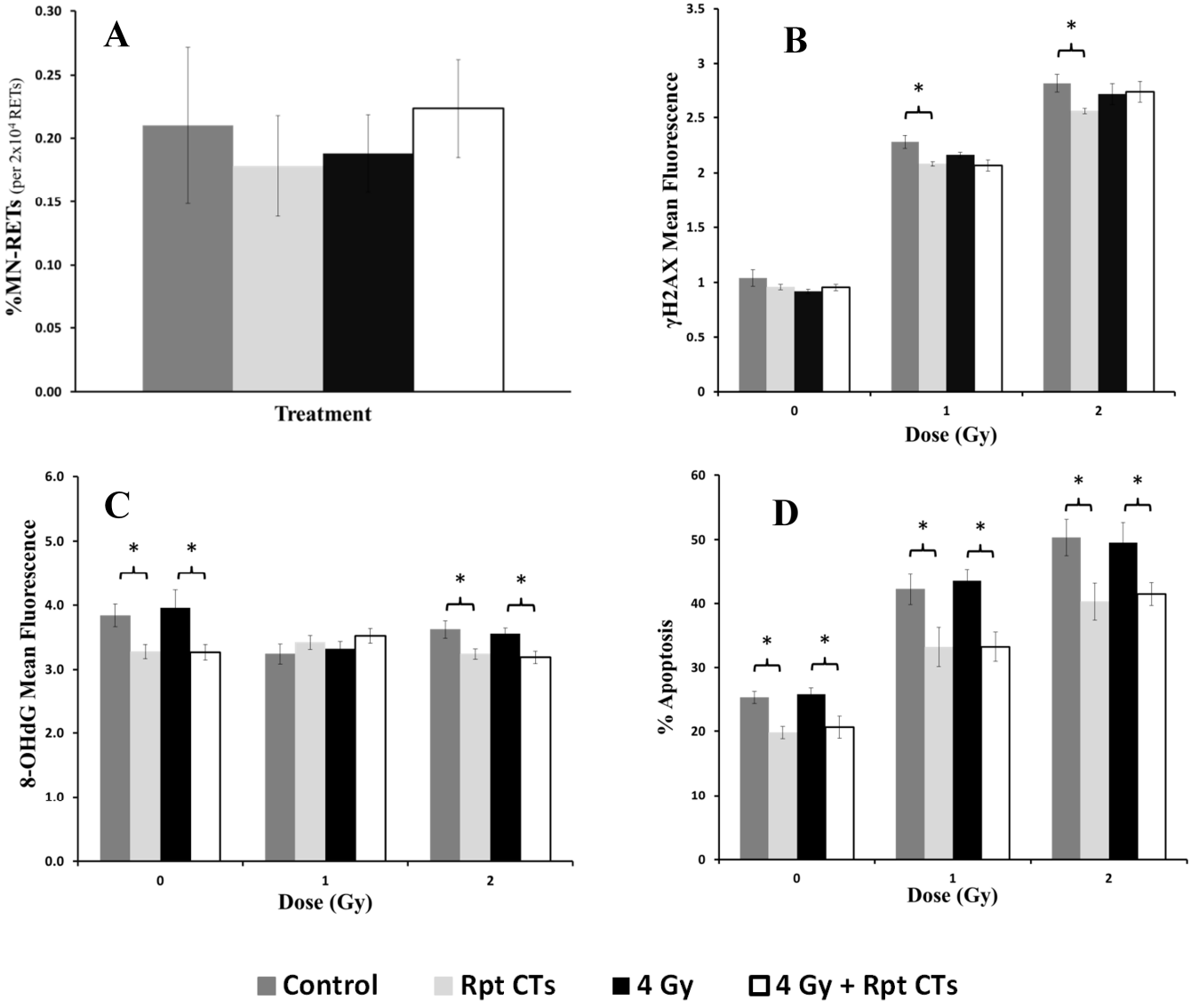

FIG. 2. Acute biological endpoints assessed five days after the last CT scan time point. Control: n=5; Rpt CTs: n=5, 4 Gy: n=5; 4 Gy + Rpt CTs: n=10. Results are sample mean values ± SE (sample analysed in duplicate); * denotes $p<0.05$. **A)** Spontaneous MN-RET frequencies in peripheral blood. **B)** Mean cellular fluorescence of labelled γH2AX in lymphocyte-rich populations of bone marrow cells after *in vitro* γ-radiation challenge doses of 0, 1 and 2 Gy. **C)** Mean cellular fluorescence of labelled 8-OHdG in lymphocyte-rich populations of bone marrow cells after *in vitro* γ-radiation challenge doses of 0, 1 and 2 Gy. **D)** Apoptosis (Annexin V+, 7AAD+) levels in CD45+ peripheral blood lymphocytes after *in vitro* γ-radiation challenge doses of 0, 1 and 2 Gy.

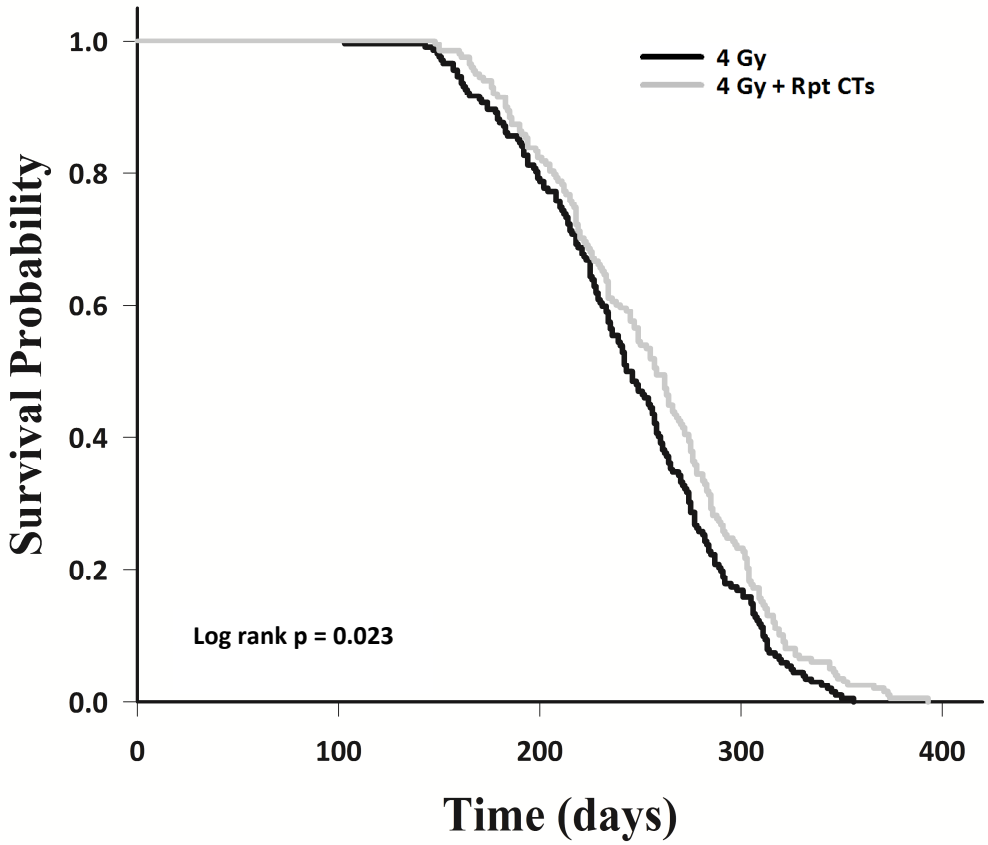

FIG. 3. Comparison of overall survival (all-cause mortality) of mice exposed to either 4 Gy alone (n=203) or 4 Gy followed four weeks later by ten weekly 10 mGy CT scans (n=198).

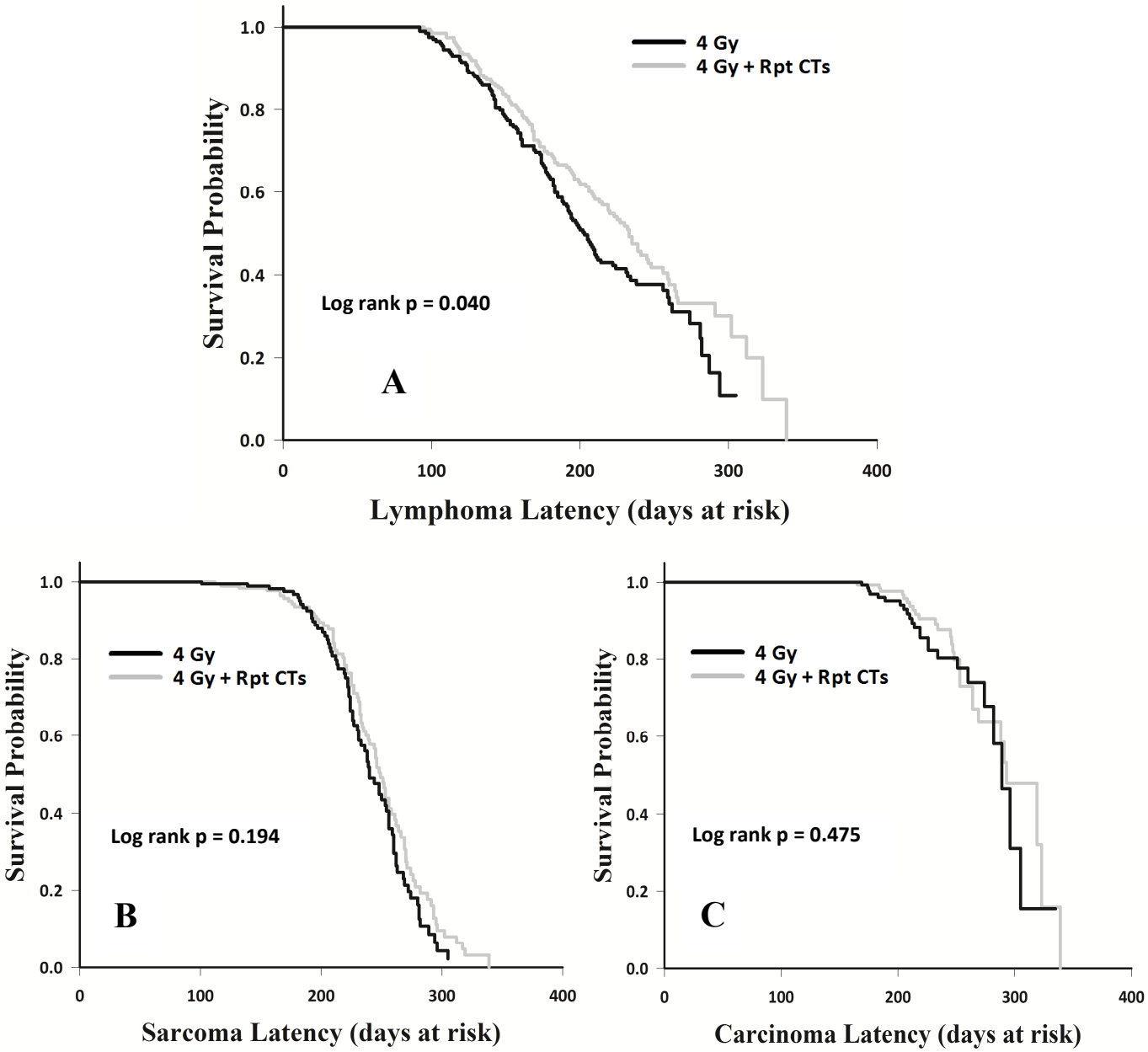

FIG. 4. Comparisons of cancer type-specific latency in Trp53+/- mice of mice exposed to either 4 Gy alone (n=203) or 4 Gy followed four weeks later by ten weekly 10 mGy CT scans (n=198). Survival probabilities were corrected for competing causes of death. **A)** Latency of mice developing lymphoma. **B)** Latency of mice developing sarcoma. **C)** Latency of mice developing carcinoma.

References

1. Feinendegen LE, Pollycove M, Sondhaus CA. Responses to low doses of ionizing radiation in biological systems. Nonlinearity Biol Toxicol Med. 2004 Jul;2(3):143-71.
2. Little MP. Cancer and non-cancer effects in japanese atomic bomb survivors. J Radiol Prot. 2009 Jun;29(2A):A43-59.
3. BEIR VII.
Health risks from exposure to low levels of ionizing radiation — BEIR VII. Washington, DC: National Academies Press; 2005.
4. Bryce SM, Bemis JC, Avlasevich SL, Dertinger SD. In vitro micronucleus assay scored by flow cytometry provides a comprehensive evaluation of cytogenetic damage and cytotoxicity. Mutat Res. 2007 Jun 15;630(1-2):78-91.
5. Maisin JR, Wambersie A, Gerber GB, Mattelin G, Lambiet-Collier M, De Coster B, et al. Life-shortening and disease incidence in C57Bl mice after single and fractionated gamma and high-energy neutron exposure. Radiat Res. 1988 Feb;113(2):300-17.
6. Fujikawa K, Hasegawa Y, Matsuzawa S, Fukunaga A, Itoh T, Kondo S. Dose and dose-rate effects of X rays and fission neutrons on lymphocyte apoptosis in p53(+/+) and p53(-/-) mice. J Radiat Res (Tokyo). 2000 Jun;41(2):113-27.
7. Leonard BE, Leonard VF. Mammogram and diagnostic X-rays--evidence of protective bystander, adaptive response (AR) radio-protection and AR retention at high dose levels. Int J Radiat Biol. 2008 Nov;84(11):885-99.
8. Feinendegen LE, Pollycove M, Neumann RD. Whole-body responses to low-level radiation exposure: New concepts in mammalian radiobiology. Exp Hematol. 2007 Apr;35(4 Suppl 1):37-46.
9. Schollnberger H, Stewart RD, Mitchel RE. Low-let-induced radioprotective mechanisms within a stochastic two-stage cancer model. Dose Response. 2006 May 22;3(4):508-18.
10. Calabrese EJ, Baldwin LA. Tales of two similar hypotheses: The rise and fall of chemical and radiation hormesis. Hum Exp Toxicol. 2000 Jan;19(1):85-97.
11. Cramers P, Atanasova P, Vrolijk H, Darroudi F, van Zeeland AA, Huiskamp R, et al. Pre-exposure to low doses: Modulation of X-ray-induced dna damage and repair? Radiat Res. 2005 Oct;164(4 Pt 1):383-90.
12. Mitchel RE. The dose window for radiation-induced protective adaptive responses. Dose Response. 2009 Nov 23;8(2):192-208.
13. Hinkal G, Parikh N, Donehower LA. Timed somatic deletion of p53 in mice reveals age-associated differences in tumor progression. PLoS One. 2009 Aug 14;4(8):e6654.
14. Christophorou MA, Ringshausen I, Finch AJ, Swigart LB, Evan GI. The pathological response to DNA damage does not contribute to p53-mediated tumour suppression. Nature. 2006 Sep 14;443(7108):214-7.
15. Marusyk A, Porter CC, Zaberezhnyy V, DeGregori J. Irradiation selects for p53-deficient hematopoietic progenitors. PLoS Biol. 2010 Mar 2;8(3):e1000324.

16. Beyan C, Kaptan K, Ifran A, Ocal R, Ulutin C, Ozturk B. The effect of radiologic imaging studies on the risk of secondary malignancy development in patients with hodgkin lymphoma. Clin Lymphoma Myeloma. 2007 Jul;7(7):467-9.
17. Pierobon J, Webber CE, Nayiager T, Barr RD, Moran GR, Gulenchyn KY. Radiation doses originating from diagnostic procedures during the treatment and follow-up of children and adolescents with malignant lymphoma. J Radiol Prot. 2011 Mar;31(1):83-93.
18. Lin C, Loberiza FR,Jr. Low-dose radiation and secondary malignancy: Is there a causal relationship? Clin Lymphoma Myeloma. 2007 Jul;7(7):450.
19. Ina Y, Tanooka H, Yamada T, Sakai K. Suppression of thymic lymphoma induction by life-long low-dose-rate irradiation accompanied by immune activation in C57BL/6 mice. Radiat Res. 2005 Feb;163(2):153-8.
20. Shin SC, Kang YM, Kim HS. Life span and thymic lymphoma incidence in high- and low-dose-rate irradiated AKR/J mice and commonly expressed genes. Radiat Res. 2010 Sep;174(3):341-6.
21. Ishii K, Hosoi Y, Yamada S, Ono T, Sakamoto K. Decreased incidence of thymic lymphoma in AKR mice as a result of chronic, fractionated low-dose total-body X irradiation. Radiat Res. 1996 Nov;146(5):582-5.
22. Mitchel REJ, Jackson JS, Morrison DP, Carlisle SM. Low doses of radiation increase the latency of spontaneous lymphomas and spinal osteosarcomas in cancer-prone, radiation-sensitive Trp53 heterozygous mice. Radiat Res. 2003;159(3):320-7.
23. Mitchel REJ, Jackson JS, McCann RA, Boreham DR. The adaptive response modifies latency for radiation-induced myeloid leukemia in CBA/H mice. Radiat Res. 1999;152(3):273-9.
24. Mitchel RE, Jackson JS, Carlisle SM. Upper dose thresholds for radiation-induced adaptive response against cancer in high-dose-exposed, cancer-prone, radiation-sensitive Trp53 heterozygous mice. Radiat Res. 2004 Jul;162(1):20-30.
25. Ina Y, Sakai K. Prolongation of life span associated with immunological modification by chronic low-dose-rate irradiation in MRL-lpr/lpr mice. Radiat Res. 2004 Feb;161(2):168-73.
26. Chen Y, Tsai Y, Nowak I, Wang N, Hyrien O, Wilkins R, et al. Validating high-throughput micronucleus analysis of peripheral reticulocytes for radiation biodosimetry: Benchmark against dicentric and CBMN assays in a mouse model. Health Phys. 2010 Feb;98(2):218-27.
27. Dertinger SD, Bishop ME, McNamee JP, Hayashi M, Suzuki T, Asano N, et al. Flow cytometric analysis of micronuclei in peripheral blood reticulocytes: I. intra- and interlaboratory comparison with microscopic scoring. Toxicol Sci. 2006 Nov;94(1):83-91.
28. Fenech M. The lymphocyte cytokinesis-block micronucleus cytome assay and its application in radiation biodosimetry. Health Phys. 2010 Feb;98(2):234-43.
29. Fenech M. In vitro micronucleus technique to predict chemosensitivity. Methods Mol Med. 2005;111:3-32.
30. Redon CE, Nakamura AJ, Martin OA, Parekh PR, Weyemi US, Bonner WM. Recent developments in the use of gamma-H2AX as a quantitative DNA double-strand break biomarker. Aging (Albany NY). 2011 Feb;3(2):168-74.

31. Rothkamm K, Horn S. Gamma-H2AX as protein biomarker for radiation exposure. Ann Ist Super Sanita. 2009;45(3):265-71.
32. Redon CE, Dickey JS, Nakamura AJ, Kareva IG, Naf D, Nowsheen S, et al. Tumors induce complex DNA damage in distant proliferative tissues in vivo. Proc Natl Acad Sci U S A. 2010 Oct 19;107(42):17992-7.
33. Kryston TB, Georgiev AB, Pissis P, Georgakilas AG. Role of oxidative stress and DNA damage in human carcinogenesis. Mutat Res. 2011 Jan 7.
34. Acharya A, Das I, Chandhok D, Saha T. Redox regulation in cancer: A double-edged sword with therapeutic potential. Oxid Med Cell Longev. 2010 Jan-Feb;3(1):23-34.
35. Samper E, Morgado L, Estrada JC, Bernad A, Hubbard A, Cadenas S, et al. Increase in mitochondrial biogenesis, oxidative stress, and glycolysis in murine lymphomas. Free Radic Biol Med. 2009 Feb 1;46(3):387-96.
36. Schmielau J, Finn OJ. Activated granulocytes and granulocyte-derived hydrogen peroxide are the underlying mechanism of suppression of t-cell function in advanced cancer patients. Cancer Res. 2001 Jun 15;61(12):4756-60.
37. Sedelnikova OA, Redon CE, Dickey JS, Nakamura AJ, Georgakilas AG, Bonner WM. Role of oxidatively induced DNA lesions in human pathogenesis. Mutat Res. 2010 Apr-Jun;704(1-3):152-9.
38. Valavanidis A, Vlachogianni T, Fiotakis C. 8-hydroxy-2' -deoxyguanosine (8-OHdG): A critical biomarker of oxidative stress and carcinogenesis. J Environ Sci Health C Environ Carcinog Ecotoxicol Rev. 2009 Apr;27(2):120-39.
39. Cheng KC, Cahill DS, Kasai H, Nishimura S, Loeb LA. 8-hydroxyguanine, an abundant form of oxidative DNA damage, causes G----T and A----C substitutions. J Biol Chem. 1992 Jan 5;267(1):166-72.
40. Bassi L, Carloni M, Meschini R, Fonti E, Palitti F. X-irradiated human lymphocytes with unstable aberrations and their preferential elimination by p53/survivin-dependent apoptosis. Int J Radiat Biol. 2003 Dec;79(12):943-54.
41. Schwartz JL, Jordan R. Selective elimination of human lymphoid cells with unstable chromosome aberrations by p53-dependent apoptosis. Carcinogenesis. 1997 Jan;18(1):201-5.
42. Belloni P, Meschini R, Lewinska D, Palitti F. Apoptosis preferentially eliminates irradiated g0 human lymphocytes bearing dicentric chromosomes. Radiat Res. 2008 Feb;169(2):181-7.
43. Phan N, De Lisio M, Parise G, Boreham DR. Biological effects and adaptive response from single and repeated computed tomography scans in reticulocytes and bone marrow of C57BL/6 mice. Radiat.Res. 2011;Submitted (in review).
44. Jacks T, Remington L, Williams BO, Schmitt EM, Halachmi S, Bronson RT, et al. Tumor spectrum analysis in p53-mutant mice. Curr Biol. 1994 Jan 1;4(1):1-7.
45. Dertinger SD, Tsai Y, Nowak I, Hyrien O, Sun H, Bemis JC, et al. Reticulocyte and micronucleated reticulocyte responses to gamma irradiation: Dose-response and time-course profiles measured by flow cytometry. Mutat Res. 2007 Dec 1;634(1-2):119-25.

46. Dertinger SD, Camphausen K, Macgregor JT, Bishop ME, Torous DK, Avlasevich S, et al. Three-color labeling method for flow cytometric measurement of cytogenetic damage in rodent and human blood. Environ Mol Mutagen. 2004;44(5):427-35.
47. Lemon JA, Rollo CD, McFarlane NM, Boreham DR. Radiation-induced apoptosis in mouse lymphocytes is modified by a complex dietary supplement: The effect of genotype and gender. Mutagenesis. 2008 Nov;23(6):465-72.
48. Donehower LA. The p53-deficient mouse: A model for basic and applied cancer studies. Semin Cancer Biol. 1996 Oct;7(5):269-78.
49. Rube CE, Grudzenski S, Kuhne M, Dong X, Rief N, Lobrich M, et al. DNA double-strand break repair of blood lymphocytes and normal tissues analysed in a preclinical mouse model: Implications for radiosensitivity testing. Clin Cancer Res. 2008 Oct 15;14(20):6546-55.
50. Cui Y, Yang H, Wu S, Gao L, Gao Y, Peng R, et al. Molecular mechanism of damage and repair of mouse thymus lymphocytes induced by radiation. Chin Med J (Engl). 2002 Jul;115(7):1070-3.
51. Ullrich RL, Jernigan MC, Satterfield LC, Bowles ND. Radiation carcinogenesis: Time-dose relationships. Radiat Res. 1987 Jul;111(1):179-84.
52. Storer JB, Ullrich RL. Life shortening in BALB/c mice following brief, protracted, or fractionated exposures to neutrons. Radiat Res. 1983 Nov;96(2):335-47.
53. Grahn D, Lombard LS, Carnes BA. The comparative tumorigenic effects of fission neutrons and cobalt-60 gamma rays in the B6CF1 mouse. Radiat Res. 1992 Jan;129(1):19-36.
54. Maisin JR, Gerber GB, Vankerkom J, Wambersie A. Survival and diseases in C57BL mice exposed to X rays or 3.1 MeV neutrons at an age of 7 or 21 days. Radiat Res. 1996 Oct;146(4):453-60.
55. Thomson JF, Grahn D. Life shortening in mice exposed to fission neutrons and gamma rays. VIII. exposures to continuous gamma radiation. Radiat Res. 1989 Apr;118(1):151-60.
56. Storer JB, Mitchell TJ. Limiting values for the RBE of fission neutrons at low doses for life shortening in mice. Radiat Res. 1984 Feb;97(2):396-406.
57. Thomson JF, Williamson FS, Grahn D. Life shortening in mice exposed to fission neutrons and gamma rays. V. further studies with single low doses. Radiat Res. 1985 Dec;104(3):420-8.
58. Hendry JH, Simon SL, Wojcik A, Sohrabi M, Burkart W, Cardis E, et al. Human exposure to high natural background radiation: What can it teach us about radiation risks? J Radiol Prot. 2009 Jun;29(2A):A29-42.
59. Preston DL, Cullings H, Suyama A, Funamoto S, Nishi N, Soda M, et al. Solid cancer incidence in atomic bomb survivors exposed in utero or as young children. J Natl Cancer Inst. 2008 Mar 19;100(6):428-36.
60. Pollycove M, Feinendegen LE. Radiation-induced versus endogenous DNA damage: Possible effect of inducible protective responses in mitigating endogenous damage. Hum Exp Toxicol. 2003 Jun;22(6):290,306; discussion 307, 315-7, 319-23.
61. Blankenbecler R. Low-dose pretreatment for radiation therapy. Dose Response. 2010 Sep 10;8(4):534-42.

62. Feinendegen LE, Pollycove M, Neumann RD. Whole-body responses to low-level radiation exposure: New concepts in mammalian radiobiology. Exp Hematol. 2007 Apr;35(4 Suppl 1):37-46.
63. Pollycove M. Radiobiological basis of low-dose irradiation in prevention and therapy of cancer. Dose Response. 2006 Nov 27;5(1):26-38.
64. Feinendegen LE. Evidence for beneficial low level radiation effects and radiation hormesis. Br J Radiol. 2005 Jan;78(925):3-7.
65. Iwasaki T, Takashima Y, Suzuki T, Yoshida MA, Hayata I. The dose response of chromosome aberrations in human lymphocytes induced in vitro by very low-dose gamma rays. Radiat Res. 2011 Feb;175(2):208-13.
66. Ma S, Liu X, Jiao B, Yang Y, Liu X. Low-dose radiation-induced responses: Focusing on epigenetic regulation. Int J Radiat Biol. 2010 Jul;86(7):517-28.
67. Azzam EI, De Toledo SM, Raaphorst GP, Mitchel REJ. Low-dose ionizing radiation decreases the frequency of neoplastic transformation to a level below the spontaneous rate in C3H 10T1/2 cells. Radiat Res. 1996;146(4):369-73.
68. de Toledo SM, Asaad N, Venkatachalam P, Li L, Howell RW, Spitz DR, et al. Adaptive responses to low-dose/low-dose-rate gamma rays in normal human fibroblasts: The role of growth architecture and oxidative metabolism. Radiat Res. 2006;166(6):849-57.
69. Shin SC, Lee KM, Kang YM, Kim K, Lim SA, Yang KH, et al. Differential expression of immune-associated cancer regulatory genes in low- versus high-dose-rate irradiated AKR/J mice. Genomics. 2011 Jan 23.
70. Day TK, Zeng G, Hooker AM, Bhat M, Scott BR, Turner DR, et al. Extremely low priming doses of X radiation induce an adaptive response for chromosomal inversions in pKZ1 mouse prostate. Radiat Res. 2006 Nov;166(5):757-66.
71. Krzyzanski W, Perez-Ruixo JJ. An assessment of recombinant human erythropoietin effect on reticulocyte production rate and lifespan distribution in healthy subjects. Pharm Res. 2007 Apr;24(4):758-72.
72. Hamasaki K, Imai K, Hayashi T, Nakachi K, Kusunoki Y. Radiation sensitivity and genomic instability in the hematopoietic system: Frequencies of micronucleated reticulocytes in whole-body X-irradiated BALB/c and C57BL/6 mice. Cancer Sci. 2007 Dec;98(12):1840-4.
73. Dertinger SD, Bemis JC, Phonethepswath S, Tsai Y, Nowak I, Hyrien O, et al. Reticulocyte and micronucleated reticulocyte responses to gamma irradiation: Effect of age. Mutat Res. 2009 Apr 30;675(1-2):77-80.
74. MacPhail SH, Banath JP, Yu TY, Chu EH, Lambur H, Olive PL. Expression of phosphorylated histone H2AX in cultured cell lines following exposure to X-rays. Int J Radiat Biol. 2003 May;79(5):351-8.
75. Fillingham J, Keogh MC, Krogan NJ. GammaH2AX and its role in DNA double-strand break repair. Biochem Cell Biol. 2006 Aug;84(4):568-77.

76. Beels L, Werbrouck J, Thierens H. Dose response and repair kinetics of gamma-H2AX foci induced by in vitro irradiation of whole blood and T-lymphocytes with X- and gamma-radiation. Int J Radiat Biol. 2010 Sep;86(9):760-8.
77. Groesser T, Chang H, Fontenay G, Chen J, Costes SV, Helen Barcellos-Hoff M, et al. Persistence of gamma-H2AX and 53BP1 foci in proliferating and non-proliferating human mammary epithelial cells after exposure to gamma-rays or iron ions. Int J Radiat Biol. 2011 Jan 27.
78. Rube CE, Fricke A, Wendorf J, Stutzel A, Kuhne M, Ong MF, et al. Accumulation of DNA double-strand breaks in normal tissues after fractionated irradiation. Int J Radiat Oncol Biol Phys. 2010 Mar 15;76(4):1206-13.
79. MacPhail SH, Banath JP, Yu Y, Chu E, Olive PL. Cell cycle-dependent expression of phosphorylated histone H2AX: Reduced expression in unirradiated but not X-irradiated G1-phase cells. Radiat Res. 2003 Jun;159(6):759-67.
80. Andrievski A, Wilkins RC. The response of gamma-H2AX in human lymphocytes and lymphocytes subsets measured in whole blood cultures. Int J Radiat Biol. 2009 Apr;85(4):369-76.
81. Svetlova MP, Solovjeva LV, Tomilin NV. Mechanism of elimination of phosphorylated histone H2AX from chromatin after repair of DNA double-strand breaks. Mutat Res. 2010 Mar 1;685(1-2):54-60.
82. Caiozzo VJ, Giedzinski E, Baker M, Suarez T, Izadi A, Lan M, et al. The radiosensitivity of satellite cells: Cell cycle regulation, apoptosis and oxidative stress. Radiat Res. 2010 Nov;174(5):582-9.
83. Umegaki K, Sugisawa A, Shin SJ, Yamada K, Sano M. Different onsets of oxidative damage to DNA and lipids in bone marrow and liver in rats given total body irradiation. Free Radic Biol Med. 2001 Nov 1;31(9):1066-74.
84. Dahle J, Kvam E. Increased level of oxidative stress in genomically unstable cell clones. J Photochem Photobiol B. 2004 Mar 19;74(1):23-8.
85. Dahle J, Kvam E. Induction of delayed mutations and chromosomal instability in fibroblasts after UVA-, UVB-, and X-radiation. Cancer Res. 2003 Apr 1;63(7):1464-9.
86. Esposito G, Campa A, Pinto M, Simone G, Tabocchini MA, Belli M. Adaptive response: Modelling and experimental studies. Radiat Prot Dosimetry. 2011 Feb;143(2-4):320-4.
87. Erker L, Schubert R, Yakushiji H, Barlow C, Larson D, Mitchell JB, et al. Cancer chemoprevention by the antioxidant tempol acts partially via the p53 tumor suppressor. Hum Mol Genet. 2005 Jun 15;14(12):1699-708.
88. Lemon JA, Rollo CD, Boreham DR. Elevated DNA damage in a mouse model of oxidative stress: Impacts of ionizing radiation and a protective dietary supplement. Mutagenesis. 2008 Nov;23(6):473-82.
89. Plews M, Simon SL, Boreham DR, Parchaliuk D, Wyatt H, Mantha R, et al. A radiation-induced adaptive response prolongs the survival of prion-infected mice. Free Radic Biol Med. 2010 Nov 15;49(9):1417-21.

90. Feinendegen LE, Pollycove M, Sondhaus CA. Responses to low doses of ionizing radiation in biological systems. Nonlinearity Biol Toxicol Med. 2004 Jul;2(3):143-71.
91. Verheij M, Bartelink H. Radiation-induced apoptosis. Cell Tissue Res. 2000 Jul;301(1):133-42.
92. Redpath JL, Short SC, Woodcock M, Johnston PJ. Low-dose reduction in transformation frequency compared to unirradiated controls: The role of hyper-radiosensitivity to cell death. Radiat Res. 2003 Mar;159(3):433-6.
93. Redpath JL, Elmore E. Radiation-induced neoplastic transformation in vitro, hormesis and risk assessment. Dose Response. 2006 Dec 6;5(2):123-30.
94. Redpath JL, Liang D, Taylor TH, Christie C, Elmore B. The shape of the dose-response curve for radiation-induced neoplastic transformation in vitro, evidence for an adaptive response against neoplastic transformation at low doses of low-LET radiation. Radiat Res. 2001;156:700-7.
95. Portess DI, Bauer G, Hill MA, O'Neill P. Low-dose irradiation of nontransformed cells stimulates the selective removal of precancerous cells via intercellular induction of apoptosis. Cancer Res. 2007 Feb 1;67(3):1246-53.
96. Thomson JF, Grahn D. Life shortening in mice exposed to fission neutrons and gamma rays. VII. effects of 60 once-weekly exposures. Radiat Res. 1988 Aug;115(2):347-60.
97. Sasaki S, Fukuda N. Temporal variation of excess mortality rate from solid tumors in mice irradiated at various ages with gamma rays. J Radiat Res (Tokyo). 2005 Mar;46(1):1-19.
98. Sasaki S, Fukuda N. Dose-response relationship for life-shortening and carcinogenesis in mice irradiated at day 7 postnatal age with dose range below 1 gy of gamma rays. J Radiat Res (Tokyo). 2006 Jun;47(2):135-45.
99. Sasaki S. Influence of the age of mice at exposure to radiation on life-shortening and carcinogenesis. J Radiat Res (Tokyo). 1991 Dec;32 Suppl 2:73-85.
100. Rossi DJ, Jamieson CH, Weissman IL. Stems cells and the pathways to aging and cancer. Cell. 2008 Feb 22;132(4):681-96.
101. Barcellos-Hoff MH. Integrative radiation carcinogenesis: Interactions between cell and tissue responses to DNA damage. Semin Cancer Biol. 2005 Apr;15(2):138-48.
102. Srivastava N, Gochhait S, de Boer P, Bamezai RN. Role of H2AX in DNA damage response and human cancers. Mutat Res. 2009 Mar-Jun;681(2-3):180-8.
103. Elmore E, Lao XY, Kapadia R, Redpath JL. The effect of dose rate on radiation-induced neoplastic transformation in vitro by low doses of low-LET radiation. Radiat Res. 2006 Dec;166(6):832-8.
104. Redpath JL, Antoniono RJ. Induction of an adaptive response against spontaneous neoplastic transformation in vitro by low-dose gamma radiation. Radiat Res. 1998;149(5):517-20.
105. Yonezawa M. Induction of radio-resistance by low dose X-irradiation. Yakugaku Zasshi. 2006 Oct;126(10):833-40.
106. Yonezawa M, Misonoh J, Hosokawa Y. Two types of X-ray-induced radioresistance in mice: Presence of 4 dose ranges with distinct biological effects. Mutat Res. 1996 Nov 4;358(2):237-43.

107. Ina Y, Tanooka H, Yamada T, Sakai K. Suppression of thymic lymphoma induction by life-long low-dose-rate irradiation accompanied by immune activation in C57BL/6 mice. Radiat Res. 2005;163(2):153-8.
108. Sakamoto K. Radiobiological basis for cancer therapy by total or half-body irradiation. Nonlinearity Biol Toxicol Med. 2004 Oct;2(4):293-316.

Chapter 6

Conclusion

Despite the differences in cell population and mouse models examined, there appears to be a common pattern in the data. Acute low-dose exposure elicits transient increases in DNA damage, unstable chromosomal aberrations, and apoptosis, while fractionated exposure shows evidence of protection against endogenous and radiation-induced damages.

Low-dose radiation exposure causes oxidative stress via production of reactive oxygen species (ROS) from hydrolysis. The elevation in ROS leads to observed increases in DNA damage and unstable chromosomal aberrations. Some of the damage is repaired via homologous recombination and non-homologous end-joining, while others trigger apoptosis. The enhanced apoptosis induced by low-dose CT scans is hypothesized to be a protective mechanism by which damaged cells are eliminated from the population. In fact, it is postulated that damaged or pre-cancerous cells that normally would not undergo apoptosis would be removed, leaving behind a robust cell population. With repeated exposure to low-dose radiation, the initial increase in ROS is speculated to trigger an up-regulation in antioxidants, thereby protecting cells from both endogenous and exogenous oxidative stress damage (i.e. a challenge radiation exposure). This resistance to oxidative stress would lead to lower cell damage and lower apoptosis.

In *Trp*53+/+ mice, repeated 10 mGy CT scans did not cause genomic instability (MN-RET). The repeated exposure significantly reduced spontaneous DNA oxidative stress damage (8-OHdG levels) and induced an adaptive response, with respect to DNA DSBs (γH2AX levels). This

decrease in genotoxicity was consistent with reduced apoptosis. Similar results were also observed in C57BL/6 mice. In cancer-prone *Trp*53+/- mice, the treatment of repeat CT scans following an acute high-dose challenge reduced spontaneous DNA oxidative stress damage (8-OHdG) that correlated with lower apoptosis. These protective biological outcomes complement observed increases in longevity and delayed cancer latency. Interestingly, the lifespan extension and delay in cancer latency were also seen following exposure to a single 10 mGy CT scan. This implies that the effects of a single low-dose CT scan can induce systemic changes that are long-lasting.

The protective effects induced by single and repeated CT scans are not exclusive to ionizing radiation exposure. Collaborative work with researchers in kinesiology has shown that exercise can induce similar adaptive responses, with respect to genotoxicity and cytotoxicity (Appendix). It is hypothesized that both CT scans and exercise employ a common pathway (i.e. oxidative stress) in producing the observed effects.

In conclusion:

1) Single CT scans cause transient genotoxicity and cytotoxicity that play a role in conferring protective effects seen with repeated CT scans;
2) A single CT scan can reduce cancer risk by delaying cancer type-specific latency, which translates to an increased lifespan.
3) Repeated CT scans can modify the acute biological responses of a prior high-dose radiation exposure, and reduce cancer risk by delaying the progression of specific types of radiation-induced cancers.

The findings of this research are not congruent with the hypothesis that dose and risk of harmful effects increase linearly, at all dose levels. The biological effects and carcinogenic investigation of diagnostic CT scans do not substantiate the presumption that low-dose radiation exposure from CT scans increase risk.

Further Investigations

The data generated from the lifetime component of this research is vast. An investigation can be conducted to examine the predictive value in correlating signs/symptoms monitored throughout life with pathology. This research can help animal care technicians and veterinarians better understand the clinical manifestations of disease within mice. For research labs conducting animal studies that do not have the resources to conduct histopathology work, some of the signs/symptoms can be used as a proxy to diagnose disease. The appropriateness of using such a method will need to be evaluated in detail (e.g. sensitivity, specificity, positive-predictive value, negative-predictive value, etc).

The work in this thesis did not examine the cancer risk of repeated CT scans alone (i.e. without the prior high-dose exposure). Another study could be conducted to investigate the latter or variations of it, such as:

1) Give pregnant mice single and repeated CT scans
    a. measure fecundity in the mothers,
    b. assess mutations, cancer incidence and latency in the offspring
    c. challenge offspring with high-dose radiation (adaptive response assessment)
        i. assess DNA damage and repair responses
        ii. assess immune functions (T-cell, B-cell, NK cell count/functions)
        iii. assess cancer risk measures (incidence, latency)

2) Give pregnant mice moderate to high dose radiation (simulate accidental exposures)
    a. same assessment measures as in 1a) and 1 b)
    b. give offspring repeated CT scans starting at adolescence
        i. same assessment measures as in 1c)
3) Give male and female mice single and repeated CT scans *before* breeding
    a. assess fecundity, and cancer risk in offspring
    b. same assessment measures as 1c)
4) Give old mice repeated CT scans (simulate diagnostic screening at old age)
    a. same assessment measures as in 1c)
5) Use a cancer animal model (or inject cancer stem cells into the mice), and starting giving repeated CT scans when the cancer has been diagnosed
    a. assess cancer latency, progression, and development of secondary malignancies

Study Design 1-2 will allow for the assessment of biological outcomes and cancer risk associated with pregnancy and CT exposure. Trans-generational carcinogenetic effects can also be examined.

Study Design 3 will allow for the assessment of diagnostic radiation risk to fecundity and sex cells /organs.

Study Design 4 will allow for the cancer risk assessment of repeated CT exposure for the elderly populations (e.g. should there be concern of cancer from repeated CT scans for people over 50?)

Study Design 5 will determine if repeated CT scans will slow or accelerate cancer development in mice *already* diagnosed with cancer. Also, the risk of secondary malignancies from repeated CT scans can be assessed. This study design is different from the “4 Gy + Rpt CT” study in this thesis because the status of the cancer is known at the time of CT exposure. In the “4 Gy + Rpt CT” study, mice did not show evidence of cancer at the time of the repeated CT scan treatments.

Appendix

Exercise-induced protection of bone marrow cells following exposure to radiation

Michael De Lisio[1]*, **Nghi Phan**[2], Douglas R. Boreham[1], and Gianni Parise[1,2]
[1]Department of Kinesiology, [2]Department of Medical Physics and Applied Radiation Sciences, McMaster University, 1280 Main St. W, Hamilton, Ontario, Canada, L8S 4K1

Manuscript is published:
De Lisio M, Phan N, Boreham DR, Parise G. Exercise-induced protection of bone marrow cells following exposure to radiation. Appl Physiol Nutr Metab. 2011 Feb;36(1):80-7.

Author Contributions:

N. Phan and M. De Lisio were responsible for experimental design and data acquisition.
M. De Lisio was responsible for the interpretation of the results and synthesis of the manuscript.
D. Boreham and G. Parise supervised and guided the research.

Exercise-induced protection of bone marrow cells following exposure to radiation

Michael De Lisio, Nghi Phan, Douglas R. Boreham, and Gianni Parise

Abstract: The hormetic effects of exercise training have previously been shown to enhance cellular protection against oxidative stress. Therefore, adaptations to exercise training may attenuate the harmful effects of radiation induced by oxidative stress. Flow cytometric analysis of genotoxicity (γH2AX foci and micronucleated reticulocytes (MN-RET)) and cytotoxicity (apoptosis and percentage of reticulocytes) were conducted on bone marrow cells isolated from acutely exercised (Acute EX), exercise-trained (EX), and sedentary (SED) mice following 1 and 2 Gy radiation challenges in vitro. Acute EX increased the percentage of cells with activated caspase-3 and -7 (32%, $p < 0.001$) and γH2AX foci formation in response to 2 Gy radiation challenge (10%, $p < 0.05$). Exercise training significantly attenuated γH2AX foci formation and MN-RET production in response to 1 Gy radiation challenge (18%, $p < 0.05$ and 22%, $p < 0.05$, respectively). Exercise training also significantly reduced basal percentages of cells with activated caspase-3 and -7 and in response to radiation in bone marrow cells (11%, $p < 0.05$). These results suggest that oxidative stress caused by acute exercise induces an adaptive response responsible for the radioprotective effects of exercise training.

Key words: exercise, high-dose radiation, radiation protection, DNA damage, apoptosis, micronucleated reticulocyte, oxidative stress.

Résumé : D'après des études antérieures, les actions hormétiques de l'entraînement physique améliorent la protection cellulaire contre le stress oxydatif. Par conséquent, les adaptations à l'entraînement physique devraient atténuer les effets néfastes des radiations suscitées par le stress oxydatif. On analyse la génotoxicité (foci γH2AX et réticulocytes micronucléés (MN-RET)) et la cytotoxicité (apoptose et pourcentage des réticulocytes) des cellules de la moelle osseuse isolées chez des souris après une séance d'exercice (Acute EX), après un programme d'entraînement physique (EX) et chez des sédentaires (SED) soumis à des radiations de 1 Gy et 2 Gy in vitro. En réponse à une radiation de 2 Gy, les souris Acute EX présentent un plus fort pourcentage de cellules avec caspase-3 et -7 activée (32 %, $p < 0{,}001$) et incluant la formation de foci γH2AX (10 %, $p < 0{,}05$). L'entraînement physique atténue significativement la formation de foci γH2AX et la production de MN-RET en réponse à une radiation de 1 Gy (18 %, $p < 0{,}05$ et 22 %, $p < 0{,}05$, respectivement). En réponse à la radiation des cellules de la moelle osseuse et à l'entraînement physique, on observe aussi une diminution significative du niveau de base des cellules avec caspase-3 et -7 activée (11 %, $p < 0{,}05$). D'après ces observations, le stress oxydatif causé par une séance d'exercice enclenche une réponse adaptative suscitant ainsi les effets radioprotecteurs de l'entraînement physique.

Mots-clés : exercice, radiation à fortes doses, radioprotection, lésion de l'ADN, apoptose, réticulocyte micronucléé, stress oxydatif.

[Traduit par la Rédaction]

Introduction

Exposure of living organisms to ionizing radiation from cosmic and terrestrial sources is a natural occurrence; however, exposure from manmade sources is becoming increasingly common. The use of medical diagnostic imaging procedures in the past 25 years has increased dramatically (Mettler et al. 2008) and is expected to increase in the future with advances in new and combined modalities (Brenner 2010). There is growing interest to better understand the biological effects of these medical exposures and to develop strategies to mitigate any resulting harmful effects produced in patients (Brenner 2010). Therefore, it would be extremely valuable to develop radioprotective strategies that can decrease the potentially harmful consequences of high-dose overexposure in normal tissues following radiation therapy (early and late effects) and also reduce potential damage caused by too many diagnostic exposures.

Received 20 August 2010. Accepted 7 October 2010. Published on the NRC Research Press Web site at apnm.nrc.ca on 16 December 2010.

M. De Lisio. Department of Kinesiology, McMaster University, Hamilton, ON L8S 4K1, Canada.
N. Phan and D.R. Boreham. Department of Medical Physics and Applied Radiation Sciences, McMaster University, Hamilton, ON L8S 4K1, Canada.
G. Parise.[1] Department of Kinesiology, McMaster University, Hamilton, ON L8S 4K1, Canada; Department of Medical Physics and Applied Radiation Sciences, McMaster University, Hamilton, ON L8S 4K1, Canada.

[1]Corresponding author (e-mail: pariseg@mcmaster.ca).

The damaging effects of low linear energy transfer radiation are primarily the result of oxidative stress caused by the production of reactive oxygen species from the radiolysis of water molecules (Prasad 1995). Enhanced production of reactive oxygen species, resulting in cellular oxidative stress, is associated with damage to proteins, lipids, and DNA. The accumulation of cellular damage can lead to dysfunction and has been linked to a myriad of diseases such as diabetes, cardiovascular disease and neurological disorders (Valko et al. 2007), as well as ageing (Harman 1956), and cancer (Marnett 2000). Therefore, identifying and developing radioprotectants could help in the management and protection of organisms from a host of diseases.

Many studies have focused on pharmacological agents (Devipriya et al. 2008) or nutritional supplements (Lemon et al. 2008*a*) as radioprotective interventions that enhance the cell's natural defense mechanisms with exogenous sources of free radical scavengers. A related area of research capitalizes on the hormetic properties of low doses of radiation to stimulate endogenous protective mechanisms (Wolff 1996; Feinendegen et al. 2007). The theory of hormesis has also been applied to exercise training (Calabrese and Nieman 1996; Radak et al. 2005, 2008; Ji et al. 2006). Like low doses of radiation, acute exercise causes cellular oxidative stress (Davies et al. 1982) and has been shown to cause apoptosis in lymphocytes (Hoffman-Goetz and Quadrilatero 2003; Mooren et al. 2004; Quadrilatero and Hoffman-Goetz 2004, 2005) and DNA damage (Hartmann et al. 1998; Tsai et al. 2001). In response to the oxidative stress induced by individual exercise bouts in a training program, cellular adaptations such as increased antioxidant activity (Venditti and Di Meo 1996; Avula and Fernandes 1999; Radak et al. 2005), DNA repair capacity (Radak et al. 2002, 2005), and decreased oxidative damage (Venditti and Di Meo 1996; Radak et al. 2002) have been observed. Traditionally, these adaptations have been associated with protection from oxidative stress in skeletal muscle (Alessio and Goldfarb 1988; Laughlin et al. 1990; Oh-ishi et al. 1997; Smolka et al. 2000); however, the beneficial effects of exercise have also been reported in tissues other than muscle, such as liver (Somani and Husain 1996; Venditti and Di Meo 1996; Nakamoto et al. 2007), brain (Somani and Husain 1996; Devi and Kiran 2004), lung (Somani and Husain 1996), and blood (Calabrese and Nieman 1996; Connolly et al. 2004; Büttner et al. 2007). In particular, trained individuals are resistant to DNA damage (Umegaki et al. 1998) and apoptosis (Avula et al. 2001; Peters et al. 2006) in peripheral lymphocytes when exposed to an oxidative challenge. Although the effects of exercise in mature, circulating blood cells have been examined, a paucity of data exist regarding immature blood progenitors residing in the bone marrow.

Given the wide-ranging tissue types that adapt to exercise, and the ability of exercise to enhance protection against oxidative stress, we hypothesized that exercise training would be protective against an oxidative challenge caused by a high-dose radiation challenge exposure. We focused on bone marrow cells, since they are highly sensitive to radiation such that failure of the hematopoietic system following high-dose radiation exposure is a primary cause of radiation lethality (Dainiak et al. 2003). Furthermore, direct study of cells from the bone marrow compartment has never been performed in the context of exercise training and modulation of radiation response.

Materials and methods

Animals

Adult male C57Bl/6 mice (Jackson Laboratory, Bar Harbor, Maine), aged 16 weeks (at the beginning of training), were used for the exercise training experiments, while 25-week-old male C57Bl/6 mice were used for the acute exercise experiments. No more than 5 mice were housed per cage (27 cm × 12 cm × 15.5 cm) and were provided food and water ad libitum. Mice were maintained on a 12 h light / 12 h dark cycle at 22 ± 2 °C. Ethics approval was granted by the McMaster University (Hamilton, Ont.) Animal Research Ethics Board, and experiments conformed to the guidelines of the Canadian Council on Animal Care.

Exercise training protocol

Mice were exercised trained (EX, $n = 10$) on a motorized treadmill (Exer 6M Treadmill, Columbus Instruments Inc., Columbus, Ohio) 3 days per week (Monday, Wednesday, Friday) for 10 weeks. The mice were allowed to acclimatize to the treadmill for the first 3 weeks with the following training protocol: warm-up at 8 m·min^{-1} for 10 min; training at 10 m·min^{-1} for 25 min (week 1), 35 min (week 2), and 45 min (week 3); cool-down at 8 m·min^{-1} for 5 min. For the remaining 7 weeks, mice were subjected to a progressive exercise protocol with the training portion of the protocol beginning at 12 m·min^{-1} for 45 min (week 4) and increasing to 20 m·min^{-1} for 45 min. The training portion of the protocol was always preceded by a 10 min warm-up at 10 m·min^{-1} and followed by a 5 min cool-down at 10 m·min^{-1}. We have previously shown that this exercise training protocol successfully increases antioxidant enzyme activities in mouse skeletal muscle (De Lisio et al., in press), and a similar training protocol has been shown to increase both antioxidant enzyme (Avula and Fernandes 1999) and base excision repair enzyme activities (Radak et al. 2007). Mice were encouraged to run using mild electric shock or hind limb stimulation with the bristles of a paint brush. Sedentary mice (SED) were handled in the same manner as exercise-trained mice but were not exposed to treadmill running. Mice from the SED group in the present study were also included in the control group for a study by Phan et al. (in review).

Acute exercise protocol

Prior to exercise, all mice were placed on the treadmill for 5 min at a speed of 8 m·min^{-1} to acclimatize them to treadmill stress. Four mice were randomly removed from the treadmill and served as unexercised controls (CON), while 4 mice remained on the treadmill and completed the acute exercise protocol (Acute Ex). Mice began running at 8 m·min^{-1}, and treadmill speed was increased by 2 m·min^{-1} every 10 min until the mice reached a speed of 16 m·min^{-1}. Mice then exercised at 16 m·min^{-1} for 30 min, then 18 m·min^{-1} for 20 min; therefore, the total time of the acute exercise protocol was 90 min. The nonexercised control mice (CON) were also used by Phan et al. (in review).

Radiation challenge

In vivo challenge

The in vivo radiation challenge took place 3 days following the final exercise bout in the 10-week training protocol and has been described previously (Lemon et al. 2008*a*; De Lisio et al., in press). Briefly, a subset of mice from each group (SED and EX) were irradiated with a Cs-137 γ ray source and received a whole-body dose of 1.116 Gy (approximately 1 Gy) at a dose rate of 0.279 Gy·min^{-1}. During irradiation, mice were placed in a polycarbonate tube and returned to their cage once the irradiation was completed. The remaining mice in each group were placed in the polycarbonate tubes for an equal amount of time to simulate the stress of the radiation challenge.

In vitro challenge

Five days following the final exercise bout of the 10-week training protocol, bone marrow was harvested from mice in each group that did not receive the in vivo high-dose radiation challenge and divided into 3 separate samples. Separate bone marrow aliquots from each mouse were exposed to 0 Gy (unchallenged), 0.969 Gy (~1 Gy) at a dose rate of 0.171 Gy·min^{-1}, and 1.938 Gy (~2 Gy) at a dose rate of 0.171 Gy·min^{-1} irradiations. Irradiations were administered with a Cs-137 γ ray source. Bone marrow from acutely exercised mice and their controls was harvested, divided, and irradiated in the same fashion 6 h following the acute exercise bout.

Sample collection and cell preparation

Mice were briefly anaesthetized with isoflurane, and blood was collected by cardiac puncture. Mice were then euthanized via cervical dislocation. Both femurs were dissected of muscle and fat, excised, and flushed with 1 mL of heparinized RPMI 1640 to remove the bone marrow. The cell suspension was disaggregated with a 23-gauge needle and placed on a water–ice slurry until the cells were counted. Cells were counted using the Z2 Coulter particle count and size analyzer (Beckman Coulter, Miami, Fla.), and the concentration was adjusted to 1×10^6 cells·mL^{-1} with ice-cold supplemented RPMI 1640 (10% fetal bovine serum (VWR International, Mississauga, Ont.), 2.5% HEPES, 1% penicillin–streptomycin, 1% L-glutamine). Cell suspensions were placed in a 37 °C water bath for the duration of the incubation.

γH2AX

The protocol for determination of γH2AX foci by flow cytometry has been previously described in detail (Lemon et al. 2008*a*). Briefly, following incubation for 30 min at 37 °C, a 500 μL aliquot of each bone marrow cell suspension was fixed in 70% ethanol for 60 min, then stored at –20 °C for future use. Cells were fixed 30 min following radiation exposure, as this time has previously been shown to correspond to the peak of γH2AX levels postradiation (Lemon et al. 2008*a*). Cells were washed in Tris-buffered saline (TBS; Trizma base plus NaCl, pH 7.4; Sigma–Aldrich, Mississauga, Ont.) then permeabilized with ice-cold Tris-buffered saline–Triton (TBST; 4% fetal bovine serum, 0.1% Triton X-100 (Sigma–Aldrich)) for 10 min. Cells were stained with anti-phospho-γH2AX (ser139) primary antibody (1:400, Upstate Cell Signaling, Charlottesville, Va.) for 2 h at room temperature. After washing, cells were incubated with AlexFluor 488 goat anti-rabbit IgG F(ab′)2 (1:500, Invitrogen Canada, Burlington, Ont.) secondary antibody for 1 h at room temperature in the dark. After washing, cells were resuspended in propidium iodide (PI; 1:60, Sigma–Aldrich) and run immediately on the Epics XL flow cytometer (Beckman Coulter, Mississauga, Ont.). Analysis was based on 5×10^3 cells from the low forward and side-scatter population, which is enriched for lymphocytes at all stages of development (Salzman et al. 1975; Hoffman et al. 1980; Terstappen et al. 1988, 1989). Each sample was analyzed in duplicate.

Apoptosis

The carboxyfluorescein FLICA caspase-3- and -7 apoptosis detection kit assay (Immunochemistry Technologies, Bloomington, Ind.) was used according to the manufacturer's instructions. Briefly, 10 μL of 30× FLICA solution was added to 300 μL aliquots of bone marrow suspension at a concentration of 1×10^6 cells·mL^{-1} and incubated for 6 h in a 37 °C, 5% CO_2 incubator. Aliquots were gently resuspended every 60 min. Cells were washed twice with 1× wash buffer (supplied) and resuspended in 400 μL of a solution of 0.5% 7AAD (Beckman Coulter) in wash buffer for the training study or 400 μL wash buffer for the acute study. Cells were put on ice and immediately run on the Epics XL flow cytometer. Percentages were determined from analysis of 2.5×10^4 cells. The gating strategy employed for the training study is shown in supplemental Fig. S2[2]. Briefly, the first gate (Fig. S2A[2]) was set to exclude all doublets with high forward and side scatter. Next, the percentage of cells expressing activated caspase-3 and -7 and either positive or negative for 7AAD was determined (Fig. S2B[2]). Total caspase-3 and -7 positive cells represent the combination of caspase-3 and -7 plus 7AAD+ and caspase-3 and -7 plus 7AAD–. The same gating strategy was performed in the acute experiments, except that 7AAD was not used. Levels of apoptosis were determined 8 h following radiation exposure. This length of incubation may contribute to the relatively high spontaneous (nonradiation-induced) levels of apoptosis reported in the present study and previously by our group (Lemon et al. 2008*b*); however, this period of incubation has previously been shown to correspond to peak levels of apoptosis postradiation (Lemon et al. 2008*b*).

Micronucleated and percentage of reticulocytes

The percentage of reticulocytes and the percentage of micronucleated reticulocytes (MN-RET) were determined using the method of Dertinger et al. (2007) using the MicroFlow PLUS kit (Litron Laboratories, Rochester, N.Y.). Dertinger et al. have previously shown MN-RET levels to be at their highest 43 h following 1–2 Gy radiation (Dertinger et al. 2007). Therefore, this assay was not performed in acutely exercised mice. Once collected, blood was immediately mixed with 350 μL of solution B (anticoagulant supplied

[2] Supplementary data for this article are available on the journal Web site (http://apnm.nrc.ca).

with kit), fixed in methanol (supplied), and stored at –80 °C for a minimum of 24 h. Samples were washed in ice-cold buffer (supplied) and incubated in 80 μL of an antibody cocktail containing RNase, FITC-conjugated CD71, and PE-conjugated CD61 on ice for 30 min, followed by 30 min at room temperature. Samples were treated with 1 mL of PI staining solution (supplied) just prior to running samples on the Epics XL flow cytometer. Cells that were double positive for CD71 and PI represented MN-RET, and cells that were CD71 positive only represent reticulocytes and were expressed as a percentage of total cells analyzed. CD61 was used as a platelet marker to differentiate between reticulocytes and platelets, as per manufacturer's instructions (Fig. S3)[2]. The percentage of reticulocytes was determined from analysis of 2×10^5 red blood cells, and the percentage of MN-RET was determined from analysis of 2×10^4 reticulocytes. All samples were analyzed at least in duplicate 43 h following radiation exposure. Certain samples were excluded from analysis because of technical problems with sample fixation causing scatter patterns in which the population of interest could not be reliably determined.

Statistics

Data were analyzed using the commercially available SigmaStat 3.1 software. Data are presented as means ± SE, with $p \leq 0.05$ considered significant. γH2AX and apoptosis data were analyzed using a 2-factor ANOVA with Tukey's post hoc test. Student's *t* tests were used to determine between-group differences in the absolute change in γH2AX, reticulocyte data, and acute H2AX data.

Results

γH2AX Foci

Cells expressing phosphorylated γH2AX foci, a surrogate marker of DNA damage, were detected by flow cytometry (Lemon et al. 2008*a*) (Fig. S1[2]). Acute exhaustive exercise did not increase basal levels of γH2AX in the lymphocyte-enriched population of bone marrow. In vitro radiation of 1 and 2 Gy increased γH2AX foci formation in both acutely exercised and nonexercised control mice ($p < 0.001$ for both doses). Acutely exercised mice had significantly higher γH2AX foci formation in response to 2 Gy in vitro radiation compared with nonexercised controls (10%, $p < 0.05$, Fig. 1A). Exercise training did not increase basal levels of γH2AX foci, and γH2AX foci were significantly increased in both exercise-trained and sedentary mice exposed to 1 and 2 Gy radiation in vitro ($p < 0.001$, Fig. 1B). Exercise training attenuated the increase from basal levels in mice exposed to 1 Gy radiation in vitro (18%, $p < 0.05$, Fig. 1C), but the protective effect was abolished by the 2 Gy dose.

Apoptosis

Cells containing activated caspase-3 and -7, with or without 7AAD positivity, were identified by flow cytometry (Fig. S2[2]). The percentage of total caspase-3 and -7 bone marrow cells was significantly greater in acutely exercised mice compared withthat in nonexercised controls (32%, $p < 0.001$, Fig. 2A). The percentage of total caspase-3 and -7 tended to increase with radiation dose ($p = 0.052$, Fig. 2A). The percentage of total caspase-3 and -7 bone marrow cells was significantly decreased in exercised-trained compared with that in sedentary mice (11%, $p < 0.05$, Fig. 2B). The percentage of total caspase-3 and -7 cells was significantly elevated from basal levels by each radiation dose in both sedentary and exercise-trained mice (1 Gy: 18%, $p < 0.05$; 2 Gy: 27%, $p < 0.001$, Fig. 2B). The percentage of cells

Fig. 1. γH2AX foci in a lymphocyte-enriched population of bone marrow cells from acutely exercised (Acute EX: 0 and 1 Gy, $n = 4$; 2 Gy, $n = 3$) and nonexercised controls (CON, $n = 4$) whose marrow was exposed to 0, 1, or 2 Gy radiation in vitro (A). γH2AX foci in a lymphocyte-enriched population of bone marrow cells from sedentary (SED, $n = 5$) vs. exercise-trained (EX, $n = 5$) mice whose marrow was exposed to 0, 1, or 2 Gy radiation in vitro (B). Increase in γH2AX foci in a lymphocyte-enriched population of bone marrow cells from exercise-trained (EX, $n = 5$) and sedentary (SED, $n = 5$) mice (C). Basal (0 Gy) values were subtracted to determine the absolute change in mean fluorescent intensity (MFI) caused by radiation. Values represent means ± SE expressed as MFI. *, $p < 0.001$ vs. 0 Gy; †, $p < 0.001$ vs. 1 Gy; ‡, $p < 0.05$ vs. CON and SED.

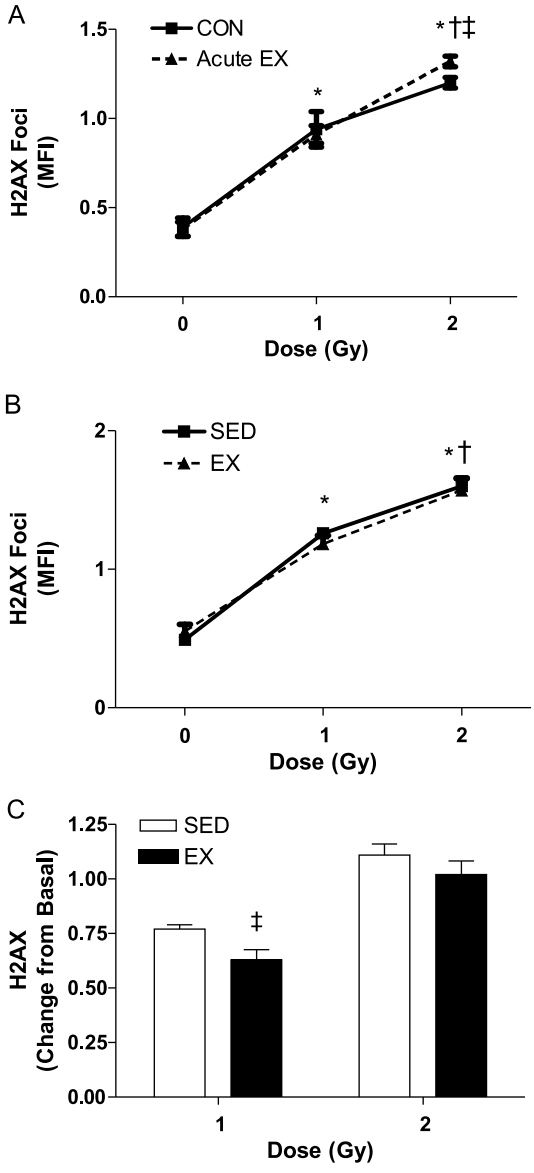

Fig. 2. The percentage of bone marrow cells with activated caspase-3 and -7 from acutely exercised (Acute EX, $n = 4$) and nonexercised controls (CON, $n = 4$) whose marrow was exposed to 0, 1, or 2 Gy radiation in vitro (A). The percentage of bone marrow cells with activated caspase-3 and -7 from exercise-trained (EX, $n = 5$) and sedentary (SED, $n = 5$) mice whose marrow was exposed to 0, 1, or 2 Gy radiation in vitro (B). The percentage of bone marrow cells with activated caspase-3 and -7 that did not stain positively for 7AAD from exercise-trained (EX, $n = 5$) and sedentary (SED, $n = 5$) mice whose marrow was exposed to 0, 1, or 2 Gy radiation in vitro (C). The percentage of bone marrow cells with activated caspase-3 and -7 that stained positively for 7AAD from exercise-trained (EX, $n = 5$) and sedentary (SED, $n = 5$) mice whose marrow was exposed to 0, 1, or 2 Gy radiation in vitro (D). Values are expressed as percentage of total cells analyzed and presented as means ± SE. *, $p < 0.05$ vs. 0 Gy; †, $p < 0.05$ vs. CON and SED.

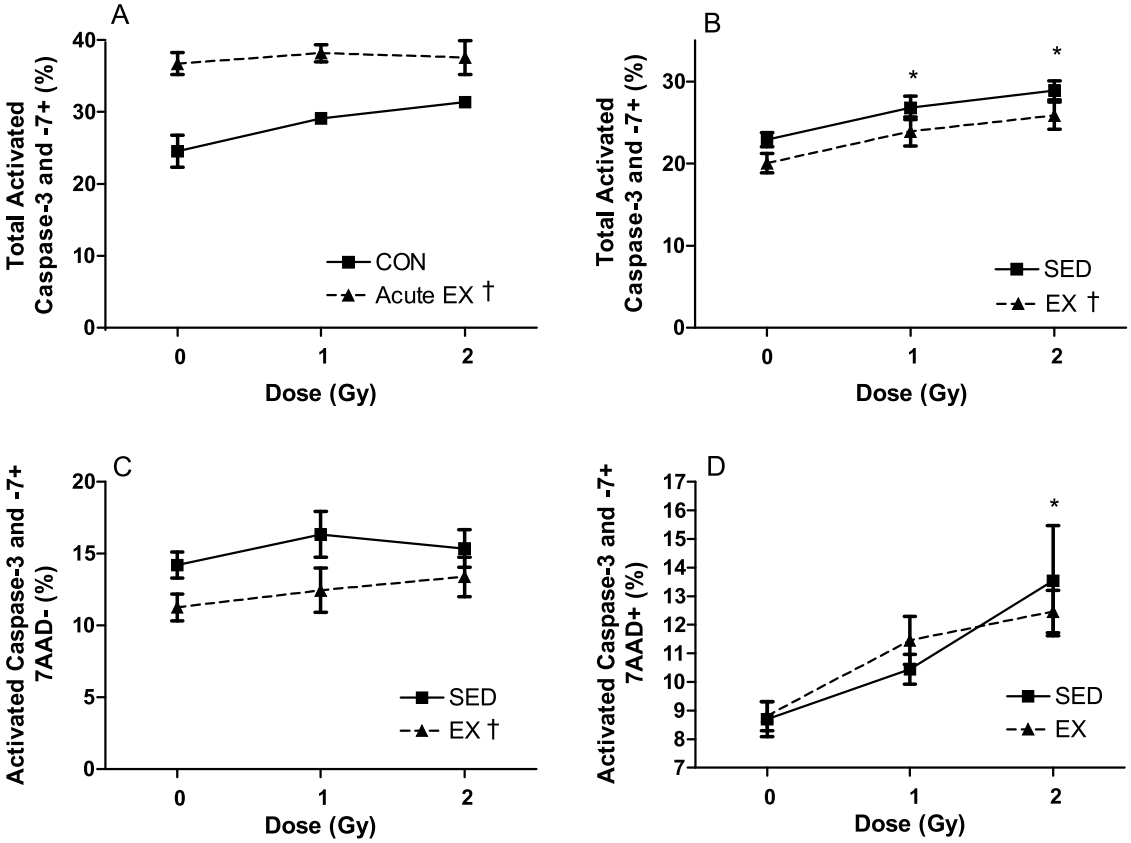

expressing activated caspase-3 and -7 and negative for the DNA dye 7AAD were significantly elevated in sedentary mice compared with that in exercise-trained mice (24%, $p < 0.05$, Fig. 2C). The percentage of cells expressing activated caspase-3 and -7 and 7AAD were not different between sedentary and exercise-trained mice; however, the percentage of cells positive for both markers was elevated with 2 Gy of radiation relative to that of nonirradiated samples (0 Gy; 48%, $p < 0.001$, Fig. 2D).

Micronucleated reticulocytes

Reticulocytes were identified with an anti-CD71 antibody and analyzed using flow cytometry (Fig. S3[2]) (Dertinger et al. 2007). The percentage of reticulocytes did not differ between the exercise-trained mice and sedentary animals basally or in response to 1 Gy radiation (Fig. 3A). The basal percentage of MN-RET did not differ between exercise-trained and sedentary mice; however, in response to 1 Gy radiation, exercise-trained mice had significantly fewer MN-RET than sedentary mice (22%, $p < 0.05$, Fig. 3B).

Discussion

To our knowledge, the present report represents the first investigation into the effects of acute exercise and exercise training in the bone marrow compartment. Results from the present investigation suggest that exercise induces acute oxidative stress in bone marrow cells, resulting in adaptations that confer protection against future oxidative challenges. Acute exercise sensitizes bone marrow cells to oxidative stress, resulting in increased DNA damage in response to a radiation challenge and elevation in the percentage of cells expressing activated caspase-3 and -7. These perturbations in redox homeostasis from acute exercise result in an adaptive response to training either through increased apoptosis of susceptible cells or an up-regulation of protective mechanisms. These adaptations following training were manifested as an attenuation of DNA damage, MN-RET formation, and reduced apoptosis in response to high challenge doses of radiation.

Each acute exercise bout in a progressive exercise training

Fig. 3. The percentage of reticulocytes from sedentary (SED) and exercise-trained (EX) mice basally (0 Gy, SED $n = 5$, EX $n = 3$) and in response to 1 Gy, whole-body, in vivo radiation (1 Gy, SED $n = 3$, EX $n = 3$) (A). The percentage of micronucleated reticulocytes (MN-RET) from sedentary (SED) and exercise-trained (EX) mice basally (0 Gy, SED $n = 5$, EX $n = 3$) and in response to 1 Gy, whole-body, in vivo radiation (1 Gy, SED $n = 3$, EX $n = 3$) (B). Values are expressed as the percentage of total cells analyzed and are presented as means ± SE. *, $p < 0.05$ vs. SED.

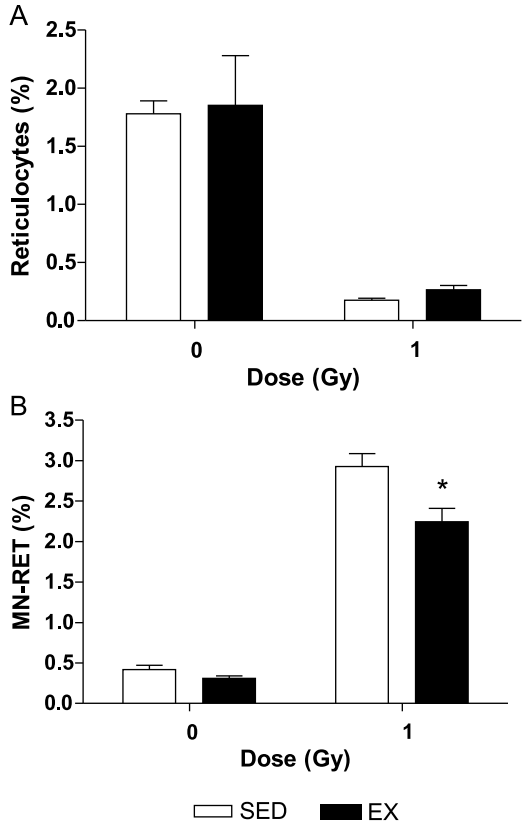

program induces oxidative stress (Venditti and Di Meo 1996) that may result in DNA damage. DNA double-strand breaks are considered the most detrimental form of DNA damage, because the potential loss of genetic information and lack of repair or disrepair can lead to cell death or genetic damage. In the present investigation, basal levels of DNA double-strand breaks, as determined by γH2AX phosphorylation, were not different between acutely exercised and nonexercised control mice 6 h following exercise. We can conclude, however, that acute exercise sensitizes the bone marrow compartment to radiation, as levels of γH2AX foci were significantly elevated in acutely exercised mice in response to 2 Gy of radiation. These data are in agreement with the data of Umegaki and colleagues, who demonstrated increased DNA damage in peripheral lymphocytes challenged with 1.5 Gy of X-rays following an acute exercise bout (Umegaki et al. 1998). Together, these data suggest that acute, exhaustive exercise sensitizes lymphocytes and lymphocyte progenitors to oxidative stress. This sensitization, however, does not cause DNA damage to accumulate over the training period, as basal levels of DNA damage were unchanged between trained and sedentary mice. This agrees with previous studies indicating that the oxidative stress caused by each exercise bout in a training program does not result in increased oxidative damage to DNA with training (Radak et al. 2002, 2007). Rather, the stress induced by exercise training resulted in protective adaptations such that, following exposure to 1 Gy radiation, the increase in DNA damage from baseline levels was attenuated in exercise-trained mice as compared with sedentary mice. These data are in accordance with previous studies demonstrating unchanged levels of DNA damage in peripheral lymphocytes from trained subjects following an acute oxidative stress in the form of 1.5 Gy of X-rays (Umegaki et al. 1998) or an acute exercise bout (Peters et al. 2006). Taken together, our data suggest that acute exercise sensitizes the bone marrow compartment to oxidative challenges, such as a high dose of radiation. With training, these repeated acute exercise bouts cause an adaptive response that confers protection against future oxidative challenges.

Apoptosis is the primary means of death in hematopoietic cells exposed to high-dose radiation exposure (Lemon et al. 2008*b*). In the present investigation, acute exercise significantly increased the percentage of cells with activated caspase-3 and -7 in bone marrow cells, an indication that the cellular apoptotic process had been initiated. Conversely, exercise training significantly decreased the percentage of bone marrow cells with activated caspase-3 and -7. The training effects were due primarily to the decrease in cells undergoing the early stages of apoptosis defined as cells positive for active caspase-3 and -7 but not positive for 7AAD. Caspase-3 and -7 activation indicates that the apoptotic machinery within the cell has been activated; however, membrane permeabilization has not occurred, as 7AAD has not yet entered the cells. These results are in agreement with previous data suggesting that peak levels of apoptosis are first seen 8 h following an acute dose of radiation (Lemon et al. 2008*b*). Previous studies have also shown increased apoptosis in lymphocytes derived from the intestines (Hoffman-Goetz and Quadrilatero 2003) and peripheral blood (Mooren et al. 2004) from untrained or poorly trained mice and humans, respectively. In further agreement with the present findings, however, peripheral lymphocytes from well-trained individuals are protected from an apoptotic response following acute oxidative stress (Mooren et al. 2004; Peters et al. 2006). These data mirror our DNA damage results, in that acute exercise induced oxidative stress to bone marrow lymphocytes, and support our hypothesis that oxidative stress induced by acute exercise is responsible for an adaptive response that increases protection against future oxidative stress. Indeed, previous studies have reported increased gene expression of the anti-apoptotic genes BCL2A, Casp8, and FADD-like apoptosis regulator (CFLAR) following exercise in mature white blood cells (Büttner et al. 2007). Results from the present study suggest that similar adaptations may be occurring in more primitive cells of the hematopoietic hierarchy. Furthermore, these data suggest that a possible mechanism for the protective effects of exercise training may be the enhanced removal of highly susceptible cells and retention of cells with more robust defenses.

Quantification of reticulocytes and micronucleated reticulocytes (MN-RET) following a high-dose radiation exposure are established measures of cytotoxicity and genotoxicity, respectively (Dertinger et al. 2007). The percentage of

reticulocytes remains unchanged in athletes (Banfi and Del Fabbro 2007), a finding that is in agreement with data from the present study showing no effects of exercise training on reticulocyte number. Additionally, basal levels of MN-RET were not different between sedentary and exercise-trained mice. These data, along with results from our γH2AX experiments, support the notion that training does not cause DNA damage in cells from the bone marrow compartment. Conversely, exercise training conferred protection to reticulocytes, as was demonstrated by a significant reduction (22% relative to SED) in the percentage of MN-RET following 1 Gy of in vivo radiation. These data agree with the results of Umegaki and colleagues (1998), who demonstrated an increase in MN-RET formation in peripheral lymphocytes from untrained subjects exposed to 1.5 Gy of X-rays, while peripheral lymphocytes from trained subjects showed no such increase. Although the 22% reduction in MN-RET relative to that in sedentary mice represents a difference of <1% in absolute terms, we believe that the biological relevance of this difference is signficant. DNA damage and proliferation and differentiation of cells containing DNA damage are critical steps in cancer initiation and progression. This type of transformation in a single cell could lead to cancer development. Therefore, an absolute difference <1%, which represents thousands of cells, is very significant biologically, as it would translate into a large decrease in the risk of cancer development. Together, these data suggest that exercise training, either through enhanced apoptosis of damaged cells or enhanced protection against oxidative damage, induce protective adaptations against the cytotoxic and genotoxic effects of high-dose radiation exposure.

Overall, the ability of cells to adapt and become resistant to high-dose radiation through exercise training could be a potentially useful strategy to protect people from the detrimental effects of radiation. This could have applications in radiation therapy for protecting normal tissues, including bone marrow, during therapy, and also reducing the risks from diagnostic overexposure or overuse.

Acknowledgements

Special thanks to Dr. Mark Tarnopolsky for kind use of his motorized mouse treadmill; Nicole McFarlane, Mary Ellen Cybulski, and Lisa Laframboise for their technical expertise; and Leeann Bellamy for her assistance with mouse training. This research was supported by the US Department of Energy Low-Dose Research Program (DE-FG02-07ER64343) to D.R. Boreham. G. Parise was supported by the Natural Sciences and Engineering Research Council of Canada (NSERC), M. De Lisio by a Canadian Institutes of Health Research (CIHR) Canadian Graduate Scholarship, and N. Phan by a CIHR Vanier Postgraduate Scholarship.

References

Alessio, H.M., and Goldfarb, A.H. 1988. Lipid peroxidation and scavenger enzymes during exercise: adaptive response to training. J. Appl. Physiol. **64**(4): 1333–1336. PMID:3378967.

Avula, C.P., and Fernandes, G. 1999. Modulation of antioxidant enzymes and apoptosis in mice by dietary lipids and treadmill exercise. J. Clin. Immunol. **19**(1): 35–44. doi:10.1023/A:1020562518071. PMID:10080103.

Avula, C.P., Muthukumar, A.R., Zaman, K., McCarter, R., and Fernandes, G. 2001. Inhibitory effects of voluntary wheel exercise on apoptosis in splenic lymphocyte subsets of C57BL/6 mice. J. Appl. Physiol. **91**(6): 2546–2552. PMID:11717217.

Banfi, G., and Del Fabbro, M. 2007. Behaviour of reticulocyte counts and immature reticulocyte fraction during a competitive season in élite athletes of four different sports. Int. J. Lab. Hematol. **29**(2): 127–131. doi:10.1111/j.1751-553X.2006.00847.x. PMID:17474885.

Brenner, D.J. 2010. Should we be concerned about the rapid increase in CT usage? Rev. Environ. Health, **25**(1): 63–68. PMID:20429161.

Büttner, P., Mosig, S., Lechtermann, A., Funke, H., and Mooren, F.C. 2007. Exercise affects the gene expression profiles of human white blood cells. J. Appl. Physiol. **102**(1): 26–36. doi:10.1152/japplphysiol.00066.2006. PMID:16990507.

Calabrese, L.H., and Nieman, D.C. 1996. Exercise, immunity, and infection. J. Am. Osteopath. Assoc. **96**(3): 166–176. PMID:8932593.

Connolly, P.H., Caiozzo, V.J., Zaldivar, F., Nemet, D., Larson, J., Hung, S.P., et al. 2004. Effects of exercise on gene expression in human peripheral blood mononuclear cells. J. Appl. Physiol. **97**(4): 1461–1469. doi:10.1152/japplphysiol.00316.2004. PMID:15194674.

Dainiak, N., Waselenko, J.K., Armitage, J.O., MacVittie, T.J., and Farese, A.M. 2003. The hematologist and radiation casualties. Hematology, 2003, 473–496. PMID:14633795.

Davies, K.J., Quintanilha, A.T., Brooks, G.A., and Packer, L. 1982. Free radicals and tissue damage produced by exercise. Biochem. Biophys. Res. Commun. **107**(4): 1198–1205. doi:10.1016/S0006-291X(82)80124-1. PMID:6291524.

De Lisio, M., Kaczor, J.J., Phan, N., Tarnopolsky, M.A., Boreham, D.R., and Parise, G. Exercise training enhances the skeletal muscle response to radiation-induced oxidative stress. Muscle Nerve. In press.

Dertinger, S.D., Tsai, Y., Nowak, I., Hyrien, O., Sun, H., Bemis, J.C., et al. 2007. Reticulocyte and micronucleated reticulocyte responses to γ irradiation: dose-response and time-course profiles measured by flow cytometry. Mutat. Res. **634**(1–2): 119–125. PMID:17686648.

Devi, S.A., and Kiran, T.R. 2004. Regional responses in antioxidant system to exercise training and dietary vitamin E in aging rat brain. Neurobiol. Aging, **25**(4): 501–508. doi:10.1016/S0197-4580(03)00112-X. PMID:15013571.

Devipriya, N., Sudheer, A.R., and Menon, V.P. 2008. Caffeic acid protects human peripheral blood lymphocytes against γ radiation-induced cellular damage. J. Biochem. Mol. Toxicol. **22**(3): 175–186. doi:10.1002/jbt.20228. PMID:18561333.

Feinendegen, L.E., Pollycove, M., and Neumann, R.D. 2007. Whole-body responses to low-level radiation exposure: new concepts in mammalian radiobiology. Exp. Hematol. **35**(4 Suppl. 1): 37–46. doi:10.1016/j.exphem.2007.01.011. PMID:17379086.

Harman, D. 1956. Aging: a theory based on free radical and radiation chemistry. J. Gerontol. **11**(3): 298–300. PMID:13332224.

Hartmann, A., Pfuhler, S., Dennog, C., Germadnik, D., Pilger, A., and Speit, G. 1998. Exercise-induced DNA effects in human leukocytes are not accompanied by increased formation of 8-hydroxy-2′-deoxyguanosine or induction of micronuclei. Free Radic. Biol. Med. **24**(2): 245–251. doi:10.1016/S0891-5849(97)00249-9. PMID:9433899.

Hoffman, R.A., Kung, P.C., Hansen, W.P., and Goldstein, G. 1980. Simple and rapid measurement of human T lymphocytes and their subclasses in peripheral blood. Proc. Natl. Acad. Sci. U.S.A. **77**(8): 4914–4917. doi:10.1073/pnas.77.8.4914. PMID:6968909.

Hoffman-Goetz, L., and Quadrilatero, J. 2003. Treadmill exercise in mice increases intestinal lymphocyte loss via apoptosis. Acta Physiol. Scand. **179**(3): 289–297. doi:10.1046/j.1365-201X.2003.01176.x. PMID:14616245.

Ji, L.L., Gomez-Cabrera, M.C., and Vina, J. 2006. Exercise and hormesis: activation of cellular antioxidant signaling pathway. Ann. N. Y. Acad. Sci. **1067**(1): 425–435. doi:10.1196/annals.1354.061. PMID:16804022.

Laughlin, M.H., Simpson, T., Sexton, W.L., Brown, O.R., Smith, J.K., and Korthuis, R.J. 1990. Skeletal muscle oxidative capacity, antioxidant enzymes, and exercise training. J. Appl. Physiol. **68**(6): 2337–2343. PMID:2384414.

Lemon, J.A., Rollo, C.D., and Boreham, D.R. 2008*a*. Elevated DNA damage in a mouse model of oxidative stress: impacts of ionizing radiation and a protective dietary supplement. Mutagenesis, **23**(6): 473–482. doi:10.1093/mutage/gen036. PMID:18644833.

Lemon, J.A., Rollo, C.D., McFarlane, N.M., and Boreham, D.R. 2008*b*. Radiation-induced apoptosis in mouse lymphocytes is modified by a complex dietary supplement: the effect of genotype and gender. Mutagenesis, **23**(6): 465–472. doi:10.1093/mutage/gen038. PMID:18644835.

Marnett, L.J. 2000. Oxyradicals and DNA damage. Carcinogenesis, **21**(3): 361–370. doi:10.1093/carcin/21.3.361. PMID:10688856.

Mettler, F.A., Jr., Thomadsen, B.R., Bhargavan, M., Gilley, D.B., Gray, J.E., Lipoti, J.A., et al. 2008. Medical radiation exposure in the U.S. in 2006: preliminary results. Health Phys. **95**(5): 502–507. doi:10.1097/01.HP.0000326333.42287.a2. PMID:18849682.

Mooren, F.C., Lechtermann, A., and Völker, K. 2004. Exercise-induced apoptosis of lymphocytes depends on training status. Med. Sci. Sports Exerc. **36**(9): 1476–1483. doi:10.1249/01.MSS.0000139897.34521.E9. PMID:15354026.

Nakamoto, H., Kaneko, T., Tahara, S., Hayashi, E., Naito, H., Radak, Z., and Goto, S. 2007. Regular exercise reduces 8-oxodG in the nuclear and mitochondrial DNA and modulates the DNA repair activity in the liver of old rats. Exp. Gerontol. **42**(4): 287–295. doi:10.1016/j.exger.2006.11.006. PMID:17204389.

Oh-ishi, S., Kizaki, T., Ookawara, T., Sakurai, T., Izawa, T., Nagata, N., and Ohno, H. 1997. Endurance training improves the resistance of rat diaphragm to exercise-induced oxidative stress. Am. J. Respir. Crit. Care Med. **156**(5): 1579–1585. PMID:9372679.

Peters, E.M., Van Eden, M., Tyler, N., Ramautar, A., and Chuturgoon, A.A. 2006. Prolonged exercise does not cause lymphocyte DNA damage or increased apoptosis in well-trained endurance athletes. Eur. J. Appl. Physiol. **98**(2): 124–131. doi:10.1007/s00421-006-0227-4. PMID:16941179.

Phan, N., De Lisio, M., Parise, G., and Boreham, D.R. Biological effects and adaptive response from single and repeated computed tomography scans in C57Bl/6 mice. Radiat. Res. In review.

Prasad, K. 1995. Handbook of radiobiology. CRC Press, New York, N.Y.

Quadrilatero, J., and Hoffman-Goetz, L. 2004. *N*-Acetyl-L-cysteine prevents exercise-induced intestinal lymphocyte apoptosis by maintaining intracellular glutathione levels and reducing mitochondrial membrane depolarization. Biochem. Biophys. Res. Commun. **319**(3): 894–901. doi:10.1016/j.bbrc.2004.05.068. PMID:15184067.

Quadrilatero, J., and Hoffman-Goetz, L. 2005. Mouse thymocyte apoptosis and cell loss in response to exercise and antioxidant administration. Brain Behav. Immun. **19**(5): 436–444. doi:10.1016/j.bbi.2004.12.004. PMID:16061151.

Radak, Z., Naito, H., Kaneko, T., Tahara, S., Nakamoto, H., Takahashi, R., et al. 2002. Exercise training decreases DNA damage and increases DNA repair and resistance against oxidative stress of proteins in aged rat skeletal muscle. Pflugers Arch. **445**(2): 273–278. doi:10.1007/s00424-002-0918-6. PMID:12457248.

Radak, Z., Chung, H.Y., and Goto, S. 2005. Exercise and hormesis: oxidative stress-related adaptation for successful aging. Biogerontology, **6**(1): 71–75. doi:10.1007/s10522-004-7386-7. PMID:15834665.

Radak, Z., Kumagai, S., Nakamoto, H., and Goto, S. 2007. 8-Oxoguanosine and uracil repair of nuclear and mitochondrial DNA in red and white skeletal muscle of exercise-trained old rats. J. Appl. Physiol. **102**(4): 1696–1701. doi:10.1152/japplphysiol.01051.2006. PMID:17204574.

Radak, Z., Chung, H.Y., Koltai, E., Taylor, A.W., and Goto, S. 2008. Exercise, oxidative stress and hormesis. Ageing Res. Rev. **7**(1): 34–42. doi:10.1016/j.arr.2007.04.004. PMID:17869589.

Salzman, G.C., Crowell, J.M., Martin, J.C., Trujillo, T.T., Romero, A., Mullaney, P.F., and LaBauve, P.M. 1975. Cell classification by laser light scattering: identification and separation of unstained leukocytes. Acta Cytol. **19**(4): 374–377. PMID:808927.

Smolka, M.B., Zoppi, C.C., Alves, A.A., Silveira, L.R., Marangoni, S., Pereira-Da-Silva, L., et al. 2000. HSP72 as a complementary protection against oxidative stress induced by exercise in the soleus muscle of rats. Am. J. Physiol. Regul. Integr. Comp. Physiol. **279**(5): R1539–R1545. PMID:11049834.

Somani, S.M., and Husain, K. 1996. Exercise training alters kinetics of antioxidant enzymes in rat tissues. Biochem. Mol. Biol. Int. **38**(3): 587–595. PMID:8829619.

Terstappen, L.W.M.M., de Grooth, B.G., Visscher, K., van Kouterik, F.A., and Greve, J. 1988. Four-parameter white blood cell differential counting based on light scattering measurements. Cytometry, **9**(1): 39–43. doi:10.1002/cyto.990090107. PMID:3409785.

Terstappen, L.W.M.M., Meiners, H., and Loken, M.R. 1989. A rapid sample preparation technique for flow cytometric analysis of immunofluorescence allowing absolute enumeration of cell subpopulations. J. Immunol. Methods, **123**(1): 103–112. doi:10.1016/0022-1759(89)90034-3. PMID:2477460.

Tsai, K., Hsu, T.G., Hsu, K.M., Cheng, H., Liu, T.Y., Hsu, C.F., and Kong, C.W. 2001. Oxidative DNA damage in human peripheral leukocytes induced by massive aerobic exercise. Free Radic. Biol. Med. **31**(11): 1465–1472. doi:10.1016/S0891-5849(01)00729-8. PMID:11728819.

Umegaki, K., Higuchi, M., Inoue, K., and Esashi, T. 1998. Influence of one bout of intensive running on lymphocyte micronucleus frequencies in endurance-trained and untrained men. Int. J. Sports Med. **19**(8): 581–585. doi:10.1055/s-2007-971963. PMID:9877151.

Valko, M., Leibfritz, D., Moncol, J., Cronin, M.T., Mazur, M., and Telser, J. 2007. Free radicals and antioxidants in normal physiological functions and human disease. Int. J. Biochem. Cell Biol. **39**(1): 44–84. doi:10.1016/j.biocel.2006.07.001. PMID:16978905.

Venditti, P., and Di Meo, S. 1996. Antioxidants, tissue damage, and endurance in trained and untrained young male rats. Arch. Biochem. Biophys. **331**(1): 63–68. doi:10.1006/abbi.1996.0283. PMID:8660684.

Wolff, S. 1996. Aspects of the adaptive response to very low doses of radiation and other agents. Mutat. Res. **358**(2): 135–142. PMID:8946018.